VU VRIJE UNIVERSITEIT AMSTERDAM

VU Research Portal

Growth potential of coral reefs and carbonate platforms

Bosscher, H.

1992

document version
Publisher's PDF, also known as Version of record

Link to publication in VU Research Portal

citation for published version (APA)
Bosscher, H. (1992). *Growth potential of coral reefs and carbonate platforms*. [PhD-Thesis - Research and graduation internal, Vrije Universiteit Amsterdam]. Elinkwijk.

General rights
Copyright and moral rights for the publications made accessible in the public portal are retained by the authors and/or other copyright owners and it is a condition of accessing publications that users recognise and abide by the legal requirements associated with these rights.

- Users may download and print one copy of any publication from the public portal for the purpose of private study or research.
- You may not further distribute the material or use it for any profit-making activity or commercial gain
- You may freely distribute the URL identifying the publication in the public portal ?

Take down policy
If you believe that this document breaches copyright please contact us providing details, and we will remove access to the work immediately and investigate your claim.

E-mail address:
vuresearchportal.ub@vu.nl

Download date: 05. May. 2023

Growth potential of coral reefs and carbonate platforms

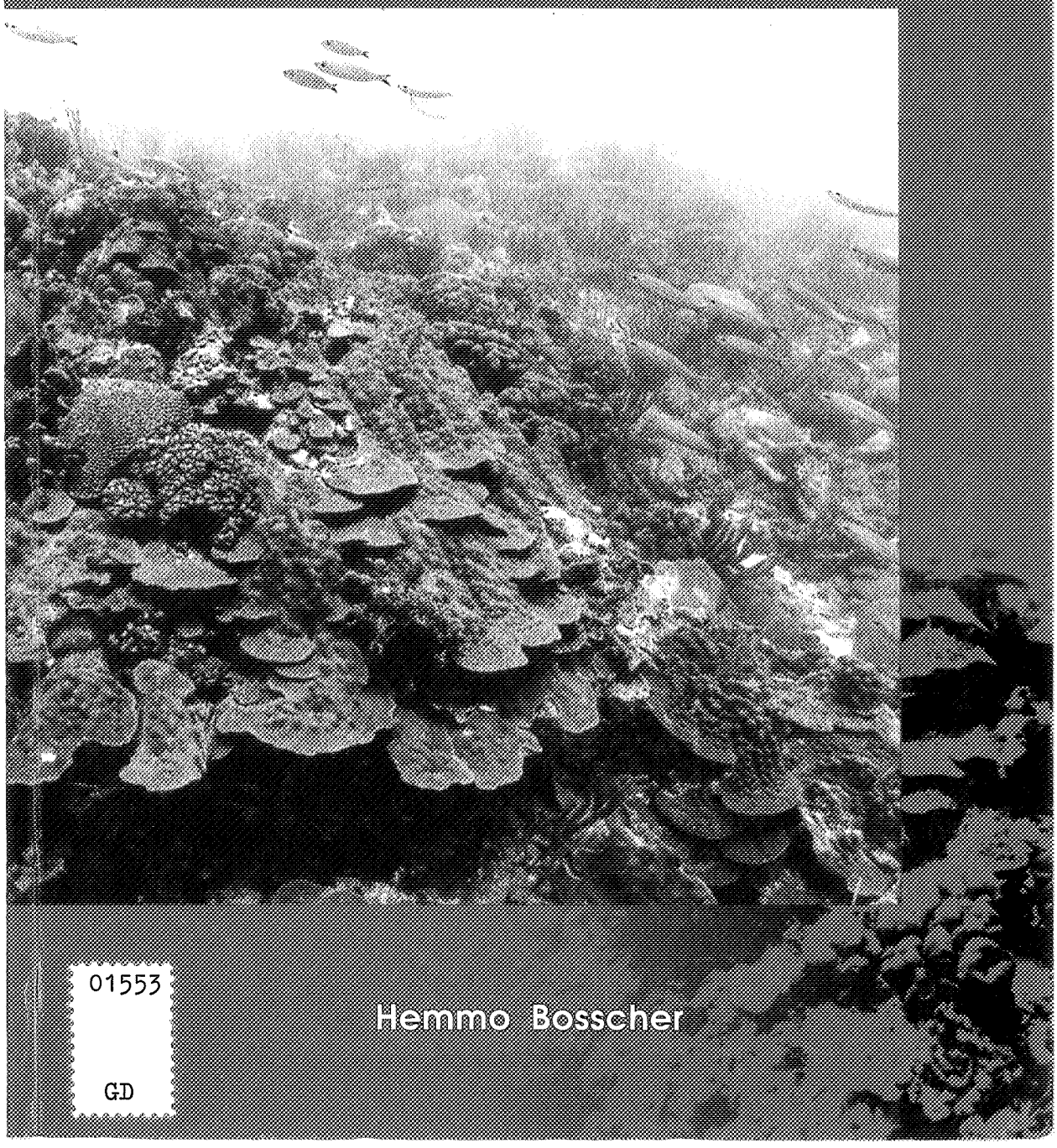

01553

GD

Hemmo Bosscher

STELLINGEN

behorende bij het proefschrift

GROWTH POTENTIAL OF CORAL REEFS
AND CARBONATE PLATFORMS

door Hemmo Bosscher

1. De veelgebruikte opmerking over de evolutie van rifbouwers, "the actors change but the play goes on", is een te eenvoudige voorstelling van zaken. De geologische geschiedenis kent vele periodes met geen of weinig rifgroei van betekenis.

(zie hoofdstuk 8 van dit proefschrift).

2. Een geoloog wordt steeds weer geconfronteerd met het probleem van dateren. Het belang van de verschillende dateringstechnieken kan derhalve niet genoeg onderstreept worden.

3. De implicatie van de bevindingen van Barnes et al. (1992) is, dat de resultaten van twee decennia isotopenonderzoek aan koralen op zijn minst met enig wantrouwen moeten worden bekeken.

4. Het definiëren van drie nieuwe soorten voor de verschillende morphotypen van *Montastrea annularis* schept meer problemen dan het oplost.

contra Knowlton et al., 1992, and in prep.

5. Het verschil in wetenschappelijke benaderingswijze tussen geologen en biologen komt sterk tot uiting in het feit dat de relatie tussen koraalgroeisnelheid en waterdiepte tot nu toe niet gekwantificeerd was.

6. Het woord modeleren in de geologie dient vervangen te worden door de woorden model leren.

7. Goede veldobservaties blijven de basis van de geologie.

8. Het hangt sterk af van de carrièrekeuze of een aio/oio nogmaals een vergelijkbare, of zelfs grotere, percentuele salarisontwikkeling zal meemaken als gedurende zijn/haar aio/oio-schap.

contra Beets, 1992 (stelling 5 gevoegd bij zijn proefschrift)

9. Vernieuwend onderzoek is meer gebaat bij het samenbrengen van enthousiaste mensen dan grote sommen gelds.

10. Het is leerzamer om in plaats van de tweede-fase opleiding Mariene Aardwetenschappen aio's/oio's in de gelegenheid te stellen enige tijd onderzoeksgroepen te bezoeken die iets kunnen toevoegen aan hun specifieke onderzoek.

11. Beagles vervullen een sleutelrol in het onderzoek naar koraalriffen.

12. Het Sinterklaasfeest maakt een wezenlijk deel uit van de Nederlandse cultuur. Een ieder die dan ook het geïmporteerde kadootjesfeest kerstmis de voorkeur geeft boven de goede Sint, dient in een stevige jute zak te worden afgevoerd in zuidelijke richting.

13. Voor een jonge vader is promoveren een welkome ontspanning.

14. Het moet wel een hobby blijven.

GROWTH POTENTIAL OF CORAL REEFS AND CARBONATE PLATFORMS

VRIJE UNIVERSITEIT

GROWTH POTENTIAL OF CORAL REEFS AND CARBONATE PLATFORMS

ACADEMISCH PROEFSCHRIFT

ter verkrijging van de graad van doctor aan
de Vrije Universiteit te Amsterdam,
op gezag van de rector magnificus
dr. C. Datema,
hoogleraar aan de faculteit der letteren,
in het openbaar te verdedigen
ten overstaan van de promotiecommissie
van de faculteit der aardwetenschappen
op maandag 7 december 1992 te 15.30 uur
in het hoofdgebouw van de universiteit, De Boelelaan 1105

door

Hemmo Bosscher

geboren te Hoorn

Amsterdam 1992

Drukkerij Elinkwijk b.v. - Utrecht

Promotor: prof.dr. W. Schlager
Copromotor: prof.dr. R.P.M. Bak
Referent: dr. J.W. Focke


BÈTA BIBL. VRIJE UNIVERSITEIT
AMSTERDAM
AARDWETEN-
SCHAPPEN
GD


voor Natalie

CIP-GEGEVENS KONINKLIJKE BIBLIOTHEEK, DEN HAAG

Bosscher, Hemmo

Growth potential of coral reefs and carbonate platforms /
Hemmo Bosscher. - [S.l. : s.n.] (Utrecht : Elinkwijk).-
Ill.
Proefschrift Vrije Universiteit Amsterdam. - Met lit. opg.
- Met samenvatting in het Nederlands.
ISBN 90-9005566-5
Trefw.: koraalriffen

© Hemmo Bosscher, 1992.

Research reported in this thesis was carried out at the Vrije Universiteit, Faculty of Earth Sciences, Department of Sedimentary Geology, Sedimentology/Marine Geology section, De Boelelaan 1085, 1081 HV Amsterdam, The Netherlands.

Financial support was provided by the Netherlands Foundation for Earth Science Research (AWON/NWO): project no.: 751.356.019.
Additional financial support was provided by the Industrial Associates of the Sedimentology/Marine Geology section at the Vrije Universiteit, the Foundation for the Advancement of Scientific Research in Surinam and the Netherlands Antilles (Studiekring) and Shell Internationale Petroleum Maatschappij.

Cover: Coral reef dominated by *Montastrea annularis* at ca. 12 meter water depth, Karpata, Bonaire, N.A. (cover design: Paul Bookelman; photograph: Rolf Bak).

CONTENTS

BIBLIOGRAPHY

Most of the chapters in this thesis have been published, or have been submitted for publication, as papers in scientific journals. The following list gives the references to these papers in the order in which they appear in this thesis:

Bosscher, H., and Meesters, E.H., 1992. Depth related changes in the growth rate of *Montastrea annularis*. Proceedings of the 7th International Coral Reef Symposium, Guam, U.S.A., in press.

Bosscher, H., 1992. Computerized tomography and skeletal density of coral skeletons. Coral Reefs, in press.

Bosscher, H., and Ganssen, G., Metabolic effect on skeletal $\delta^{13}C$ of the Caribbean reef-building coral *Montastrea annularis*. Palaeogeography, Palaeoclimatology, Palaeoecology, submitted.

Bosscher, H., and Schlager, W., 1992. Computer simulation of reef growth. Sedimentology, v.39, p.503-512.

Bosscher, H., and Southam, J.R., 1992. CARBPLAT - a computer model to simulate the development of carbonate platforms. Geology, v.20, p.235-238.

Reijmer, J.J.G., Schlager, W., Bosscher, H., Beets, C.J., and McNeill, 1992. Pliocene/Pleistocene platform facies transition recorded in calciturbidites (Exuma Sound, Bahamas). Sedimentary Geology, v.78, p.171-179.

Bosscher, H., and Schlager, W., 1992. Accumulation rates of carbonate platforms. Journal of Geology, in press.

Schlager, W., and Bosscher, H., Platform drowning and scaling of sedimentation rates. Geology, submitted.

SAMENVATTING

Inleiding

Carbonaat (kalk) sedimenten ontstaan voor een belangrijk deel door middel van kalkvormende organismen. De kalkskeletten van verschillende groepen organismen vormen de bouwstenen van koraalriffen, carbonaat platformen (grote plateaus met vaak een rand van koraalriffen) en diepzee kalkafzettingen. Het belang van het biologische proces van kalkvorming onderscheidt kalkstenen van de andere grote sediment familie, de siliciclastische gesteenten (zand, klei etc.). De belangrijkste hedendaagse rifbouwers zijn de z.g. steenkoralen. Deze dieren bezitten in hun weefsel een-cellige algen. Koralen zijn door deze symbiose met planten voor hun groei sterk afhankelijk van fotosynthese en dus licht. Doordat de licht-intensiteit afneemt met toenemende water diepte, neemt ook de groei van koralen af met diepte. Rifbouwende koralen komen voor tot de diepte waar de lichtintensiteit nog slechts 1% van de oppervlakte lichtintensiteit bedraagt (de eufotische zone). Deze diepte varieert van ca. 30 to 150 m. Koraalriffen kunnen dus 'verdrinken' wanneer bijvoorbeeld een snel stijgende zeespiegel het rif beneden de eufotische zone doet belanden.

Vraagstelling

Het onderzoek dat wordt beschreven in dit proefschrift heeft zich bezig gehouden met het groei-potentieel van koraalriffen en carbonaat platformen. Wat bepaalt het vermogen van deze systemen om te groeien en het hoofd te kunnen bieden aan zeespiegel-veranderingen.? Hoe snel groeien koralen en in hoeverre is de groeisnelheid van koralen bepalend voor de groei van het gehele koraalrif?

In de geologische geschiedenis vormen koraalriffen en carbonaat platformen verreweg het grootste gedeelte van de totale hoeveelheid afgezette kalksteen. Wat was de accumulatie-snelheid van deze fossiele koraal riffen en carbonaat platformen ? Wat kan de oorzaak zijn geweest voor het verdrinken van veel van deze fossiele platformen?

Het onderzoek

Het onderzoek, en ook dit proefschrift, bestaat uit drie delen. Deel I behandelt de groei van het belangrijkste rifbouwende koraal in het Caraïbisch gebied, Montastrea annularis, of sterkoraal. Het kalkskelet van dit koraal bevat jaarlijkse groeiringen die het mogelijk maken de groeisnelheid te bepalen. Samen met dichtheidsbepalingen van het skelet en de variatie van de koolstof isotopen die in het skelet worden opgenomen, leveren deze groeigegevens informatie over de totale groei van het kalkskelet van dit koraal. Door middel van onderwater licht-metingen is het verband tussen koraalgroei en licht bestudeerd. De koraal-boorkernen die voor dit onderzoek zijn gebruikt, zijn genomen op Curaçao tot een diepte van zo'n 30 meter.

Deel II behandelt de groei van koraalriffen en carbonaat platformen. Computer simulaties van rifgroei, gebaseerd op de bevindingen uit deel I, illustreren het belang van licht voor rifgroei. De reactie van rifgroei op zeespiegelveranderingen kan voor een groot deel worden verklaard door de afname van koraalgroei met toenemende diepte. Dit model

is uitgebreid met observaties van sediment afzetting op carbonaat platformen. Dit heeft geresulteerd in CARBPLAT, een computer model dat de ontwikkeling van dergelijke carbonaat platformen beschrijft. De observaties die aan dit model ten grondslag liggen zijn voor een deel onderbouwd met een studie naar de ontwikkeling van een carbonaat platform in de Bahama's.

Deel III geeft een overzicht van de groeisnelheid van riffen en carbonaat platformen gedurende de laatste 600 miljoen jaar van de geologische geschiedenis. De waargenomen variaties in de groeisnelheid van riffen en carbonaat platformen is voor een groot deel te relateren aan de evolutie van rifbouwende organismen. Voor het verdrinken van riffen en carbonaat platformen is het vooral van belang te weten wat de maximale groeisnelheid bedraagt voor een periode van enkele duizenden tot tienduizenden jaren. Dit is de de periode die relatieve zeespiegelveranderingen doorgaans nodig hebben om de dikte van de euphotische zone te bereiken. Dit groei-potentieel van riffen en carbonaatplatformen is bepaald door het vergelijken van groeisnelheden van recente en fossiele riffen en carbonaat platformen.

Conclusies

De groeisnelheid van het belangrijkste rifbouwende koraal in het Caraïbische gebied, *Montastrea annularis* neemt af met de diepte op een manier die vrijwel geheel wordt bepaald door de hoeveelheid licht. Tot een diepte van ca. 15 meter is de groei van dit koraal 'licht-verzadigd' en vertoont het weinig variatie. Beneden deze 'licht-verzadigingsdrempel', die afhangt van de helderheid van het water, neemt de groeisnelheid vrijwel exponentieel af tot de ondergrens van de eufotische zone. Deze relatie tussen groei, licht en diepte, geldt niet alleen voor de groei van individuele koralen, maar speelt ook een belangrijke rol in de groei van het gehele koraalrif.

De groei van carbonaat platformen hangt voor een belangrijk deel af van de groei van koraalriffen, die doorgaans de rand van het platform vormen. Platformen groeien het beste als ze geheel onder water staan, en slechts dan zijn ze in staat zijn om grote hoeveelheden sediment te maken en te transporteren naar de omliggende diepzee bodem. Beneden de 'licht-verzadigings drempel' echter, neemt het groeipotentieel van de rifrand, en dus het gehele platform snel af. Het is voor een platform, of koraalrif, dus voordelig in de 'licht-verzadigde zone' te blijven om te overleven. Of dit lukt hangt af van de balans tussen relatieve zeespiegelveranderingen en het groei-potentieel. Het groei-potentieel zoals dat blijkt uit de vergelijking tussen recente en fossiele platformen, bedraagt zo'n 1000 meter per miljoen jaar. Dit maakt het voor normale snelheden van zeespiegelverandering, die doorgaans veel lager zijn, onmogelijk om riffen en platformen permanent te verdrinken. De aanwezigheid van vele voorbeelden van verdronken riffen en platformen in de geologische geschiedenis is hiermee in tegenspraak. Om hiervoor een verklaring te vinden moeten we kijken naar milieufactoren die het groei-potentieel aantasten, of extreem snelle daling van de aardkorst en dus een zeer snelle relatieve zeespiegelstijging.

Dit proefschrift belicht enkele van de basis-principes binnen de carbonaat sedimentologie. De resultaten van dit onderzoek hebben echter ook belangrijke consequenties voor de biologie van koraalriffen en andere disciplines binnen de geologie, niet in de laatste plaats gezien de rol van riffen en carbonaat platformen als olie reservoir en hun belangrijke aandeel in de koolstofkringloop van de aarde.

SUMMARY

Introduction

Calcification by organisms is the most important sediment producer in carbonate environments. By building carbonate skeletons these organisms form the basic building blocks of coral reefs, carbonate platforms, and pelagic carbonates. This link to biologic processes distinguishes carbonates from siliciclastics.

Today's most important reef-building organisms are scleractinian, or stony corals. These animals have a symbiotic relationship with uni-cellular algae called zooxanthellae. Light-enhanced calcification through the photosynthetic activity of these symbionts allows corals to grow at rates that would otherwise be impossible. The photic requirements of the coral/algal symbiosis limits the depth distribution of reef-building corals to the euphotic zone. Below this depth (generally 30 - 150 m) coral reefs cannot survive and consequently drown.

The research reported in this thesis deals with the growth potential of coral reefs and carbonate platforms. What determines the growth of these systems? What is the growth rate of individual corals and to what extent can coral growth be taken as a measure of reef growth? Most of the carbonate rock mass in the geologic record is formed by reefs, carbonate platforms and other shoalwater carbonates. At what rate did these reefs and platforms accumulate? What could have been the reason for the drowning of many of these ancient reefs and platforms?

This thesis is divided into three parts. Part I deals with the skeletal growth of the most important reef-building coral in the Caribbean, *Montastrea annularis*. Growth rate, skeletal density, and carbon isotope composition were determined to evaluate the role of decreasing light with increasing water depth.

Part II discusses the growth of coral reefs and carbonate platforms. Observations on the growth of modern reef-building corals (part I) have been incorporated into a computer model to simulate the growth of coral reefs. Combined with sedimentological principles of carbonate platform development this reef model resulted in CARBPLAT, a simulation model for carbonate platform development. A case study on carbonate platform development illustrates one of the basic assumptions that underlies CARBPLAT.

Part III gives an overview of the accumulation rates of Phanerozoic reefs and carbonate platforms. The results of this study are used to assess the importance of scaling law's in determining the growth potential of carbonate platforms.

Conclusions

The results presented in part I of this thesis illustrate the dominant control of light on skeletal growth rates of *Montastrea annularis*. The decrease of skeletal growth with depth can be described using a combination of a photosynthetic function and the exponential

decrease of light with depth. To a depth of ca. 15 m growth is light-saturated and shows little variation. Below this light-saturation threshold growth rates decline rapidly towards the base of the euphotic zone.

This relation between coral growth rates and depth has been succesfully used to simulate Holocene reef growth. CARBPLAT incorporates this growth/depth relation into a model that combines observations on the sedimentology of carbonate slopes with the notion that carbonate platforms are highstand shedding depositional systems. This is illustrated by an example of platform development from the Bahamas. CARBPLAT illustrates that not only sea-level changes can produce stratigraphic unconformities on carbonate platform slopes, but also changes in the sediment composition at different stages of platform growth.

To survive, carbonate platforms and coral reefs have to remain within the euphotic zone and preferably within the zone of light-saturation. Whether they can accomplish this depends on the balance between relative sea-level changes and growth potential. The growth potential of coral reefs and carbonate platforms, as estimated from a comparison between recent and fossil reefs and platforms, is in the order of 1000 B (m/Ma). This rate renders normal rates of sea-level rise incapable of permanently drowning coral reefs and carbonate platforms. To explain drowning in the geologic record we have to look at a reduction of growth potential by environmental stress or extremely rapid relative sea-level rises as result of rapid tectonic subsidence.

This thesis discusses some of the basic principles in carbonate sedimentology. The results presented here are also important in other earth sciences disciplines, and coral reef biology, not in the least because of the role of coral reefs and carbonate platforms as hydrocarbon reservoirs and their important contribution to the global carbon budget.

ACKNOWLEDGMENTS

Much of what I have learned about carbonate sedimentology, I learned from my promotor Wolfgang Schlager. I would like to thank him for the opportunity he offered me to pursue this Ph.D. His support and many questions have been of great help.

To my copromotor Rolf Bak I would like to express my gratitude for his cooperation and interest. I am very pleased that he got involved with this project and hope he learned that sraightforward is not always straight. Jaap Focke is gratefully acknowledged for being a referee to this thesis.

My fellow Ph.D. students from the Sedimentary Geology Department, John Reijmer, Jeroen Kenter, Erik Zwart, Ewan Campbell, Arnout Everts, and Jan Stafleu (the 'wolfgang'), Tim Peper, Menno de Ruig, Jan Diederik van Wees, Paul Saager, and many others have always, seemingly undisturbed, tolerated my presence. I thank them for this. They contributed to this thesis, by answering my questions, attempting discussion, lending a patient ear or two, or sharing a beer or two.

For their help in various stages of my Ph.D. project I would like to acknowledge Gerald Ganssen, Simon Troelstra, Juul Everaars, Flora Vijn, and John Southam.

Annemiek Bredius and Peter Derriks are thanked for their help in operating the CT at the Academic Hospital of the Vrije Universiteit

During my stay at the Vrije Universiteit many people have helped me getting this thesis finished. I would particularly like to thank Saskia Kars, Peter Willekes, Nanda Rave-Koot and all the other members of the technical support staff and photograpy department hat have helped me during the last four years.

I thank the CARMABI Institute for the use of their facilities. Staff and students at the CARMABI who helped me are gratefully thanked. Especially Erik Meesters and Manfred van Veghel contributed to the timely completion of this thesis. I wish them succes with the completion of their own thesis.

I will never forget the hospitality offered by various people during fieldwork or visits abroad. Bill and Joni Precht, Harold and Elizabeth Hudson, Mike McClain, Frank and Eva Peerdeman and Vicki Nelson are very warmly thanked.

I consider it a great honour that Kay Beets and Johan Dorenbos have accepted my request to act as 'paranimfen' for this promotion. Especially Dr. C.J. Beets should be mentioned for offering me much needed practice and help in the preparation of a Ph.D. thesis.

The support of my father and my parents-in-law has kept me and my family running. Arno is thanked for his help with chapter 5 of this thesis. Paul Bookelman is thanked for his help in the final preparation of the manuscript.

My children Hemmo and Isabeau have been great friends and always shared my interest in cojals and gelology. To my wife, Natalie, I owe everything. It is to her that I dedicate this thesis.

Chapter 1

INTRODUCTION

"If it be asked, at what rate in years I suppose a reef of coral favourably circumstanced could grow up from a given depth; I should answer that we have no precise evidence on this point, and comparatively little concern with it. We see, in inumerable points over wide areas, that the rate has been sufficient, either to bring up the reefs from various depths, or, as is more likely, to keep them at the surface, during progressive subsidences; and this is a much more important standard of comparison than any cycle of years."

(Charles Darwin, 1842)

INTRODUCTION

Ever since the stromatolites of the Woonawarra group in Australia some 3500 million years ago, photosynthetically powered calcification has been present (Cowen, 1988). Especially since the advent of calcifying metazoans in the Early Cambrian carbonates have dominated shallow tropical seas. It is a long way from these Early Cambrian archeocyathid/ algal communities to the modern coral reefs dominated by scleractinian corals. Calcification by benthic organisms, however, has remained the building stone of shallow water carbonate deposition throughout the Phanerozoic.

Coral Reefs and Carbonate Platforms

Corals thrive in clear, warm tropical waters. There they grow to form reefs from small atoll islets to impressive structures such as the Australian Great Barrier Reef. Their growth is limited ultimately by sea level. Coral reefs will try to fill the accommodation space created by a rising sea level and keep up with sea level. If the sea-level rise is too fast they will have to give up and 'drown" or wait for the sea-level rise to slow down and catch up with it. If sea level falls, however, coral reefs will become emerged and the living reef is forced to step down with sea level and migrate oceanward. Sea level exerts a major control on coral reef growth (Precht, 1988).

Carbonate platforms act much in the same way. The anatomy of carbonate platforms can be described in a simple way by the 'bucket principle' (Schlager, 1981): a modern rimmed platform consists of a stiff rim of reefs or cemented sand shoals (the 'bucket') filled by soft lagoonal or platform interior sediments, and surrounded by a steep fore-reef slope. Through the construction of the stiff rim and trapping of the loose sediments that form the

platform interior, coral reefs determine the way in which carbonate platforms respond to sea-level changes. The growth potential of the coral reef rim, therefore, determines the growth potential of the entire platform.

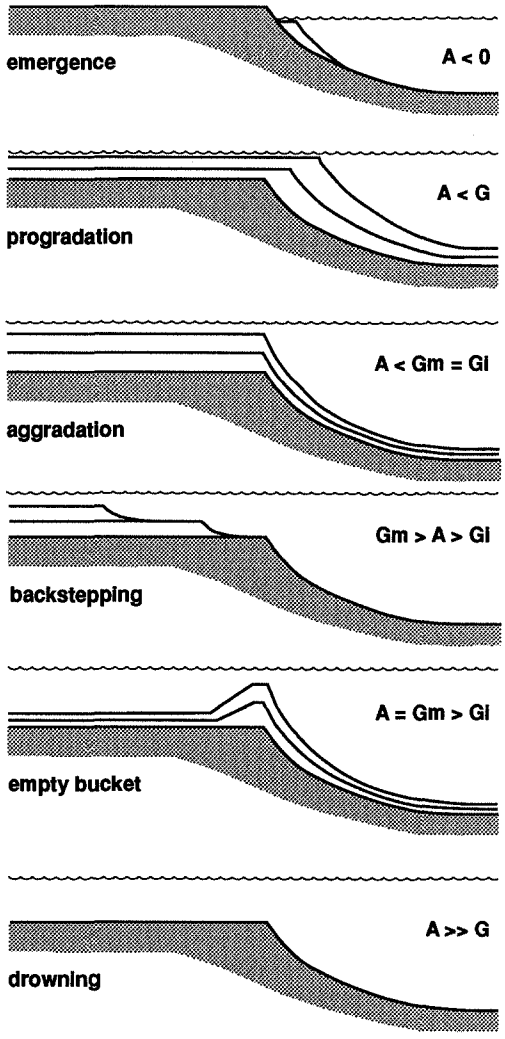

Figure 1. Sedimentologic interpretation of basic geometries in carbonates (after Schlager, 1992). A = rate of creation of accommodation space; G = growth potential, Gm = growth potential platform margin, Gi = growth potential platform interior.

Growth potential

The growth potential of coral reefs and carbonate platforms can be defined as the maximum rate at which they grow upward, i.e. their aggradation potential. Another measure of growth potential is the volume of sediment a carbonate platform can produce, i.e. production potential. Throughout this thesis growth potential is used in the meaning of aggradation potential. Accumulation rates in this thesis will be given in Bubnoff units (B: m/Ma; Fischer, 1969). Growth rates of individual corals will be given in mm/yr for easier comparison with existing literature. The growth rates of Holocene reefs can be measured relatively accurate. From their growth response to the rapid Holocene sea-level rise it is apparent that the growth potential of these coral reefs was less than the maximum rate of sea-level rise. During at least some parts of the Holocene reefs were forced to grow at their full potential, thus providing an estimate of upper limit of the growth potential of such depositional systems.

The growth potential of fossil reefs and carbonate platforms can only be deduced from several observations. Numerous platforms attained vertical thicknesses of more than a kilometer containing only shallow water carbonates. Not only did they grow up to sea level and maintained that position for several millions of years, but often they grew outward and prograded basinward. This means that the accumulation rate of fossil platforms is the lower limit, and most probably an underestimate, of their growth potential. From a compilation of Phanerozic carbonate platforms it appears that they accumulated at rates to over 200 B (m/ Ma). From the Holocene we know that the maximum growth rate of coral reefs subjected to the very fast Holocene sea-level rise has been between 10000-12000 B. The Holocene growth potential provides thus an estimate of the upper limit of the growth potential. Part III of this thesis will deal with the connection between accumulation rates of fossil platforms and Holocene reef accretion rates to provide an estimate of growth potential.

Drowning of reefs and carbonate platforms

If the growth potential of a carbonate platform is insufficient to match a fast rise of relative sea level, the platform will drown and eventually become submerged below the euphotic zone. Such drowned platforms occur throughout the geologic record. Reef or platform drowning can have many causes, from rapid rises of relative sea level and oceanographic changes to the extinction of reef-builders. To determine the cause of platform drowning we must consider that such mechanisms have to either destroy the platform's production system or outpace the platform's growth potential for a period of time long enough to prevent the platform to catch up with sea level again. Whether drowning occurs depends on the growth potential of a platform and the depth at which this growth potential has been reduced to rates too low to cope with even a slight relative sea-level rise.

Thesis lay-out

The growth potential of coral reefs and carbonate platforms, i.e. the maximum rate at which they can grow up to sea level, is one of the main themes of this thesis. A related

question is to what depth coral reefs can maintain this growth. At what depth will the growth potential be reduced to rates that are insufficient to cope with even small relative rises in sea level? To find answers to these questions the problem was tackled from two sides. On the one side I looked at the controls on modern coral reef growth .On the other side, I compiled accumulation rates of what is left from nearly 600 Million years of reef and platform growth in the geologic record. This two-prong approach is reflected in the lay-out of this thesis

This thesis consists of a number of papers that have either been published or submitted for publication, and an introduction and discussion/conclusions section. The main body is subdivided into three parts: I. Coral Growth, II. Growth of Coral Reefs and Carbonate Platforms, and III. Accumulation Rates of Reefs and Carbonate Platforms Trough Time. Part I consists of three papers that deal with various aspects of the skeletal growth of the most important reef-building coral in the Caribbean, *Montastrea annularis*. Part two describes computer simulation of coral reef and carbonate platform growth. This is followed by a case study on carbonate platform development . The last part of this thesis consists of a literature compilation of accumulation rates of most of the extensive carbonate platforms from the Phanerozoic. The results of this study form the basis for a discussion on scaling laws in sedimentation rates of carbonates and their significance for assessing the growth potential of fossil platforms.

PART I

CORAL GROWTH

INTRODUCTION

This part of the thesis deals with the growth of modern reef-building corals and its controls. The introduction discusses general characteristics and controls of modern coral reef development. Chapters 2,3, and 4 discuss the skeletal growth of the scleractinian coral *Montastrea annularis*. The growth rate of this important Caribbean reef-building coral and its relation to underwater light is discussed in chapter 2. Chapter 3 illustrates the use of Computerized Tomography for measuring the density of coral skeletons. A study on the carbon isotopic composition of coral skeletons, and its relation to decreasing photosynthetic rates with depth is presented in chapter 4.

What is a coral ?

A coral is an animal that belongs to the phylum Coelenterata and the class Anthozoa. This class includes, amongst others, the extinct groups of rugose and tabulate corals that formed reefs during much of the Paleozoic and early Mesozoic. Present day coral reefs are dominated by the reef-building (hermatypic) order of scleractinians (stony corals). They are mostly colonial organisms that consist of numerous polyps. These polyps form a thin living tissue layer that covers the coral skeleton. The individual polyps have a three-layered bodywall and consist of a row of tentacles lining the mouth and the gullet that leads to the digestive body cavity (coelenteron) This cavity is divided by radial partitions (mesenteries). From the outer layer of the body wall (the ectoderm) they excrete their carbonate skeleton. Each polyp sits in its own cup in the skeleton, the calice, from which the septa (six or a multiple of six), that project between pairs of mesenteries, radiate.

The skeleton mainly consists of these vertical (septa) and horizontal elements (dissepiments). The dissepiments are actually the floors on which the polyps live. New dissepiments are formed during growth to cut of the part of the skeleton the polyp has withdrawn from and provide a new floor. Within their inner tissue layer (the endoderm) these corals have symbionts. These symbionts, often called, zooxanthellae, are unicellular dinoflagellate algae known as *Symbiodinium microadriaticum*. This symbiosis between autotrophic algae and heterotrophic animals is the key to the succes of scleractinian corals. The corals get nearly all of their energy requirements through their photosynthesizing symbionts and the coral host offers nutrients and protection to the symbionts. This symbiosis allows the corals to behave like autotrophic organisms and inhabit oligotrophic (nutrient poor) parts of the world's oceans. It also permits them through light-enhanced calcification

to build their skeleton at rates that would otherwise have been impossible. According to Hallock (1981) the symbiosis is only advantageous to the algae in oligotrophic waters. But most important, it makes corals strongly dependent on light for their growth.

Skeletal banding

This thesis concentrates on *Montastrea annularis*, the most important reef-building coral in the Caribbean. Like many others this coral deposits a high and low density layer in its skeleton each year. This gives a pattern of high and low density bands similar to growth rings of trees. X-radiography of these skeletons reveals this banding and allows the measurement of annual growth rates (Knutson et al., 1972; Hudson et al., 1976; Fig. 1).

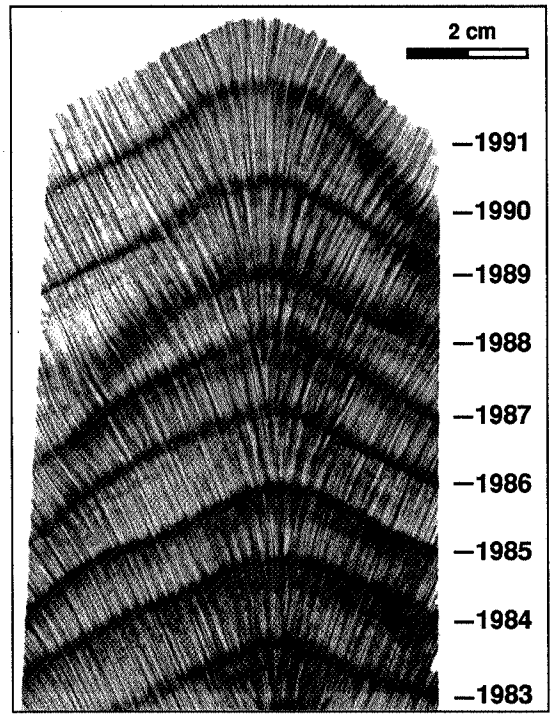

Figure 1. X-radiograph of *Montastrea annularis* showing yearly density banding (core HB10; see Fig.3).

These density bands form mainly through variations in the size of the exothecal (space between adjacent corallites) dissepiments (Dodge et al., 1992). Variations in the endothecal elements (the part of the skeleton in which the polyp lives) or microstructure of the carbonate skeleton play only a minor role. The coral skeleton consists almost entirely of the carbonate mineral aragonite. This mineral forms needle-like crystals that appear in layers or bundles in the coral skeleton (Fig. 2). The timing of deposition of these bands has often been the

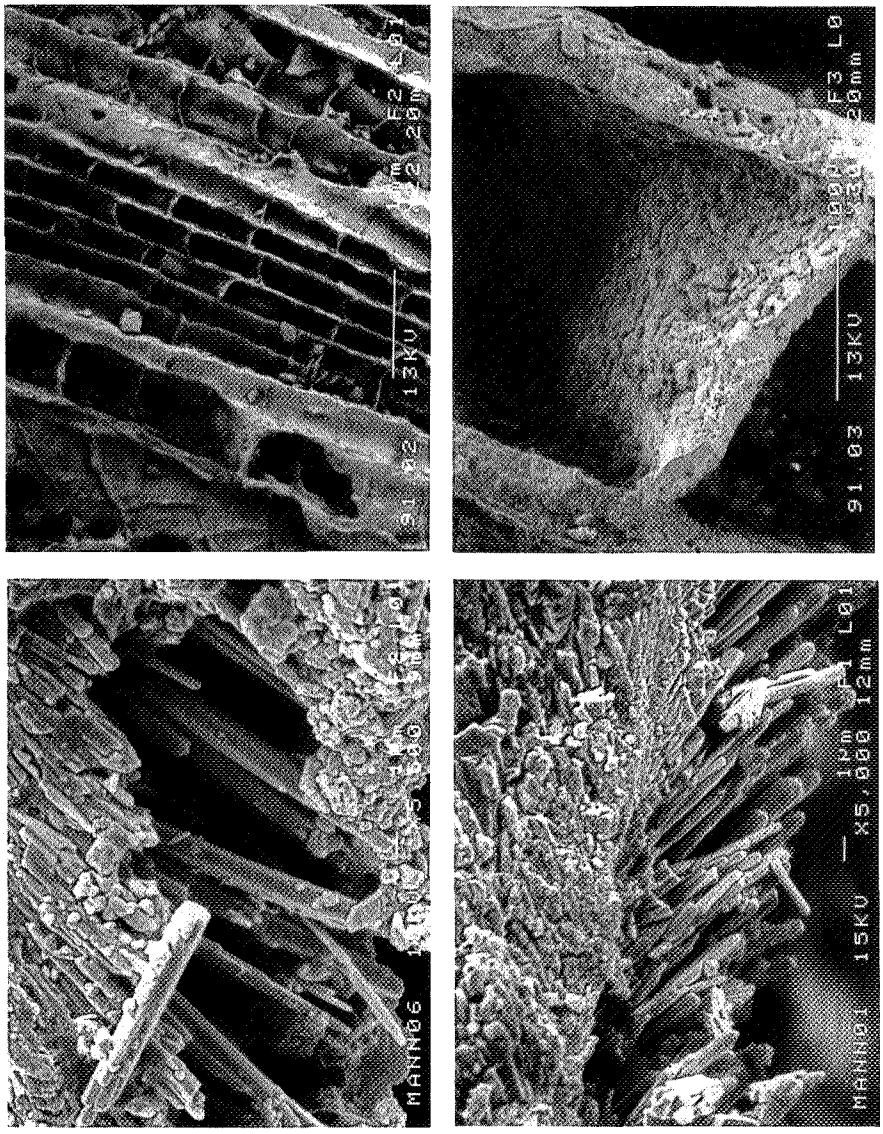

Figure 2. SEM-microphotographs showing skeletal architecture of the coral *Montastrea annularis*. **A** (top left): Septa walls and dissepiments (x 22). **B** (top right): Enlargement of dissepiment between two septa (x 300). **C** (bottom left): Aragonite needles in a dissepiment from a *M.annularis* colony from a water depth of 30.5 m (x 5500). **D** (bottom right): idem, from a water depth of 4 m (x 5000).

subject of discussion (Barnes et al.,'1992). From the cores taken in Curaçao it is clear that the high density bands form sometime in the late summer and early fall (September-October).

This is the period of the highest water temperatures and coincides with the reproductive period of *M. annularis* in Curaçao. More generally high density bands are formed during the period of the year that is least suited for coral growth. This also means that unusual stress, e.g. extremely cold water, or 'bleaching', are recorded in the coral skeleton besides the annual variations. Such 'stress bands' have been described by Hudson et al., (1976). Figure 1 shows an X-rayed slab of a core from a *M. annularis* colony from Boca Santu Pretu, Curaçao. Two examples of growth records of corals ('sclerochronology') form Boca Santu Pretu, Curaçao, are shown in Figure 3. Large coral heads of *M. annularis* from the Caribbean and large colonies (sometimes up to 10 m in size) from the Great Barrier Reef have revealed climatological and environmental records for many hundreds of years (see for example Hudson, 1981). From Figure 3 it is clear that adjacent coral heads of *M.annularis* from Curaçao can exhibit different and sometimes even opposite growth patterns. The extraction of environmental parameters from coral growth records should, therefore, be based on a large number of colonies.

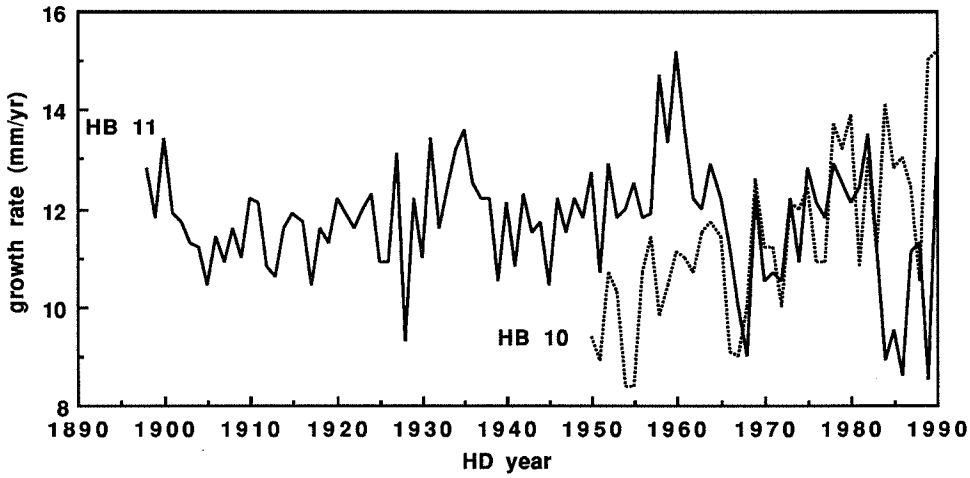

Figure 3. Growth records for two *Montastrea annularis* colonies from Boca Santu Pretu, Curaçao, Netherlands Antilles (HB10: 9.7 m water depth, average growth rate: 11.4 mm/y; HB11: 9.1 m. water depth, average growth rate: 11.7 mm/yr).

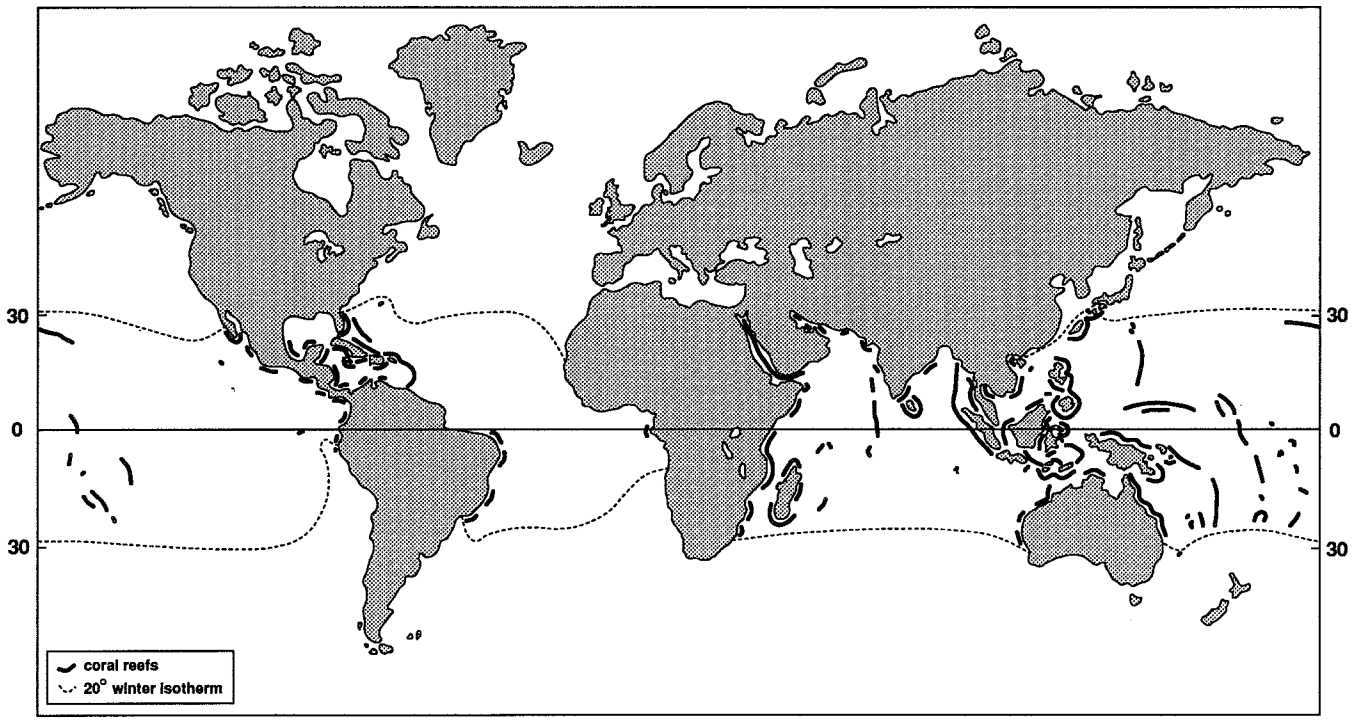

Figure 4. Global distribution of coral reefs and the 20 °C winter isotherm (coral data from: Darwin, 1842; Goureau et al., 1979; Schuhmacher, 1976; various other sources; temperature data from: Van Loon, 1984).

CONTROLS ON CORAL GROWTH

Temperature

Hermatypic corals and coral reefs are restricted to warm tropical waters. The optimum temperature for coral growth is ca. 26-27 °C (Coles and Jokiel, 1978; Kinsman, 1964). Temperature tolerance may vary among species but generally the upper limit for coral growth is 32-33 ° C (Jokiel and Coles, 1977). The lower temperature limit for coral growth is 20 °C (Barnes et al., 1986; Buddemeier and Kinzie, 1976; Marcus and Thorhaug, 1981). Figure 4 shows the global distribution of coral reefs, with the 20 °C winter isotherm. Latitudinal limits of coral growth are clearly related to temperature. Generally coral reefs occur in the tropics between 30° N and 30° S.

Upwelling of cold, nutrient-rich water can prevent reef development in this favourable belt of reef growth as can be seen along the Pacific coast off South America and off Western Africa. The presence of oceanic currents that carry relatively warm waters may extend reef growth beyond 30°, e.g. on Bermuda (Gulf Stream) and the Ryukyu Islands at the southern tip of Japan (Ryukyu Current).

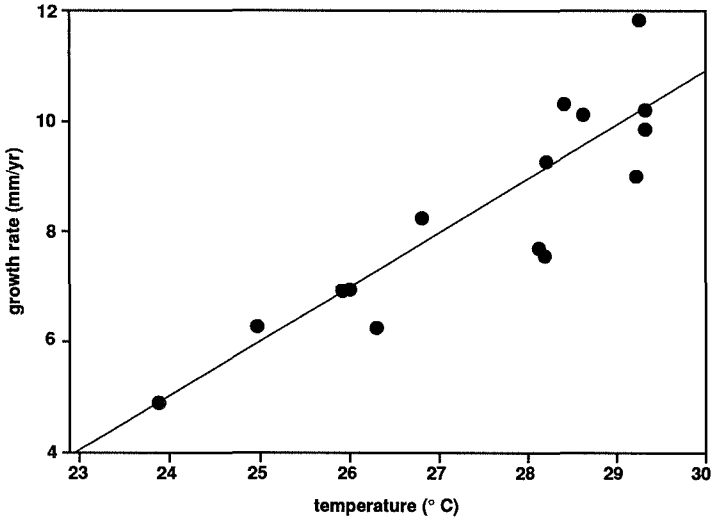

Figure 5. Relation between the average sea-water temperature and growth rate of the Indo-Pacific reef-building coral *Platygyra sp.* (data from Weber and White, 1974).

Weber and White (1974) investigated the influence of variations in temperature and solar radiation for different geographical locations on the growth rate of corals. Their data for the Indo-Pacific scleractinian coral *Platygyra sp.* indicate that reduced water temperature cause a reduction of coral growth rates (Fig. 5). They found no relation between changes

in solar radiation and coral growth rates. Variations in solar radiation seem to be subordinate to temperature in determining the latitudinal variation of coral growth. In the Hawaiian chain of islands the northern treshold for coral reef formation lies at 29° N (Kure Atoll). Grigg (1982) has described the variation of reef and coral growth along this chain towards the treshold for atoll formation which he termed 'the Darwin point'. The decrease of coral growth rates towards this northern limit for coral reef development is shown in Figure 6 .

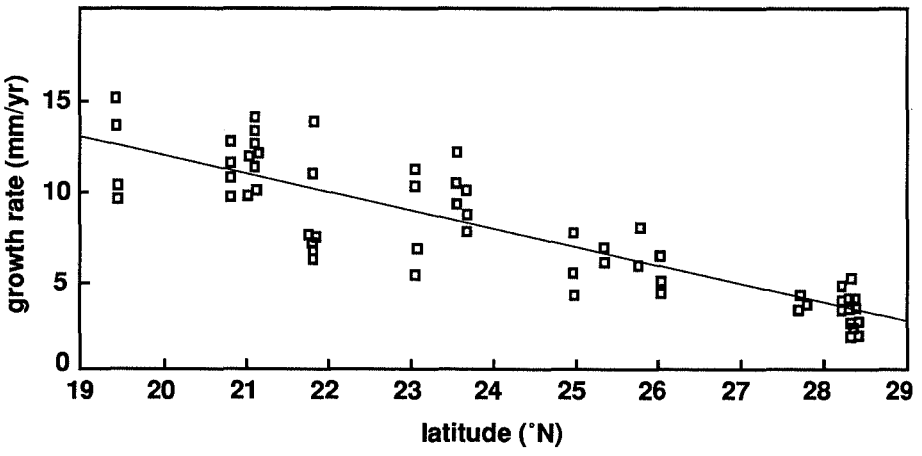

Figure 6. Decrease of coral growth rates along the Hawaiian Archipelago towards the northern treshold (Darwin point) of coral reef growth at 29° N (Kure Atoll) (after Grigg, 1982)

Salinity

Coral reefs flourish best at salinities from 34-36‰ The average salinity of oceanic waters is 35‰ (Sverdrup et al., 1942). Corals can tolerate salinities from 27 to 37‰ for a short period of time. They can also adapt to permanent levels of high salinity and shift their tolerance range upwards. In the Red Sea and the Arabian Gulf corals grow at salinities well over 40‰ (Coles and Jokiel, 1978). Increased salinity in the Mediterranean during the late Messinian resulted in reefs entirely dominated by *Porites sp.* and the eventual disappearance of coral reefs from this part of the world. Also today *Porites sp.* is one of the coral species that is best adapted to salinity changes (Kinsman, 1964).

Nutrients

Because the coral/alga symbiosis is largely autotrophic coral reefs are not directly limited by the nutrient load of the water. Corals get most of their energy requirements through their symbionts and only have to feed themselves in order to obtain necessary nutrients such as nitrogen (Dubinsky, 1992). Healthy coral reefs only occur in oligotrophic waters. An increase in the nutrient load of the waters will lead to the demise of the coral reef.

Other more opportunistic organisms such as certain algae, sponges and soft corals will smother coral growth. This can be illustrated by the example of Kaneohe Bay in Hawaii. Major sewage outfall caused eutrophication of the bay waters and the once flourishing coral reef community became smothered by algae and coral cover and diversity declined dramatically. Diversion of the sewage outfall to the open ocean has resulted in an amazing recovery of the reef community. Five years after cessation of sewage discharge live coral cover had nearly doubled while the algal cover was reduced by as much as 75% (Maragos et al., 1985).

It has been suggested that also in the geologic history the demise of coral reefs and carbonate platforms can be attributed to increased amounts of nutrients (Hallock and Schlager, 1986). This would imply that throughout the geologic record coral reefs were adapted to oligotrophic waters through algal symbiosis (Cowen, 1988).

Wave energy

The influence of wave energy on coral reefs is best illustrated by reef zonation. Geister (1977) described the zonation of Caribbean coral reefs and showed that wave energy exerted a major control on the observed zonation pattern. With increasing wave energy, i.e. with decreasing depth, the following zones could be observed: mixed coral zone (*Porites/ Montastrea annularis* head coral assemblage), *Acropora cervicornis* zone (fragile branching), *Acropora palmata* zone (robust branching) and *Millepora*/encrusting corraline algae zone. In the Pacific with its much larger number of coral species, zonation patterns are more complicated. The general zonation characteristics of Pacific coral reefs are similar to those described for the Caribbean (Chappel, 1980). In the high wave energy zone encrusting growth forms dominate (algal pavement). With decreasing wave energy these are replaced by robust branching corals, fragile branching and massive head corals, respectively.

The zonation patterns described above are derived from windward margins. On leeward margins which are protected from high wave energy the encrusting and robust branching forms are generally absent. In these more protected environments the ability to cope with high sedimentation rates becomes more important, favouring fragile branching forms such as *A. cervicornis* or staghorn coral. The fact that the high energy zones of the reef front are often occupied by branching corals instead of masssive head corals probably results from their better ability to shed sediment that is resuspended by wave action and their reduced, more streamlined, surface. Severe storms may often largely destroy these branching corals and turn them into rubble. The *A. palmata* zone on Jamaican reefs, for example, was completely destroyed by Hurricane Allen in 1980 (Woodley et al., 1981). Their high growth rate of over 100 mm/yr and rapid regeneration capacity allow them to grow back very fast and outgrow their competitors. Much of the observed zonation patterns occur within the upper 10 - 20 m of the water column, i.e.within the zone of light saturation. The difference depth ranges of leeward and windward zonation patterns suggest wave energy, and not light, exerts the major control on shallow reef zonation. It has to be noted that wave energy is not the only control on reef zonation. The infuence of light on reef zonation will be discussed below. Another important role of wave action is the constant renewal of the waters overlying the reef and providing the reef organisms with the necessary nutrients (Patterson et al., 1991).

Sediment resuspension and turbidity

The resuspension of bottom sediments as a result of wave action and increased turbidity will result in reduced water transparency. The influence of water transparency on coral.growth will be discussed in the next section. Another negative effect of sediment resuspension is the settling of sediment particles on the surface of a coral colony. Most corals will try to remove this sediment by tentacular movements and excretion of mucus. The energy costs of this are very high and are at the expense of coral growth. The influence of sediment resuspension on the growth rate of *M. annularis* is illustrated in Figure 7. In this example increased sedimentation has lead to a nearly 100% decrease in growth rates.

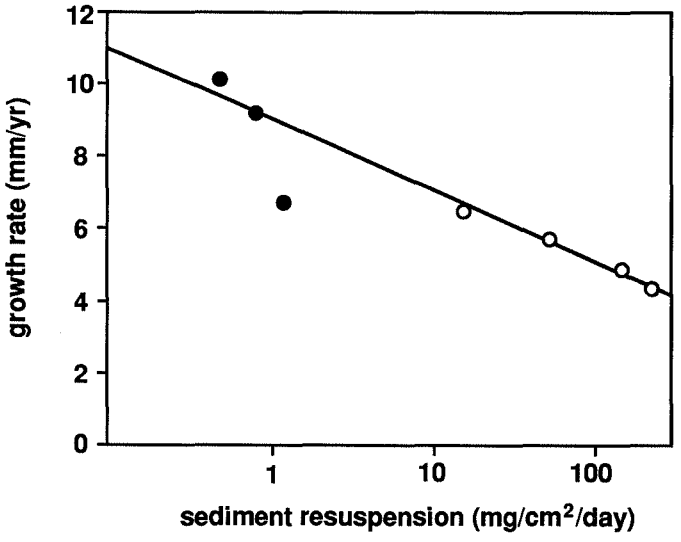

Figure 7. Decrease of growth rate of *Montastrea annularis* as a result of increased sediment resuspension (open circles: Costa Rica; filled circles: Jamaica). Data from Cortés and Risk (1985), and Aller and Dodge (1974).

Light

Each second the sun emits $2x10^{45}$ photons of which approximately $2x10^{35}$ enter the ocean (Tett, 1990). As the radiation penetrates the water, it is absorbed rapidly in the upper layers of the ocean. The depth at which the light intensity has been reduced to 1% of the surface light level (lower limit of the euphotic zone; Jerlov, 1976) varies roughly from 30 to 150 m for different oceanic water types (Jerlov, 1976; Kirk, 1983). The biologic definition of the euphotic zone, i.e. the depth at which respiration and photosynthesis in the water

column are in equilibrium roughly coincides with the 1% surface light level. Due to selective absorption of sea water the light spectrum also changes. Red and ultraviolet wavelengths are readily absorbed within the first few meters. Clear ocean water is most transparent to the bluegreen region of the spectrum. Only bluegreen light, with a maximum wavelength of ca. 470 nm can penetrate to appreciable depths. The most important fraction of the light spectrum for photosynthesis is that with wavelengths of ca. 400-700 nm. This is generally referred to as Photosynthetically Active Radiation (PAR). A quantitative assessment of light energy for biological processes involves the measurement of quanta, a measure of the number of photons of a particular wavelength.

The extinction of light in the water column follows an exponential function known as the Beer-Lambert law:

$$I_z = I_0 \, e^{-kz},$$

where I_z = light intensity at depth z; I_0 = light intensity at the surface; k = light extinction coefficient (Figs. 8 and 9). If light intensity is plotted versus depth on a semi-log scale a straight line is produced. The slope of this line is defined by the light extinction coefficient (k).

The light extinction coefficient for PAR can be used to characterize the transparency with respect to PAR for oceanic water bodies. A k-value of 0.035 m^{-1} is characteristic of clear ocean waters while more turbid coastal waters can exhibit values of 0.2 m^{-1} to 1.0 m^{-1} or more (Jerlov, 1976; Kirk, 1983).

Light and coral growth

The effects of light (irradiance) on coral growth have most frequently been studied with regard to photosynthesis. The relation between coral photosynthesis and irradiance can be described with so-called P vs. I, or light-saturation curves. These show the photosynthetic activity, either as oxygen production or as carbon uptake, versus the intensity of Photosynthetically Active Radiation. These light saturation curves for corals have a very characteristic shape. Chalker (1981) has shown that the best function to describe these curves is the hyperbolic tangent. An example of an idealized light saturation curve for corals is shown in Figure 8. Initially photosynthesis increases proportional to the increasing light intensity. At higher light intensities the increase in photosynthesis decreases gradually until it reaches a horizontal assymptote that is defined by the maximum photosynthetic performance of the coral/alga symbiosis. The intercept between the initial slope of the curve (α) and the horizontal assymptote defines the light saturation point (I_k). Photoinhibition of growth, sometimes observed in other marine organisms, does not occur in corals.

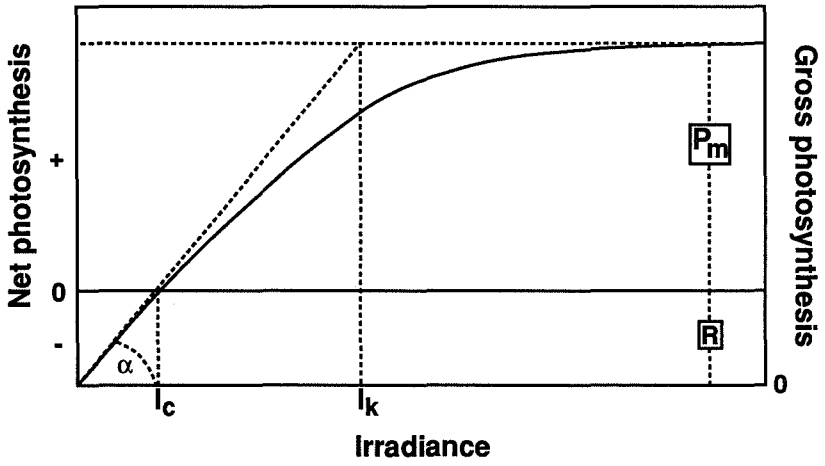

Figure 8. Idealized light-saturation curve for coral photosynthesis (after Chalker et al., 1988). For explanation see text.

Light enhancement of calcification in corals is evident but the exact way in which photosynthesis controls calcification is still poorly understood (Rinkevich and Loya, 1984). Calcification rates increase with photosynthetic rates and show a similar reponse to changes in light intensity. Corals appear to have their own calcification mechanism which is assisted by the photosynthetic activity of their symbionts. During the night, calcification by corals continues but these dark calcification rates are much lower than those during the day (dark/light 1:3; Chalker et al., 1988). Corals without symbionts are also known to build carbonate skeletons, although at much lower rates. In general calcification rates of hermatypic scleractinians behave in a similar fashion as their photosynthetic rates (Chalker et al., 1988). Szmant et al. (1992) have shown that calcification and photosynthesis of *Montastrea annularis* are indeed linearly correlated.

Most corals have adapted in one way or another to deal with different light conditions. Species that have hemispherical growth forms in shallow water often develop more plate-like growth to improve light capture and increase the surface to volume ratio (Dustan, 1975). The deeper zones of coral reefs are dominated by platy or sheet-like corals. Corals can optimize the light utilization of the zooxanthellae through an increase of photosynthetic pigments (Dustan, 1982) and increased carbon fixation (Battey and Porter, 1988). Photoadaptive trends that have been observed in coral photosynthesis include an increase of the initial slope (α) of P vs. I curves, decreased light saturation (I_k) and compensation light intensity (I_c), and reduced respiration rates. Because the maximum photosynthetic rate (normalized to chlorophyll-a content) remains constant this leads to increasing Photosynthesis/Respiration (P/R) ratios with increasing depth (Chalker et al., 1988).

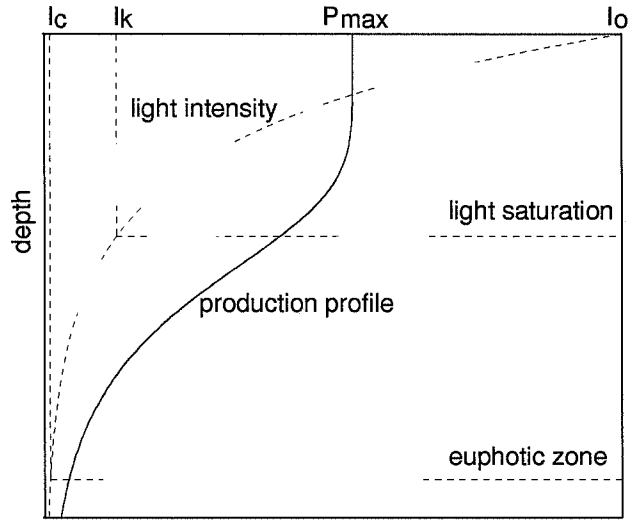

Figure 9. Schematic diagram of the relation between light, depth, and photosynthesis (from Bosscher and Schlager, 1992a)

Depth limits of coral growth

The energy requirements for sustained coral growth (i.e. light) limits the vertical distribution of corals in the water column. By definition the depth at which photosynthesis and respiration are in equilibrium will be the maximum depth for sustained coral growth. This means that growth of hermatypic corals is restricted to the euphotic zone. As the depth of the euphotic zone changes with the water transparency, the depth distribution of corals also varies with geographical location. Figures 10 and 11 show a compilation of the depth distribution of reef-building scleractinians for reef locations throughout the world's oceans. It should be noted that active coral growth is different from active reef-building by corals. The depth for high rates of reef growth is much shallower and, in many instances, close to the zone of light saturation. It is clear from Figures 10 and 11 that large geographical variations are present in depth limits of hermatypic scleractinians. The average depth limit for coral growth in the Caribbean ranges from 90-100 m. Abundant coral growth occurs here to a depth of ca. 50 m. In the Indo-Pacific variations are much larger. Depth limits in the oligotrophic gyres of the Pacific are around 140 m. Such euphotic depths correspond to a k of 0.035 m^{-1}. Indepent oceanographic estimates of light extinction values agree with the observed depth ranges of reef-building corals (Gundersen et al., 1976; Kirk, 1983). Areas with large terrigenous run-off and thus reduced water transparency show reduced depth ranges for coral growth (e.g. SE Asia). The depth of the euphotic zone in oceanic waters that overlie coral reefs ranges roughly from 30 to 150 m.

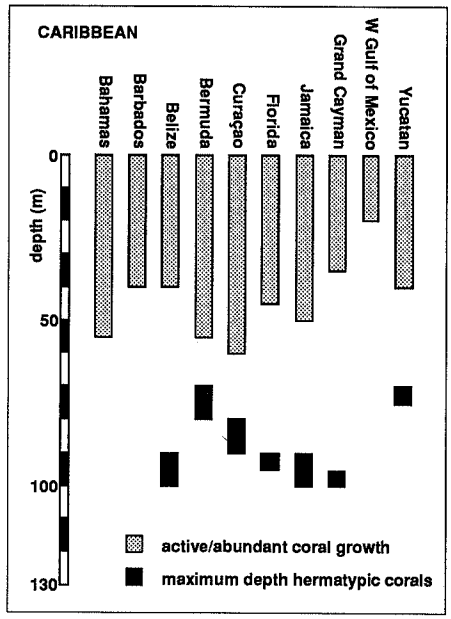

Figure 10. Depth distribution of reef-building corals in the Caribbean (compiled from: Bak, 1974; James and Ginsburg, 1979; Fricke and Meisschner, 1985; Reed, 1985; Liddel and Ohlhorst, 1988; Acevedo et al., 1989; and other sources).

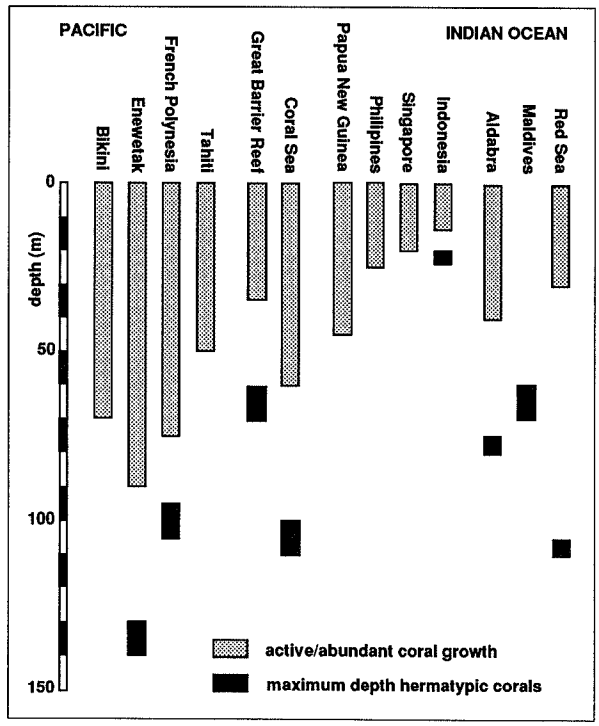

Figure 11. Depth distribution of Indo-Pacific reef-building corals (compiled from: Davies, 1977; James and Ginsburg, 1979; Harmelin-Vivien, 1985; Sarano and Pichon, 1988; and other sources sources)

Other reef organisms

Of course corals are not the only organisms in the reef ecosystem, but they are by far the most important in terms of primary and carbonate production, area and biomass. Most of the carbonate produced on coral reefs is coral skeleton. Hubbard et al. (1990) have shown that over 85% of the carbonate produced by a coral reef is derived from coral calcification. Other major sediment producers include red and green algae and, to a minor extent, foraminifera and molluscs. But like scleractinian corals, the algae and many foraminifera depend on light for photosynthesis. Their depth distribution may, therefore, be expected to follow similar trends as the depth distribution of corals. Figure 12 shows the depth limits of scleractinian corals combined with the depth limits of another major sediment producer the green alga *Halimeda*. This alga has segmented branches that consist of aragonite. In Figure12 it is shown that the depth limits of both groups of organisms are nearly identical. *Halimeda* usually persists to somewhat greater depths. For example in the very clear water surrounding Pacific atolls *Halimeda* have been observed to depths of ca. 145 m similar to the 140 m depth limit for hermatypic scleractinians. The depth limit for *Halimeda* in the Caribbean is 100-110 m compared to a depth limit for hermatypic corals of 90-100 m.

The typical depth limit for abundant coralline algae in the tropics is about 80 m, while below 100 m they occur only rarely (Adey, 1986)

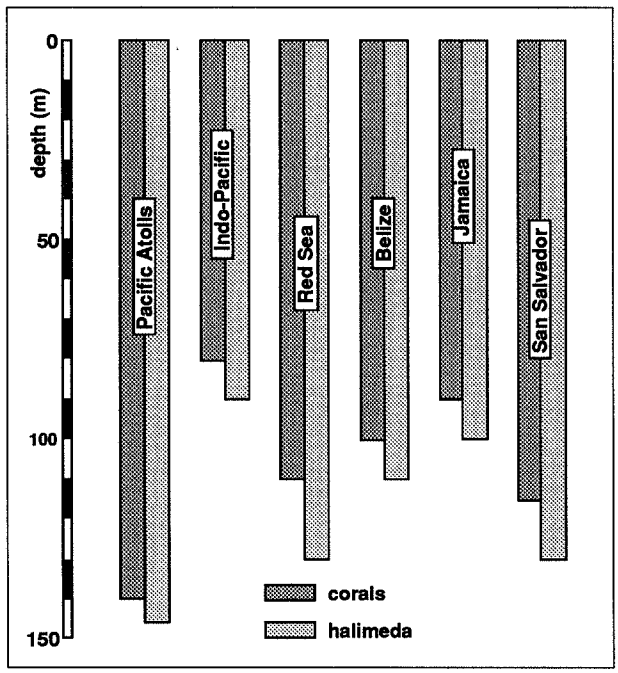

Figure 12. Depth limits of hermatypic scleractinian corals and the green alga *Halimeda* (compiled from: James and Ginsburg (1979); Hillis-Collinvaux, 1985; and other sources).

Recent corals and growth potential

Reef-building organisms have been a major building block of carbonate platforms throughout the geologic record. The controls on reef and platform development are therefore strongly linked to the controls on the growth of these organisms. To understand the role of various factors that controlled Phanerozoic reef development and determined the growth potential of reefs and platforms it is necessary to first understand the various controls on modern coral growth. All important environmental parameters can be directly measured and the interaction between coral growth and its controls can be evaluated. Extrapolation of these findings back into the geologic record will help to recognize the controls on coral reef and carbonate platform development.

Chapter 2

DEPTH RELATED CHANGES IN THE GROWTH RATE OF *MONTASTREA ANNULARIS*

Abstract

Growth rates of massive colonies of *Montastrea annularis* from Curaçao, Netherlands Antilles, were related to light extinction profiles to evaluate the role of light in growth. The observed decrease of growth rate with depth was related to the exponential decrease in light by a photosynthetic hyperbolic tangent function. Growth was light-saturated to a depth of 15 m. Saturated rates were in the range of 8 to 16 mm/yr. Growth rates rapidly decreased below 15 m to values of 2 to 3 mm/yr at 30 m. Our data, in conjunction with other examples from the Caribbean, suggest that light has a dominant control on the decreasing growth rates of the most important Caribbean reef-building coral *M. annularis*.

INTRODUCTION

Light has long been recognized as the primary environmental factor controlling growth of reef-building corals (Vaughan, 1919). Light-enhanced calcification is responsible for most of the skeletal growth of reef-building corals (Goreau, 1959; Chalker et al., 1988).

Several authors have shown that the growth (vertical linear extension) of the main Caribbean reef-building coral *Montastrea annularis* (Ellis & Solander) exhibits a pattern of decreasing rates with depth (Baker and Weber , 1975; Dustan, 1975; Hubbard and Scaturo, 1985; Huston, 1985). It is suggested by these authors that the decrease in light is in part responsible for this pattern. Similar patterns of decreasing growth rates with depth are observed for other species, for example, the Pacific reef-building coral *Porites lutea* (Buddemeier et al., 1974; Highsmith, 1979).

Here we provide a mathematical description of the relationship between depth and growth rate. Decrease in Photosynthetically Active Radiation (PAR) causes reduced photosynthesis by reef-building corals following so-called light-saturation curves (Barnes and Taylor, 1973; Chalker, 1981). If reduced light levels and consequently reduced rates of coral/symbiont photosynthesis are responsible for the reduction of growth rates at greater depths, these rates might be expected to follow light-saturation curves similar to those for photosynthesis. We fitted growth and light data to a hyperbolic tangent function to obtain a light-response curve for growth rates. In combination with the exponential decrease of light with increased water depth it is then possible to describe the decrease of growth rate with depth.

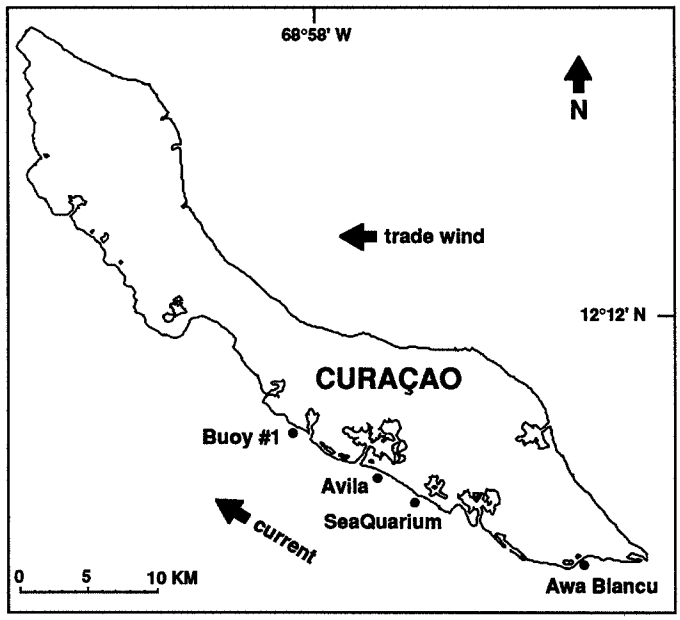

Figure 2.1. Schematic map of Curaçao, Netherlands Antilles, showing sample locations. Main wind and current directions are indicated.

MATERIALS AND METHODS

Core samples were taken in October 1990 and July and August 1991 at three localities on the leeward fringing reefs of Curaçao, Netherlands Antilles (Fig. 2.1). Here a gently sloping submarine terrace stretches ca. 100 m from the coast to the drop-off at a depth of 10 to 12 m, from where the reef slopes steeply to a depth of 50 to 60 m (Bak, 1977; Focke, 1978). Only massive growth forms of *Montastrea annularis* were sampled. Although colonies tend to become flattened with increasing depth, platy, columnar and other growth forms were avoided.

We extracted cores from colonies using a small hand-held pneumatic drill, connected to a SCUBA tank, and a 25 cm long diamond-tipped core barrel with an internal diameter of 25 mm. The cores were sawn into 4 to 6 mm thick slabs. Slabs were X-rayed for 2-3 minutes at 60 KeV and 3 mA to display annual density banding (Knutson et al., 1972; Hudson et al., 1976). Growth rates were measured from X-ray positive prints along the major (vertical) growth axis. Growth rate is given as the average width of the annual bands. The number of bands measured per colony ranges from 5 to 10, depending on the quality of the banding, core length and colony growth rate. Light was measured with an IL 1400A Radiometer/Photometer (International Light) using a cosine corrected, underwater sensor as Photosynthetically Active Radiation (PAR: wavelength 400 - 700 nm) and is given here in $\mu E\ m^{-2}\ s^{-1}$ ($1\mu E\ m^{-2}\ s^{-1}$ is ca. $0.435\ W\ m^{-2}$). Measurements were carried out using SCUBA gear. Light extinction profiles were measured several times for each locality for different weather conditions and times of day, in July and August 1991. Individual measurements were integrated over 60 seconds at each depth. Daily radiation measurements were obtained from the Curaçao Meteorologic Survey at Hato Airport.

Light extinction coefficients were calculated by exponential regression of the depth profiles. On a semi-log scale, light extinction values produced a straight line. The slope of this line represents the light extinction coefficient (k).

RESULTS

Growth rates of *Montastrea annularis* in this study ranged from 8 - 16 mm/yr in the shallow part of the reef, and from there decreased rapidly to 2 mm/yr for the deepest colony (31.8 m; Fig. 2.2). The rates for shallow-water colonies are similar to those reported for individual colonies from St. Croix, 6 - 14 mm/yr (Dodge and Brass, 1984). Average growth rates reported for other localities in the Caribbean are shown in Figure 2.3.

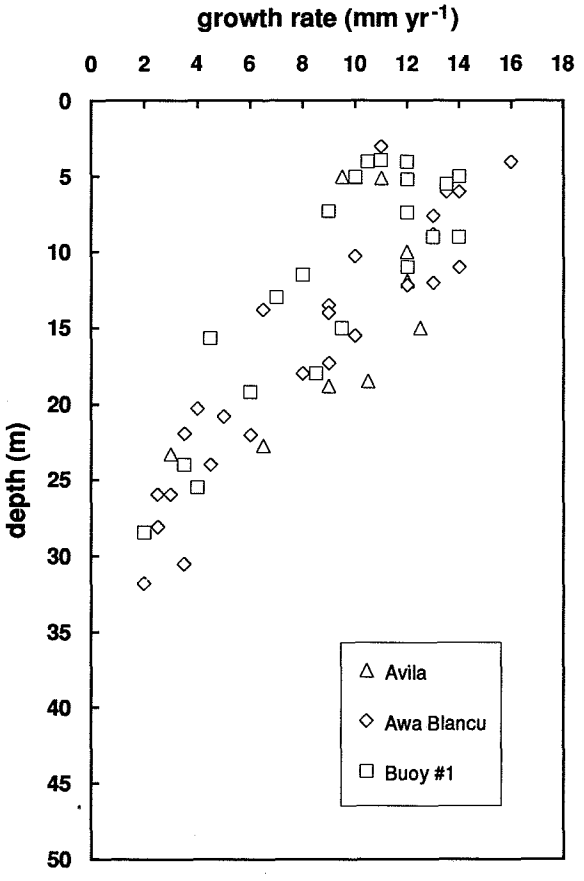

Figure 2.2. Growth rates of *Montastrea annularis* versus water depth for Curaçao, (n = 57).

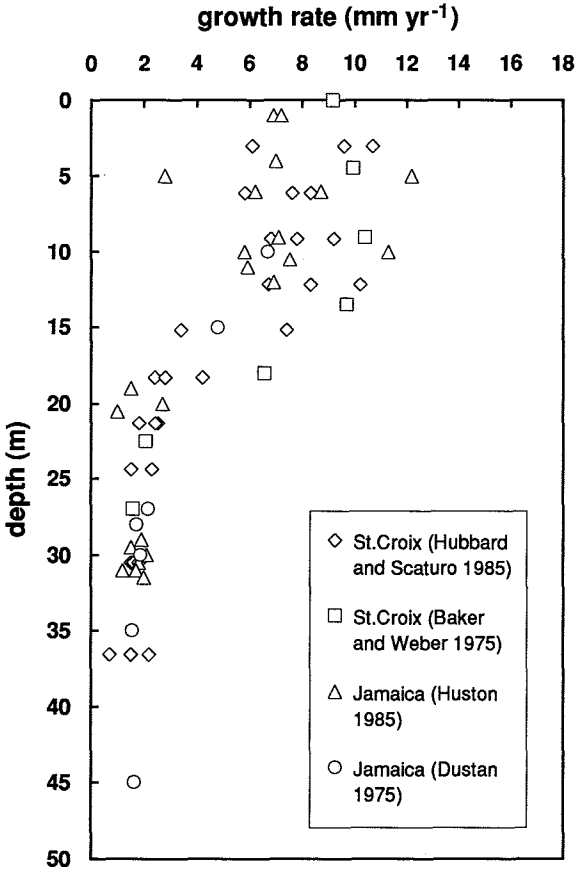

Figure 2.3. Growth rates of *Montastrea annularis* versus water depth for Jamaica and St. Croix, USVI (n = 66).

The average light extinction coefficient for the Curaçao reef waters was -0.115 m^{-1} (Fig. 2.4). We did not observe significant variations in the light extinction coefficient for different weather conditions during the sampling period. Light extinction values reported here are similar to those reported by Van den Hoek et al. (1978) for September and October (start of the wet season on Curaçao). Noon surface light values during the sampling period varied from 1500 to 2700 mE $m^{-2} s^{-1}$ depending on weather conditions. The monthly average maximum solar radiation around solar noon was ca. 2000 mE m^{-2} s^{-1} (Fig. 2.5). These light conditions are similar to those reported for Jamaica (Porter, 1985). Light extinction coefficients for oceanic waters typically range from 0.04 to 0.16 m^{-1} (Jerlov, 1976).

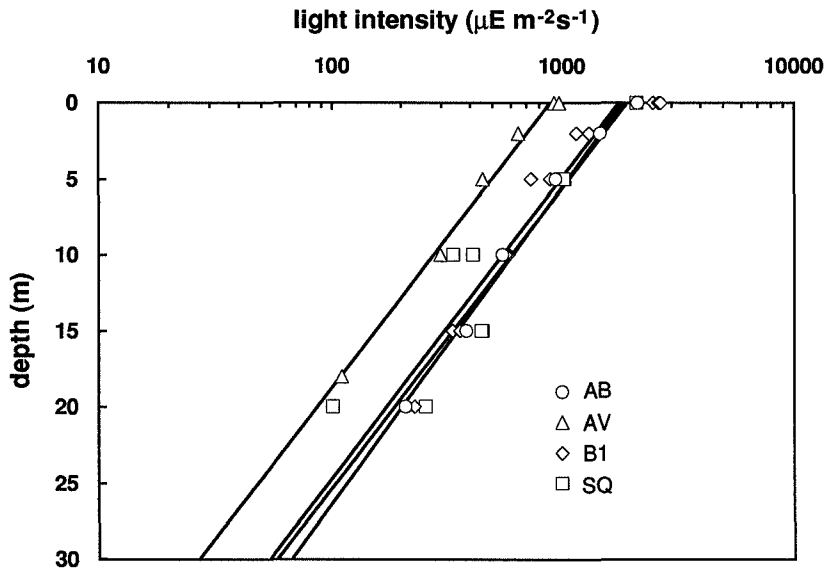

Figure 2.4. Light extinction profiles for different localities on the leeward fringing reef of Curaçao. Profiles for Buoy #1 (B1:k=-0.117 m^{-1}), Awa Blancu (AB:k=-0.111 m^{-1}) and SeaQuarium (SQ:k=-0.116 m^{-1}) were measured around local solar noon. The profile for Avila (AV:k=-0.117 m^{-1}) was taken at 16.30 h. Each data point represents three individual measurements on a specific day. Profiles are representative of the entire sampling period. Extinction coefficients were calculated by exponential regression.

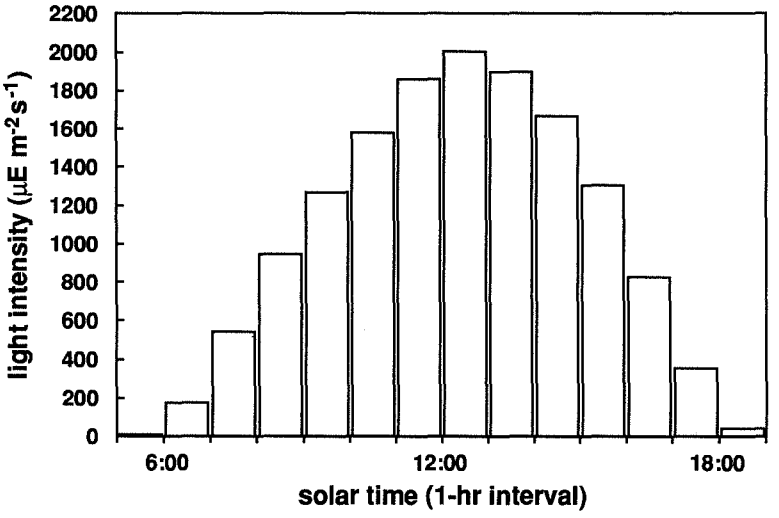

Figure 2.5. Average daily variation of solar radiation for July 1991 at Hato Airport, Curaçao (dat from Curaçao Meteorological Survey).

Chalker (1981) demonstrated that a hyperbolic tangent function can be used successfully in simulating light-saturation curves for gross photosynthesis and calcification by reef-building corals:

$$P = P_{max} \tanh (I/I_k) \quad \text{(Chalker, 1981),}$$

where P = gross photosynthetic rate, P_{max} = maximum photosynthetic rate, I = light intensity, and I_k = saturating light intensity. Initially, photosynthesis increases linearly with increasing light intensity until a horizontal assymptote is reached. The light intensity at which the initial slope of the curve intercepts the horizontal assymptote is the light-saturation intensity (I_k). The maximum photosynthetic rate, P_{max} , defines the horizontal assymptote (see also Fig. 8 in introduction to part I).

Photosynthesis and calcification follow similar light-saturation curves (Chalker, 1981). Because light-enhanced calcification and linear growth rate are proportional (Chalker et al., 1988), we replaced P (photosynthetic rate) by G (growth rate). The light-saturation curve for the growth rate of *M. annularis* colonies was then obtained by fitting the light and growth rate data to the hyperbolic tangent function, using a least-squares method (Fig. 2.6).

This resulted in the following function: $G = 12.15 \tanh (I/351.6)$,

where G is the growth rate (mm/yr), and I the light intensity ($\mu E\ m^{-2}\ s^{-1}$) obtained from the light extinction profiles (Fig. 2.4). The maximum growth rate of 12.15 mm/yr and the light saturation intensity (I_k) of 351.6 $\mu E\ m^{-2}\ s^{-1}$ are calculated by the curve-fitting program. Statistical results of this regression are given in Table 2.1.

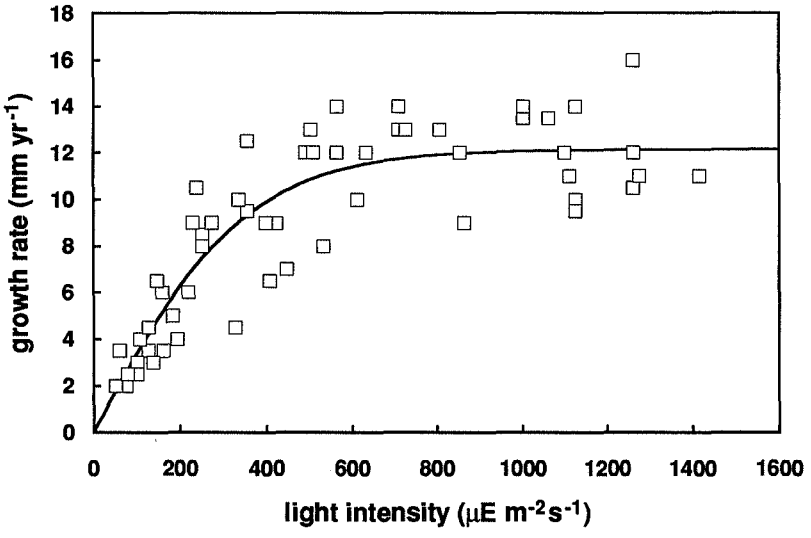

Figure 2.6. Growth rate of *Montastrea annularis* versus light intensity. Data fitted to photosynthetic function: $G = G_{max} \tanh(I/I_k)$ (for explanation see text). This resulted in the following values: $G_{max} = 12.15$ mm/yr, $I_k = 351.6\ \mu E\ m^{-2}\ s^{-1}$ ($R^2 = 0.97$).

Table 2.1. One-way Analysis Of Variance.

Source	SS	df	MS	F
Model	5205.6	2	2602.8	768.9 ($p<0.0001$)
Residual	186.7	55	3,4	
Total	5392.3	57		

By converting the light intensities from Figure 2.6 to depth using the exponential decrease of light in water, we obtain a function for the decrease of growth rate with depth:

$$G_z = 12.15 \tanh ((I_0 e^{-kz})/351.6),$$

where G_z is the growth rate at depth z, I_0 the surface light intensity (2000 $\mu E\ m^{-2}\ s^{-1}$), and k the light extinction coefficient (-0.115 m^{-1}). The predicted curve closely follows the observed decrease of *M. annularis* growth rates with depth (Fig. 2.7). The correlation coefficient between the predicted curve and the actual data was $R^2 = 0.97$.

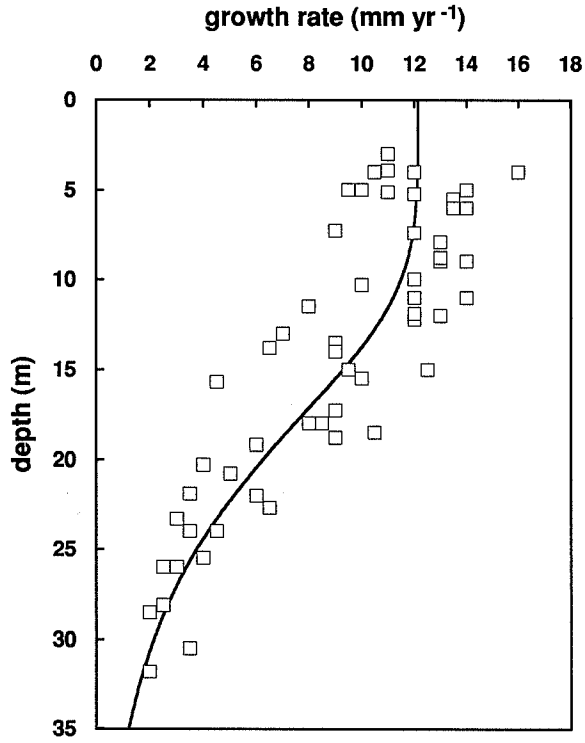

Figure 2.7. Observed and predicted decrease of growth rate for *Montastrea annularis* from Curaçao, based on data from Figure 2.6.

DISCUSSION

The relation between light and coral growth has long been acknowledged (Vaughan, 1919; Goreau, 1959; Chalker et al., 1988). Our findings confirm the importance of light to the growth rate of *Montastrea annularis*. Photoadaption might have been expected to obscure the observed relationship between light and growth rate (Chalker et al., 1988). Light-adaptive strategies to increase light utilization with increasing depth have been reported for *M. annularis* (Dustan, 1982; Wyman et al., 1987). Our results suggest that photoadaption does not have a significant influence on growth rate. Part of this discrepancy may arise from the increased skeletal density of deeper colonies (Baker and Weber, 1975; Dodge and Brass, 1984; Hughes, 1987). The photosynthetic gain from photoadation seems to go towards a denser skeleton rather than increased vertical growth rate. Light-adaptive strategies may, however, be responsible for growth rates deeper than 30 m being somewhat higher than predicted. Deep growth rates remain relatively constant to a depth of ca. 50 m (Fig. 2.3). The latter effect may be a result of increased heterotrophy. Muscatine et al. (1989) show that specimens of *M. annularis* at depths of 30 and 50 m indeed draw significantly on allochtonous sources of carbon.

Caribbean

The depth for light saturation in *Montastrea annularis* from Curaçao is 15.1 m (based on I_k=351.6 μE m-2 s-1). This depth is similar to the depth of 18 m reported as the critical depth that divides shallow and deep populations of *M. annularis* at St. Croix (no data between 13.5 and 18 m; Baker and Weber, 1975). Hubbard and Scaturo (1985) give a depth range of 12 to 18 m for the "curious" drop in growth rates at St. Croix. For Jamaica, Dustan (1975) reported a depth of 15 m.

The pattern of decreasing growth rate of *M. annularis*, observed by the above mentioned authors (Fig. 2.3) is similar to that reported here for *M. annularis* from Curaçao. The correspondance between light-saturation depths and overall trend of decreasing growth rate with depth, for various localities throughout the Caribbean suggests light, rather than local environmental factors, to be the most important control on the growth rate of *M. annularis*.

Other environmental controls

We should consider, however, other environmental factors that may influence the growth rate of corals and contribute to the observed relationship between depth and growth rate. Temperature, water motion, sediment resuspension and other factors can be expected to affect coral growth rates and vary with depth. We will here discuss briefly the possible effects of some of these factors.

Curaçao reef waters are isothermal over the studied depth-interval. Oxygen isotopic composition of the samples used in this study does not show a temperature effect (chapter 4). Jamaica reef waters are, likewise, isothermal in the upper 50 m of the water column (Fairbanks and Dodge, 1979). We can thus assume that temperature plays no role in the observed relationship between depth and growth rate.

Water motion and sediment resuspension are predominant in the shallow reef within the zone of wave action. Sediment resuspension has been shown to decrease the growth rate of *Montatrea annularis* (Cortés and Risk, 1985). This is, however, opposite to the trend observed here, where shallow growth rates are higher than growth rates well below wavebase. Water motion has been shown to also influence metabolic rates of *M. annularis* (Patterson et al., 1991). It has, however, only a minor effect on the net production of the coral (Patterson et al., 1991). The effect of sediment resuspension and water motion, if any, may be reflected in the increased variation in shallow growth rates as opposed to deep growth rates (Fig. 2.7). But most important, none of the discussed parameteres can be expected to change exponentially with depth but rather abruptly at wavebase. We assume, therefore, that these factors do not significantly contribute to the observed decrease of growth rate of *M. annularis* with depth.

Decreasing growth rates with depth are found in many photosynthetic reef organisms (Huston, 1985). The observed relationship between light and growth may therefore be a key factor in growth of the entire reef. Adey (1978) already stated that 15 m is a critical depth for reef initiation after the Holocene sea-level rise slowed. Below this light-saturation depth the growth rate of corals will become insufficient to cope with even slight sea-level variations. Bosscher and Schlager (1992) simulated Holocene reef growth based on the relationship between depth and growth rate reported here. Their results indicate that light may well be a key factor in the response of reef growth to changing sea level.

The decrease of growth rate of *M. annularis* with depth can be attributed almost entirely to the decrease in light (PAR). The observed sharp decrease in growth rates at 15 m probably reflects the lower limit of light saturation. Although other factors cannot be ruled out our data suggest that light is the dominant, if not only, control on the decrease of growth rate of *M. annularis* with depth.

Chapter 3

COMPUTERIZED TOMOGRAPHY AND SKELETAL DENSITY OF CORAL SKELETONS

Abstract

This paper describes and discusses the use of medical X-ray Computerized Tomography (CT) in the study of coral skeletons. CT generates X-ray images along freely chosen sections through the skeleton and offers the possibility of density measurements based on X-ray attenuation. This method has been applied to measure the skeletal density of the Caribbean reef-building coral *Montastrea annularis*, from Curaçao, Netherlands Antilles. The observed, non-linear, increase of skeletal density with depth can be attributed to decreasing photosynthetic rates with increasing water depth. A comparison with extension rate measurements shows the inverse relationship between extension rate and skeletal density. CT proves to be a quick and non-destructive method to reveal growth structures (density banding) and measure skeletal density.

INTRODUCTION

Conventional X-radiography has been a widely used technique in the study of coral skeletons for nearly twenty years. The deposition of annual pairs of high and low density bands in the coral skeleton has allowed detailed reconstruction of coral growth records (Knutson et al., 1972; Hudson et al., 1976). Measurements of coral skeletal densities have been made by various techniques: photodensitometry of X-radiographs (Dodge and Thompson, 1974; Buddemeier, 1974; Buddemeier et al., 1974; Baker and Weber, 1975; Dodge and Brass, 1984), displacement in water (Graus and Macintyre, 1982; Hughes, 1987) and mercury displacement (Dustan, 1975). Recently Chalker and Barnes (1990) described the use of gamma densitometry and reviewed several methods for measuring skeletal densities in corals.

Computerized tomography (CT), widely used in the medical world since its introduction in 1972 (Hounsfield, 1973), offers a 'conventional' X-ray image of the coral skeleton, combined with the possibility to measure skeletal densities based on X-ray attenuation. Outside the medical world applications of CT have been reported from various earth science disciplines, such as reservoir geology, sedimentology and paleontology (for reviews of applications see: Haubitz et al., 1988; Kenter, 1989). Dodge (1980) was the first to suggest the use of CT in the study of coral growth. CT scanning of corals has been reported by Kenter (1989) and Logan and Anderson (1991), who discussed the use of CT scan imagery to assess coral growth rates.

This paper deals with applications of Computerized Tomography to the study of coral skeletons. The methodology of CT is outlined briefly before discussing CT-scans, density calibration, density measurements of samples of the Caribbean reef-building coral *Montastrea annularis*, and some implications of these measurements.

MATERIALS AND METHODS

Coral samples

Coral samples were taken in October 1990 and July/August 1991 at three localities on the leeward fringing reef off Curaçao, Netherlands Antilles (Fig. 3.1). Here a gently sloping submarine terrace stretches ca. 100 m from the coast to the drop-off at a depth of 10 to 12 m, from where the reef slopes steeply to a depth of 50 to 60 m (Bak 1977). At each location coral cores were taken from 0 down to 30 m water depth at ca.2 m depth intervals. A small hand-held pneumatic drill was used, connected to a SCUBA tank, with a 25 cm long diamond-tipped core barrel with an internal diameter of 25 mm. Care was taken to sample only the massive growth form of *Montastrea annularis* (morphotype 2 of Knowlton et al. 1992). Cores were taken along the major (vertical) growth axis of each colony. From the obtained cores slabs of ca. 5 mm thickness were sawn and X-rayed for linear extension measurements. The results of these measurements and underwater light measurements used in this study are discussed elsewhere (chapter 2). The remaining part of the cores was used in this study (chapter 2).

Reference density standards were obtained by sawing rectangular blocks of coral using a precision rocksaw. The blocks had slightly varying dimensions (approximately 2x2x1.5 cm) and a volume of ca .5 cm^3. Coral blocks were sawn from *M. annularis* colonies from different depths and localities (Belize, Curaçao, and Florida). Blocks were accurately weighed and measured, using an analytical balance and a precision caliper. The bulk density of these blocks was estimated by simply dividing weight by volume. To obtain samples with a wider range of densities than the coral skeletons we used material taken from all coral specimens. This material was ground and powdered in an agate mortar and analytical cups (of known volume) were filled with different grainsize fractions. These cups were weighed and the bulk density was calculated. The difference between the dry bulk density and the density of aragonite (i.e. porosity) was used to convert dry into wet bulk density, using the following formula:

$$\rho_{wet} = \rho_{dry} + ((\rho_{ar} - \rho_{dry})/\rho_{ar}),$$

where ρ_{wet} = wet bulk density; ρ_{dry} = dry bulk density; ρ_{ar} = density of aragonite (2.94 g cm^{-3}).In total 25 density standards were used (15 blocks and 10 ground samples).

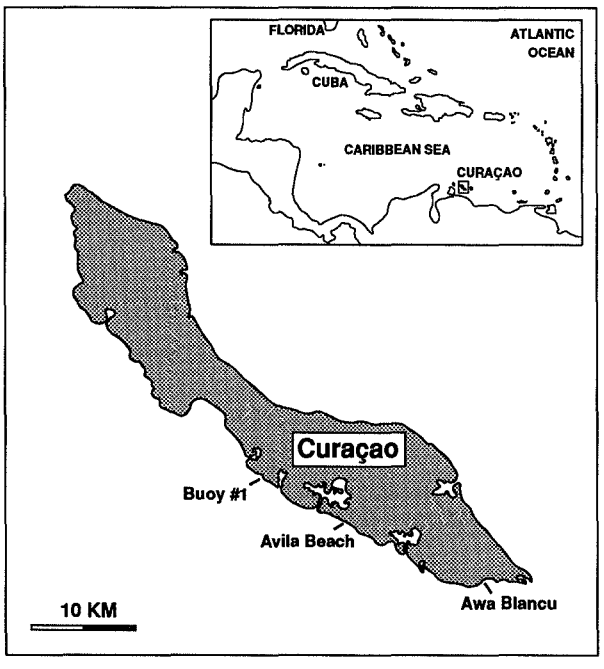

Figure 3.1. Schematic map of Curaçao, Netherlands Antilles, showing sample locations.

Computerized Tomography

A CT-scanner consists of a rotating collimated X-ray beam and an array of detectors. The basic quantity measured in CT is the linear attenuation coefficient m, as defined by:

$$I/I_0 = e^{-mx},$$

where I_0 = incident X-ray intensity; and I = attenuated X-ray intensity after passing through thickness x of an object with an attenuation coefficient m. The detectors obtain a series of one-dimensional projections of attenuation through an object at various angles. These projections are then computer-processed to construct a two-dimensional matrix of attenuation values of volume elements. The resulting picture or 'tomoscan' is displayed on a monitor, with the various attenuation values being represented by different grey values, similar to conventional X-radiographs. To construct a density profile, a line can be selected on the monitor along which a density profile will then be computed (Fig. 3.2a). Similarly, if an object is outlined on the monitor, a histogram, showing the density distribution within the outlined object, can be computed (Fig. 3.2b). If the object is slowly moved through the scanner, a three-dimensional matrix is generated, allowing reconstruction of cross-sections along any plane through the object.

To avoid image reconstruction artifacts caused by a large contrast in densities, all samples were scanned submerged in water. We waited several minutes for the water to fill all the pores. The few air bubbles that remained were easily removed by gently shaking the container with the samples. The presence of air in the samples could easily be detected using the density histograms that were conctructed for each sample. If water filled all the pore space CT density values should not be negative, i.e. below the density of water (see calibration section). Standard blocks were scanned submerged in water. The cups containing the ground standard samples were filled with water and then scanned. Only the relatively coarse samples (>120 m), in which water filled all the pore space, were used for calibration. Coral densities were measured by outlining the sample on the CT monitor to construct a CT density histogram (Fig. 3.2b). The thus obtained mean CT densities were then converted into mean skeletal densities in g cm^{-3} (see calibration section). Densities were measured for the entire length of each core. This means that we measured the average density for the last 7 to 11 years of growth of each colony, depending on length of the core and the extension rate of the colony. The error associated with the different time spans is assumed to be relatively minor.

All experiments were conducted using a Philips Tomoscan 350. Scanning time was 9.6 sec at 120 keV and 200mA. The scanned slice thickness was arbitrarily set at 2 mm.

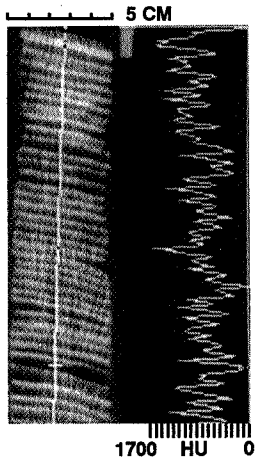

Figure 3.2a. Tomoscan of a core (4" diameter) of *Montastrea annularis* from Looe Key, Florida, to show yearly banding as revealed by CT-imagery (core provided by J.H.Hudson; uppermost high density (white) band = 1988). Density profile shown is constructed along the white line. Yearly density variation is very clear and can easily be related to the skeletal banding. The uppermost, anomalously thick, high density band, actually results from the blending of the 1987/1988 high density bands as a result of the 1987 'bleaching' event in the Caribbean. CT density scale shown below the scan converts into 0 to 2.93 g cm^{-3} (0 to 1700 HU).

Figure 3.2b. Tomoscan of coral samples of *Montastrea annularis* from Curaçao. Density characteristics of the outlined sample are shown to the left of the scan. Histogram of density distribution applies to sample A (outlined). Text and histogram are redrawn from original photograph.

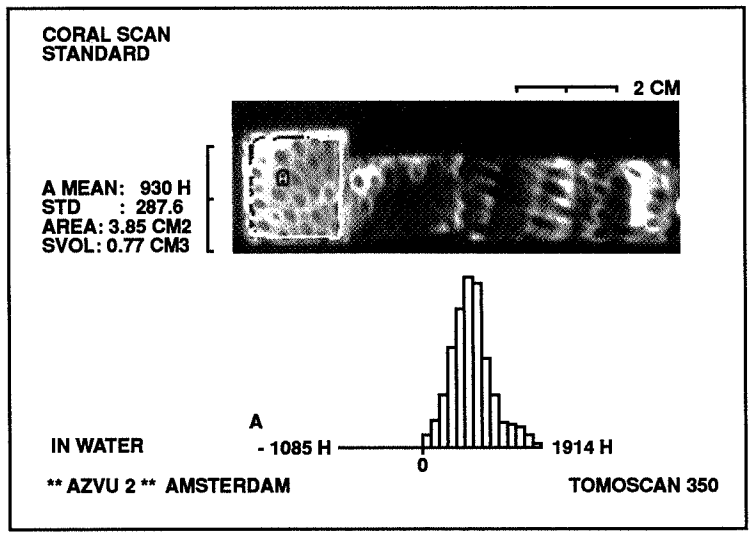

Calibration

The linear attenuation coefficient measured in CT is not in conventional units of cm^{-1}, but in a standardized CT scale known as Hounsfield units. CT scanners are calibrated internally to this scale. It is defined by setting the absorption of air at -1000, and that of water at 0. Attenuation is caused both by Compton scattering (dependent on electron density and predominant for energies above 100 keV) and photoelectric absorption (for energies well below 100 keV, dependent on the effective atomic number). For a constant chemical composition and energy levels used in medical CT-scanners Hounsfield units are linearly correlatable to bulk density. In addition to the internal calibration of the scanner, a set of coral aragonite standards was used to construct a calibration curve for coral skeletal densities. The linear conversion of CT densities into densities in g cm^{-3} (wet bulk density) is shown in Fig.3. The difference between the density of aragonite and the wet bulk density results from water filling pore space. If this difference is divided by the difference in density between aragonite and water, the weight and volume of water, and thus dry bulk density, can be calculated:

$$\rho_{dry} = \rho_{wet} - ((\rho_{ar}-\rho_{wet})/(\rho_{ar}-\rho_{water})),$$

where ρ_{dry} = dry bulk density; ρ_{wet} = wet bulk density; ρ_{water} = density of water (1 g cm^{-3}); ρ_{ar} = density of aragonite (2.94 g cm^{-3}). Reproducability of CT densities was within 5% for 15 samples that were scanned twice.

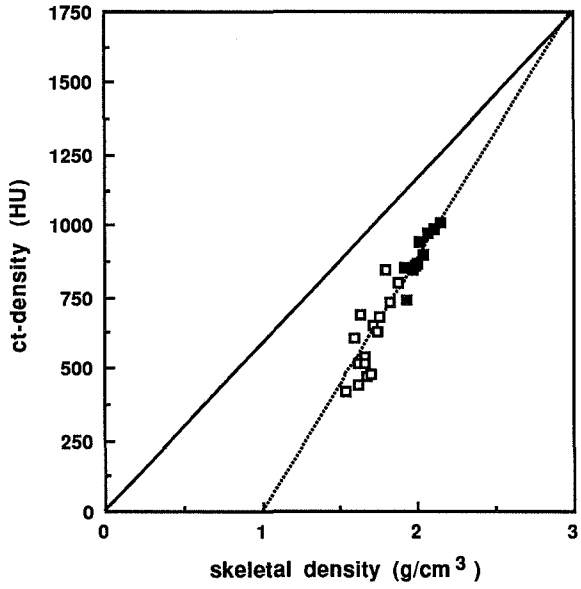

Figure 3.3. Calibration curve to convert CT - densities (in Hounsfield units) into wet bulk densities in g cm^{-3} (dotted line). Curve is defined by the X-ray attenuation of water (0 Hounsfield units and 1 g cm^{-3}) and 25 coral aragonite standards (regression equation y = (x-1) 881.2; R^2 = 0.99,p << 0.001). Open symbols: coral block density standards (n=15); filled symbols: ground coral samples (> 120 m; n = 10). Solid line is calibration curve for dry bulk density, based on formula given in materials and methods section.

RESULTS

The results of the density measurements are shown in Figure 3.4. The mean skeletal density for *Montastrea annularis* colonies from Curaçao ranges from 0.91 g cm^{-3} to 2.24 g cm^{-3}. Shallow colonies (0 - 15 m) show densities that range from 0.94 g cm^{-3} to 1.45 g cm^{-3}. Between a water depth of ca. 15 to 25 m the skeletal density increases to maximum values of 1.92 to 2.24 g cm^{-3} for colonies below 25 m. Rather than a linear increase, as suggested by previous authors (Baker and Weber, 1975; Graus and Macintyre, 1982), the observed increase shows a rather abrupt jump around 20 m. Densities for shallow colonies remain more or less constant to a depth of 15 m. From a water depth of 15 to 20 m density gradually increases and below 20 m rapidly reaches the highest values of up to 2.24 g cm^{-3}. No differences between localities were observed.

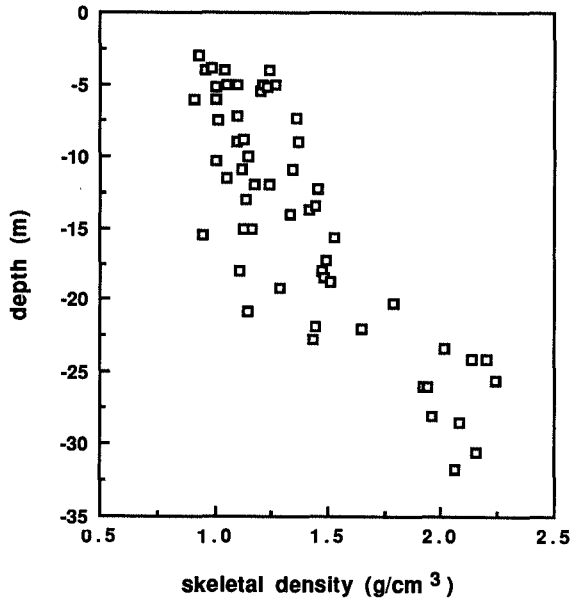

Figure 3.4. Mean skeletal density (dry bulk density) of *Montastrea annularis* versus water depth, based on CT - density measurements (n=57). CT - density data converted into g cm^{-3} using linear calibration of Figure 3.3.

DISCUSSION

Skeletal density

Table 3.1. Skeletal density of *Montastrea annularis*

location	depth (m)	density (g cm^{-3})	method	remarks	reference
St.Croix	0-27	1.57-2.17	photodensitometry	hemispherical/platy	
	0-13.5	1.57-1.79		hemispher./columnar	Baker and Weber, 1975
Jamaica	8-24	1.66-1.94	mercury displacement	hemispherical	Dustan, 1975
Belize	0-30	1.58-2.20	water displacement	hemispherical/platy	Graus and Macintyre, 1982
St.Croix	2.5-8	0.78-1.63	photodensitometry	columnar	Dodge and Brass, 1984
Jamaica	10-30	1.78-2.05	water displacement	foliaceous (platy)	Hughes, 1987
Curaçao	3-31.8	0.91-2.24	X-ray attenuation (CT)	hemispherical	this study

Table 3.1 gives skeletal densities for *Montastrea annularis* from various localities throughout the Caribbean. Nearly all studies report an increase of skeletal density with increasing depth. Data from Dustan (1975) form an exception, because no density/depth relation was observed. The reported skeletal densities fall more or less within the density range reported here (Table 3.1). There are however some striking differences between the various density ranges. Considering the variety of methods used this may not be surprising. The maximum density reported here for *M. annularis* from Curaçao was 2.24 g cm^{-3} which is comparable to the maximum values of 2.05, 2.17, and 2.2 g cm^{-3}, for corals from a similar depth range from Jamaica (Hughes, 1987), Belize (Graus and Macintyre 1982), and St. Croix (Baker and Weber, 1975) respectively (Table 3.1). The minimum values, however, do not compare equally well. Minimum densities reported for colonies from a water depth of 0 to 10 m range from 0.78 g cm^{-3} (Dodge and Brass, 1984) to values of 1.57 g cm^{-3} (Baker and Weber, 1975) and 1.58 g cm^{-3} (Graus and Macintyre, 1982). The minimum value of 0.91 g cm^{-3} reported here compares well with the data from Dodge and Brass (1984). But even if we consider that Baker and Weber (1975) reported average values for a number of colonies per depth, a minimum value of ca. 1.6 g cm^{-3} as reported by those authors as well as Graus and Macintyre (1982) does not agree with results reported here. Although these differences may be caused by environmental factors that vary between localities, a discussion of the various methods is appropriate.

The method used by Graus and Macintyre (1982) and Hughes (1987), where blocks of corals are weighed in water, suspended briefly from an analytical balance, is rather crude. It is almost impossible to submerge highly porous coral skeleton without water flowing in, at least part of, the skeleton if no precautions are taken to prevent this (Scoffin et al., 1992). This would lead to an overestimation of the skeletal density and could be the reason for the higher minimum density values reported by Graus and Macintyre (1982) and Hughes (1987). The magnitude of the error associated with this method should decrease with the porosity of the sample. The maximum values estimated using this method are indeed in better agreement with values reported here.

Baker and Weber (1975) used a different method, photodensitometry of X-radiographs, to measure skeletal density. The difference between their data and those of Dodge and Brass (1984), who used the same method, warrants some caution when comparing absolute density measurements based on photodensitometry. Baker and Weber (1975) reported a range of 1.57-1.79 g cm^{-3} for hemispherical/columnar colonies (0-13.5 m water depth), while Dodge and Brass (1984) give a range of 0.78-1.61 g cm^{-3} for columnar colonies (2.5-8 m water depth). Both studies were carried out at St. Croix. There may be variations between localities and indeed Dodge and Brass (1984) only used the less dense columnar growth form as opposed to the use of both columnar and hemispherical colonies by Baker and Weber (1975). But the question remains wether this can adequately account for the difference between the two reported ranges (Table 3.1). Different calibration thechniques may be another source for the observed differences. More accurate calibration for photodensitometry of X-radiographs should improve comparison between results obtained using this method (Chalker et al., 1985).

From this study it appears that CT density measurements, based on X-ray attenuation, are quick and might prove to be more accurate than conventional methods that have been applied to measure skeletal densities of *M. annularis*. Calibration of CT densities is relatively easy and does not call for specialized equipment. The internal calibration of CT scanners to air and water would enable easy comparison of results from different studies.

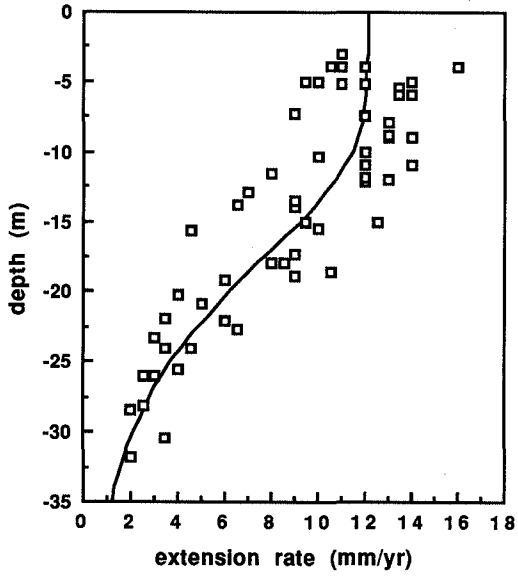

Figure 3.5a. Extension rate of *Montastrea annularis* versus water depth. Decrease of extension rate is described by the following function (shown as solid line):

$G_z=G_{max}\ (I_0e^{-kz}/I_k)$,

where G_z = extension rate at depth z (mm/yr); G_{max} = maximum rate (12.15 mm/yr ; I_0 = light intensity at the surface (2000 µE m^{-2} s^{-1}); k = light extinction coeficient (-0.115 m^{-1}); z = depth (m); I_k = saturation light intensity (351.6 µE $m^{-2}s^{-1}$ 15.1 m water depth). Values in brackets result in R^2 = 0.97 (see chapter 2).

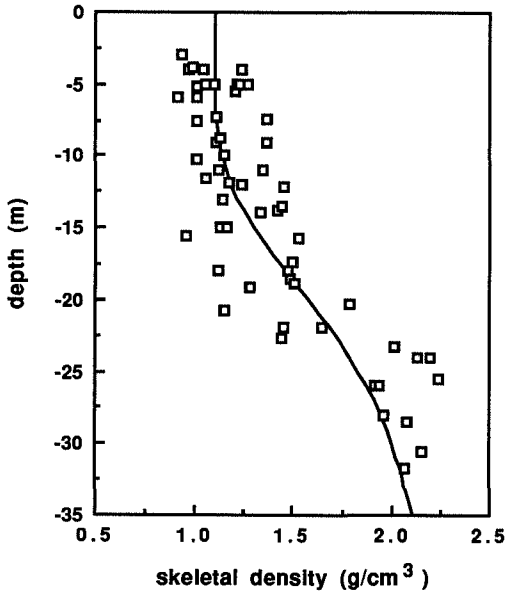

Figure 3.5b. Skeletal density of *Montastrea annularis* versus water depth. Data from Figure 3.4 are fitted to the same function (solid line) as in Figure 5a, where now G_z = skeletal density (g cm^{-3}) at depth z (m); G_{max} = surface density value; maximum density is set at 2.24 g cm^{-3} (see Fig.4); light data as in Figure 5a. Resulting values for the estimated parameters were: I_k (saturation light intensity) = 301.7 µE $m^{-2}s^{-1}$ 16. 4 m water depth; G_{max} = 1.14 g cm^{-3} (R^2=0.96;p<<0.001). Note increase of skeletal density similar to the decrease of extension rate shown in Figure 3.5a.

Density vs. depth

Several authors have recognized the relation between decreased extension rates and increased skeletal densities with increased water depth (Baker and Weber, 1975; Graus and Macintyre, 1982; Highsmith, 1979). It is proposed by these authors that this is the result of decreasing amounts of light with depth. Slower growing colonies build denser skeletons and generally coral extension rates decrease with depth. The decrease of coral extension rates can be attributed to the decreased amounts of light available for photosynthesis (Bosscher and Meesters, 1992; Chalker et al., 1988). Bosscher and Meesters (1992) demonstrated the possible control of light on the growth rate of *Montastrea annularis* using the same samples used in this study (Fig. 3.5a). The relation between light and photosynthesis for reef-building corals is best described by a hyperbolic tangent function (Chalker, 1981). Initially photosynthesis increases proportionally to increasing light intensity until it reaches a horizontal assymptote defined by the maximum photosynthetic performance of the coral. The light saturation point (I_k) is defined as the intercept between the initial slope of the curve and the horizontal assymptote (Chalker, 1981).

Light decreases with depth following an exponential function. A combination of the two functions describes the non-linear relationship between photosynthesis and depth. The use of a linear regression to evaluate the possible relationship between photosynthesis, skeletal density and depth is therefore inappropriate. Photosynthesis is at its maximum in a zone of light saturation. Below the depth of light saturation photosynthesis decreases rapidly, more or less exponentially, following the extinction of light in the water column.

Here the possible relationship between decreasing rates of photosynthesis with depth and increasing skeletal densities is tested.

Skeletal density data were fitted to a hyperbolic tangent function using an iterative curve-fitting program (Fig. 3.5b). From light intensity (at sample depth; chapter 2) and skeletal density data the program calculated the best fitting hyperbolic tangent function. The program does so by adjusting the mean skeletal density at the surface and the light saturation point, using a least squares method. It is apparent that indeed the increasing skeletal densities fit the trend predicted by decreasing rates of photosynthesis (Fig. 3.5b).

From a comparison with the results of extension rate measurements of the same colonies it appears that the increase of skeletal density with depth follows a similar trend as the decrease of extension rates (Figs. 3.5a and b; chapter 2). Skeletal densities remain relatively constant in the zone of light saturation. An increase in skeletal density occurs at 15-20 m water depth (Fig. 3.5b). The increase of coral skeletal densities around this depth is also apparent in a compilation of the data from Baker and Weber (1975) and Graus and Macintyre (1982) in Figure 3.6. The light saturation depth found for skeletal density of 16.4 m is similar to the light saturation for extension rate at 15.1 m water depth. This light saturation depth seems to be responsible for the drop in extension rates of *M. annularis* that occurs around 15-20 m throughout the Caribbean (Hubbard and Scaturo, 1985; Huston, 1985). From Figure 3.5a and b it follows that skeletal density and extension rate are inversely correlated. In Figure 3.7 it is shown that the skeletal density of *M. annularis* is indeed inversely proportional to the extension rate. This agrees with observations made by others

(e.g. Dodge and Brass, 1984). A linear regression through the extension rate and skeletal density data is shown to be nearly identical to a combination of the fitted functions from Figures 3.5a and b.

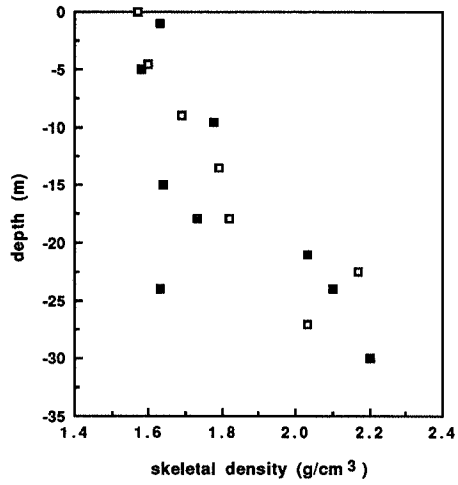

Figure 3.6. Skeletal density of *Montastrea annularis* versus water depth. Open symbols: Jamaica (Baker and Weber, 1975); each point represents 6 to 22 measured colonies. Filled symbols: Belize (Graus and Macintyre, 1982); each point represents one individual measurement. Note similarity of the overall trend of decreasing skeletal density with depth to the trend shown in Figure 3.4, with the exception of one individual measurement at a depth of ca. 24 m.

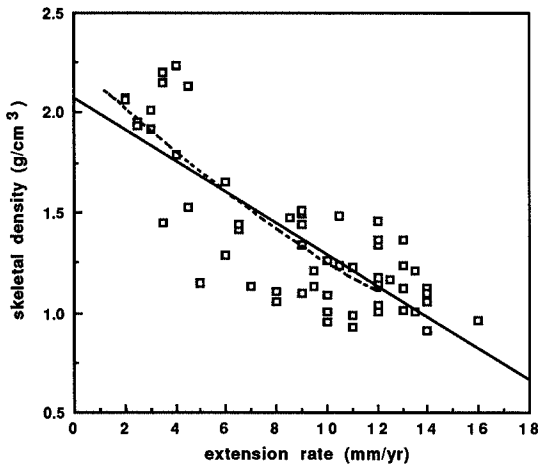

Figure 3.7. Relation between growth rate and skeletal density of *Montastrea annularis* (n = 57). Solid line is based on linear regression: $y = 2.07-0.0779X$ ($R^2 = 0.64$; $p < 0.01$). Dashed line is based on the fitted functions from Figures 3.5a and b.

CONCLUSIONS

A major advantage of the use of CT for the study of coral skeletons is that it is quick and non-destructive. Coral heads and small cores can be scanned without cutting them first or to select the best section before cutting. CT-scanners can accommodate cores and coral colonies up to the size of a human body. Extension rates can be estimated using scale bars, shown on the scans, but for precise measurements of the yearly growth increments the conventional, true-scale, X-radiographs are preferable. CT offers great possibilities for the measurement of skeletal densities. Density profiles or mean skeletal densities can be accurately measured. Computerized Tomography is available at many hospitals and especially academic hospitals may make time available for coral "patients".

The increasing skeletal density of the reef-building coral *Montastrea annularis* with increasing depth (Baker and Weber, 1975; Graus and Macintyre, 1982; Hughes, 1987) is confirmed using CT density measurements. The results, however, suggest a non-linear trend with an abrupt change around 15-20 m, similar to the decrease of photosynthetic rates with depth. The decrease of extension rate and the increase of skeletal density follow a similar trend with depth and are, therefore, inversely correlated.

Chapter 4

METABOLIC EFFECT ON SKELETAL $\delta^{13}C$ OF THE CARIBBEAN REEF-BUILDING CORAL *MONTASTREA ANNULARIS*

Abstract

The isotopic composition of the Caribbean reef-building coral *Montastrea annularis* shows a decrease in the $\delta^{13}C$ of the skeleton of ca. 2.8‰ from 0 to 30 m water depth, attributed to the decreasing rates of gross photosynthesis. Skeletal $\delta^{18}O$ remains constant over this depth range at 4.33‰. Our results agree with models that propose increasing skeletal $\delta^{13}C$ with increasing photosynthesis, whereas $\delta^{18}O$ appears to be unaffected by changes in the photosynthetic rate with depth. The discrepancy between the observed decrease of skeletal $\delta^{13}C$ with depth and other skeletal growth parameters can be explained by photoadaption of the coral.

INTRODUCTION

Stable isotope ratios in coral skeletons

The oxygen and carbon isotopic composition of coral skeletons has been the subject of many studies in the last two decades. The progress in this field has recently been summarized in several thorough reviews (Swart, 1983; McConnaughey, 1989; Aharon, 1991). Corals precipitate aragonite in disequilibrium with ambient seawater. Isotopic fractionation is influenced by both so-called "kinetic" and "metabolic" effects (Swart, 1983; McConnaughey, 1989). With increasing temperatures kinetic effects cause depletion of ^{18}O with respect to ^{16}O and to a lesser extent of ^{13}C with respect to ^{12}C. This is probably the result of fractionation during hydration and hydroxylation of CO_2 (Aharon 1991). The preference of photosynthesis for the lighter ^{12}C isotope allows the use of the depletion in ^{13}C of the coral skeleton as an indicator of changes in photosynthetic performance of coral/alga symbiosis (McConnaughey, 1989). Oxygen isotope fractionation is attributed mainly to kinetic effects. The dependence of oxygen isotope ratios of coral skeletons on the isotopic composition of ambient sea-water (temperature) makes them possible recorders of reef environment history. The use of oxygen isotopes from corals as paleothermometers has been described by Emiliani et al. (1978), Fairbanks and Dodge (1979), Weil et al. (1981), Pätzold (1984) (among others). A study on the effect of "bleaching" on the stable isotopic composition of *Montastrea annularis* from Florida (Leder et al., 1991) shows the difficulties in assessing the environmental factors that cause variations in the isotopic composition of a coral skeleton.

The changes of the carbon isotopic signature of coral skeletons are generally attributed to the changing rates of photosynthesis and respiration, the so-called metabolic or vital effects. The carbon needed in calcification comes from the internal inorganic carbon pool of the coral. The carbon in this pool is derived from two sources, ambient seawater and zooxanthellae respiration (Weber and Woodhead, 1970; Goreau, 1977;Swart, 1983). Preferential fixation of ^{12}C by zooxanthellae photosynthesis will enrich this pool in ^{13}C. Skeletal material precipitated from this pool should, therefore, exhibit a decrease in $\delta^{13}C$ with decreasing photosynthestic activity and thus with depth (Swart, 1983). Fairbanks and Dodge (1979) combined data from Land et al. (1975) and Weber et al. (1976) in a discussion of the aboved mentioned depth/$\delta^{13}C$ relation for *M. annularis*. Data indeed show an overall lower $^{13}C/^{12}C$ ratios with depth. They (Fairbanks and Dodge, 1979) relate this decrease to the exponential decrease of light with depth. The $\delta^{13}C$ of *M. annularis* animal tissue and zooxanthellae shows a similar reduction in $\delta^{13}C$ attributed to reduced rates of photosynthesis (Muscatine et al., 1989). Here we describe the bulk isotopic composition of skeletons of massive *M. annularis* sampled over a 30 m depth range and its relation to different growth parameters. The main objective of this study is to relate the variation in $\delta^{13}C$ with depth to the decrease of photosynthesis.

MATERIALS AND METHODS

Coral samples

Coral core samples were taken in October 1990 and July/August 1991 at three localities on the leeward fringing reefs of Curaçao, Netherlands Antilles (Fig. 4.1). We used a small hand-held pneumatic drill, connected to a SCUBA tank, and a 25 cm long diamond-tipped core barrel with an internal diameter of 25 mm. The obtained cores were sawn into slabs of ca. 5 mm thickness and X-rayed for extension measurements. The results of these measurements and underwater light measurements are discussed elsewhere (chapter 2). Polyp spacing (distance between centres of adjacent corallites) was measured on the top of the cores using a precision caliper and is given as the average of 5 measurements per core. Care was taken to sample only *Montastrea annularis* colonies of the massive morphotype (morphotype 2 of Knowlton et al., 1992). Cores were taken along the major (vertical) growth axis of each colony.

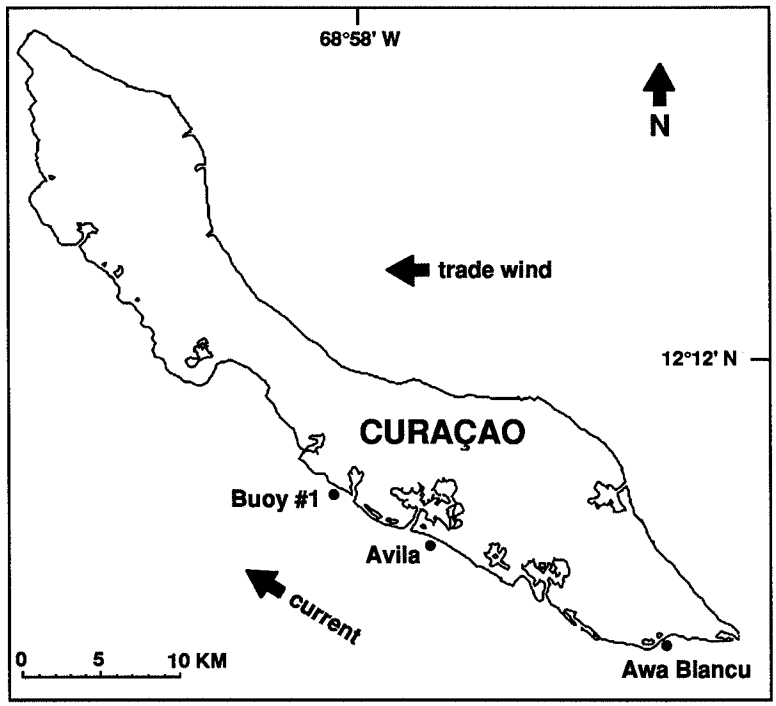

Figure 4.1. Schematic map of Curaçao, Netherlands Antilles, showing the location of the study sites. Cores were taken at Buoy #1, Avila Beach and Awa Blancu.

Sampling technique

X-ray positive prints were used to identify the last four years of skeletal growth. With a rocksaw sticks were sawn from the slabs measuring ca. 4 x 4 mm and comprising four years of growth (i.e. four pairs of high and low density bands). This minimized the influence of both seasonal variations in the stable isotopic composition and the different isotopic signatures of the various skeletal elements (Land et al., 1975). Sticks were subsequently ground and homogenized using an agate mortar. Additional samples were taken from the slabs by using a micro-drill with a 1 mm drill bit, along the growth axis of the skeleton. This was done to address the discrepancy between the isotopic composition of paired samples as a result of the sampling technique. Aharon (1991) compared "dry" drilling with "wet" drilling techniques and concluded that the dry drilling technique shows great deficiencies when compared to wet micro-coring and grinding of the skeleton. Although our sampling technique (see above) is comparable to the "wet" drilling technique as described by Aharon (1991) we compared micro-samples obtained using "dry" drilling with the bulk skeleton results (Table 4.1). We found no deviations that could be attributed to the sampling technique and must conclude, in agreement with Leder et al. (1991), that such an effect could well be caused by high pressure and/or dull drill bits, but does not normally occur.

Table 4.1. Isotopic composition of *Montastrea annularis*.

colony depth (m)	dry sampling $\delta^{18}O$ (‰ ± 1 s.d.)	$\delta^{13}C$ (‰ ± 1 s.d.)	wet sampling $\delta^{18}O$ (‰ ± 0.10)	$\delta^{13}C$ (‰ ± 0.05)
4	3.82 ± 0.08	0.47 ± 0.16	4.12	0.86
11	4.11 ± 0.11	2.11 ± 0.29	4.14	2.23
15.5	4.31 ± 0.33	2.47 ± 0.33	4.25	2.87
20.8	4.63 ± 0.16	2.68 ± 0.18	4.43	2.68
26	4.30 ± 0.15	2.63 ± 0.18	4.16	2.44
31.8	3.17 ± 0.13	1.23 ± 0.29	3.17	1.48

Isotope analyses

Approximately 0.5 to 1 mg of powdered coral sample was used. To each sample 5 droplets of 100% phosphoric acid were added in vacuum at 50 °C to liberate CO_2. Isotope analysis was carried out off-line on a Finnigan MAT 251 mass spectrometer. Analytical precision of a continuously run internal standard ("Merck" 100% calcite) was ± 0.10‰ for $\delta^{18}O$ and ± 0.05‰ for $\delta^{13}C$. Standard deviation of repeatedly measured coral samples was similarly within 0.10‰ for $\delta^{18}O$ and 0.05‰ for $\delta^{13}C$. Results are expressed as deviations in permil from the PDB standard, calibrated through NBS 19 and 20 carbonate standards.

RESULTS

Oxygen isotopes

The oxygen isotopic composition over the sampled 30 m depth interval is nearly constant with a mean value of -4.33 (± 0.16‰; Fig. 4.2). We therefore assume that the reef waters at the study sites are isothermal in the upper 30 m of the water column. Over a similar depth range at St. Croix, Weber et al. (1976) found an average $\delta^{18}O$ of -4.06‰. Land et al. (1975) reported an average $\delta^{18}O$ of -4.49 ‰ for Jamaica reef waters for a water depth of 0 to 60 m. Both studies did not report variations in $\delta^{18}O$ with depth and concluded that the reef waters were isothermal over the studied depth interval. This also shows that the oxygen isotopic composition of *Montastrea annularis* skeletons seems indeed unaffected by changing rates of photosynthesis. Photosynthetic rates can be expected to change substantially in the studied depth interval (0 - 30 m).

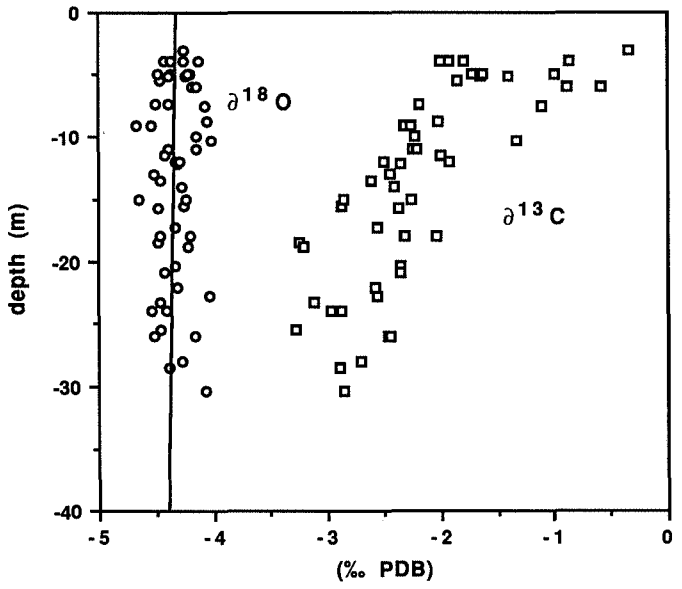

Figure 4.2. $\delta^{18}O$ and $\delta^{13}C$ for *Montastrea annularis* versus water depth (n = 53). Solid line is linear regression of $\delta^{18}O$ vs. depth: y = 4,304 - 0.0002x; R^2 = 0.99. Mean $\delta^{18}O$ is -4.33‰ (± 0.16).

Carbon isotopes

The carbon isotopic composition of *Montastrea annularis* vs. depth does show large variations (Fig. 4.2). $\delta^{13}C$ of skeletons of *M. annularis* from Curaçao decreases from ca. -0.5‰ for the shallowest colonies to -3.3‰ for the deepest colonies. This range is similar to the range reported by Land et al. (1975) and Weber et al. (1976): -0.49 to -3.5‰ for Jamaica and St. Croix.

DISCUSSION

Intraspecific variation

Although care was taken to sample only one morphotype of *Montastrea annularis* we found several colonies with extremely dense polyp packing and anomalously high $\delta^{18}O$ and $\delta^{13}C$ (Table 4.2). Over a 30 m depth range we found corallite spacing to range from 2.9 to 4.6 mm and generally increasing with depth, in accordance with the findings of Weber et al. (1976). These authors reported a corallite spacing ranging from 3 to 4.2 mm (over a 0-27 m depth range). A similar range has been reported by Dustan (1979). Both authors report a non-linear decrease of polyp packing with depth. If we consider that photoadaption by *M. annularis* results in decreased polyp packing densities, lowering the metabolic demands of the coral (Dustan 1979), we consider the colonies with narrow corallite spacings to be especially autotrophic polymorphs. The simultaneous offset of both oxygen and carbon isotopic ratios when compared to "normal colonies" indicates decreased kinetic fractionation as a result of higher metabolic demands. These results warrant extreme caution when isotopic composition is used to differentiate between morphotypes of *M. annularis* (Knowlton et al., 1992). The results of these anomalous samples were not incorporated in the $\delta^{13}C$ vs. depth study discussed below.

Table 4.2. Isotopic composition of *Montastrea annularis*.

depth range (m)	polyp spacing (mm)	$\delta^{13}C$ (‰)	$\delta^{18}O$ (‰)	
13.8-31.8	2.1 (1.9-2.3)	-1.086 ± 0.34	-3.262 ± 0.08	(n:4)
14.0-30.5	3.8 (2.9-4.6)	-2.676 ± 0.35	-4.343 ± 0.16	(n:23)

Carbon isotopes

The decrease of $\delta^{13}C$ with depth is often attributed to the decrease of photosynthesis with decreasing amounts of light (Fairbanks and Dodge, 1979; Swart, 1983). Light decreases exponentially with depth, but photosynthesis, the driving force behind $\delta^{13}C$ variations does not (Chalker et al., 1988). The relationship between light (irradiance) and

photosynthesis (so-called P vs. I curves) can accurately be described using a hyperbolic tangent function (Chalker, 1981). Initially photosynthesis (P) increases proportionally to irradiance (I) until a horizontal assymptote is reached defined by the maximum gross photosynthetic performance of the coral/zooxanthellae symbiosis. The intercept of the initial slope of the P vs. I curve and the horizontal assymptote defines the light saturation point (I_k). The decrease of photosyntheis with depth depends on a combination of the exponential function for the decrease of light with depth and the hyperbolic tangent function to describe the relation between light and photosynthesis (see Figs. 8 and 9 in introduction to part I). The assumption of a direct relationship between the exponential decrease of light with depth, photosynthesis, and $\delta^{13}C$ would imply a linear relationship between light and photosynthesis. We know that such a linear relation ship does not exist (e.g. Chalker et al, 1988). Thus, rather than assuming an exponential decrease of skeletal $\delta^{13}C$ (Fairbanks and Dodge 1979; Fig. 4.3a) we fitted our carbon isotope data to a hyperbolic tangent function (Fig. 4.3b). Unfortunately the statistical results are far from conclusive, although the resulting fit for the hyperbolic tangent function is slightly better than for the exponential function (R^2 = 0.88 for the exponential function vs. R^2 = 0.97 for the hyperbolic tangent function). As can be seen on Figures 4.3a and b, variation of $\delta^{13}C$ is greatest in shallow waters (from -0.33 to -1.99‰). As yet we have no good explanation for this. Both models fail to give a good fit for the upper part of the water column. The average $\delta^{13}C$ for shallow colonies, however, is best predicted using the hyperbolic tangent function. The exponential function predicts positive values for the shallowest colonies (Fig. 4.3a). The value obtained by fitting a photosynthetic function for shallow colonies (-1.09‰; Fig. 4.3b) is in better agreement with the vaues of -0.5 to -2.0‰ reported in the literature (Baker and Weber, 1975; Land et al., 1975; Fairbanks and Dodge, 1979). Because of the large variation in $\delta^{13}C$ in shallow colonies, we observed only a vague correlation between coral extension rates and the $\delta^{13}C$ of the skeleton (Fig. 4.4).

The light saturation depth for skeletal $\delta^{13}C$ predicted by using a hyperbolic tangent funtion is 6.7 m (Fig. 4.3b). This is remarkably different from the light saturation depth for the extension rate (15.1 m) and skeletal density (16.4 m) for the same colonies (chapters 2 and 3). This can be explained by photoadaptive strategies that corals employ to optimize the use of photosynthetic products, thus expanding the depth of light saturated growth (Dustan, 1979). Corals respond to decreasing light levels by reducing both respiration and photosynthesis (Chalker et al., 1988). Gross photosynthesis decreases rapidly with depth as shown by the decrease of $\delta^{13}C$ in Figure 4.2. The simultaneous decrease of respiration results in an increased P/R ratio and a more gradual decrease of net photosynthesis. The decrease of net photosynthesis with depth could, therefore, show a trend more similar to the above mentioned skeletal growth parameters. Because net photosynthesis is responsible for coral growth this could well explain the observed difference between skeletal growth rates of the coral and the $\delta^{13}C$ of its skeleton versus water depth.

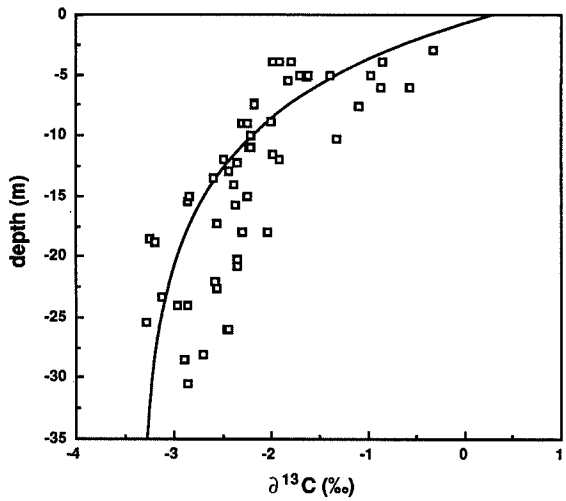

Figure 4.3a. Carbon isotopic data fitted to an exponential function. Minimum value is set at lowest $\delta^{13}C$ value obtained from Figure 4.2 (-3.28‰). Light data for Curaçao from chapter 2.
Resulting curve: $\delta^{13}C(z) = -3.28 + 3.447\ e^{-0.115*z}$, where z is depth (m); value of 0.115 is light extinction coefficient (k) in m^{-1} ($R^2 = 0.88$).

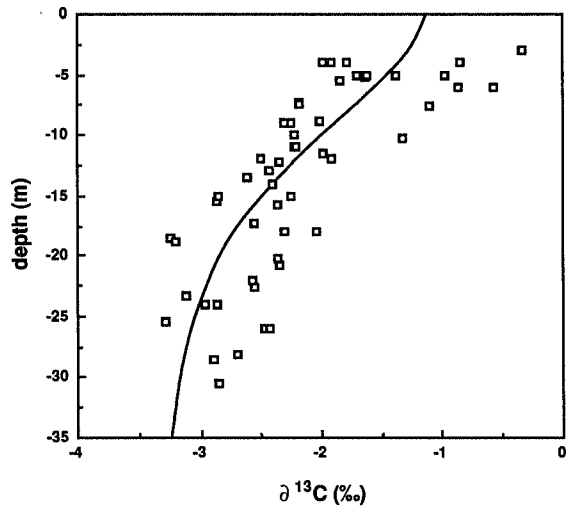

Figure 4.3b. Carbon isotopic data fitted to a photosynthetic hyperbolic tangent function (Chalker, 1981). Parameter values as in Figure 4.3a. Resulting curve: $\delta^{13}C\ (z) = -3.28 + 2.193 \tanh(I/926.2)$, where the maximum ratio (z = 0) is -1.09‰, I is the light intensity and I_k (saturation light intensity) is represented by a value of 926.2 (light data in µE $m^{-2}\ s^{-1}$)($R^2 = 0.97$).

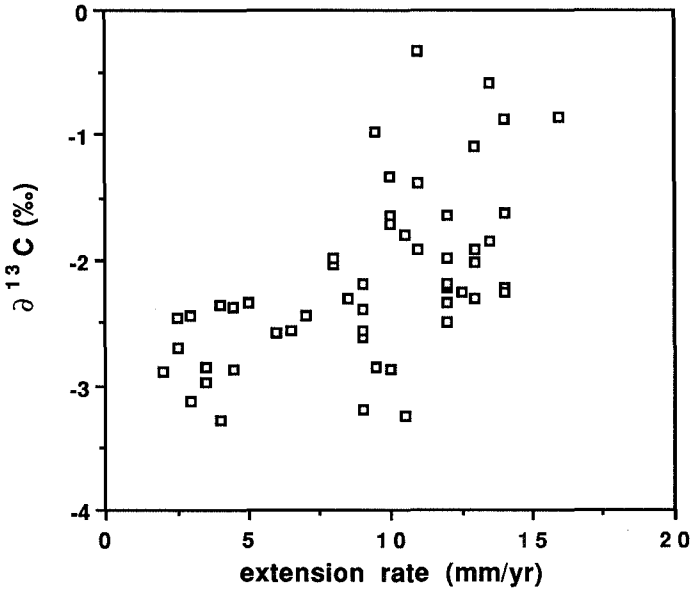

Figure 4.4. Growth rate versus $\delta^{13}C$ for *Montastrea annularis* (n = 53).

CONCLUSIONS

Skeletal $\delta^{13}C$ of the Caribbean reef-building coral Montastrea annularis decreases from -0.5‰ for shallow colonies (3 m water depth) to -3.3‰ at a depth of 30 m. This seems to be the result of increased fractionation of carbon isotopes at higher gross photosynthetic rates. The sharp decrease in gross photosynthesis with depth as illustrated by the observed decrease in $\delta^{13}C$ does not agree with the more gradual decrease of other skeletal growth parameters. Photoadaptive strategies resulting in higher P/R ratios probably result in a more gradual decrease of net photosynthesis and thus coral growth.

PART II

GROWTH OF CORAL REEFS AND CARBONATE PLATFORMS

INTRODUCTION

There are several ways to study the growth of coral reefs and carbonate platforms. One is to go to outcrops of fossil reefs, another one is to try to make a computer model and make one's own outcrop. In trying to construct computer models for complex sedimentary systems such as carbonate platforms one has to come to grips with the underlying controls. If one can not constrain the most important geological processes there is no use in making a model. This is where the observations on modern reefs and outcrops come in. In chapter 5 observations on the growth of recent corals and reefs from part I have been incorporated in a simulation model for Holocene reef growth. Adding to this, sedimentological observations on carbonate platforms resulted in CARBPLAT - a computer model for carbonate platforms (chapter 6). In CARBPLAT development of carbonate platforms depends largely on flooding and/or emergence of the platform interior. Chapter 7 illustrates this mechanism for the Pliocene/Pleistocene development of the Bahamas carbonate platforms based on the composition of calciturbidites.

What is a reef ?

A reef is a buildup of carbonate in which organic framework builders play an important role. These framework builders trap sediment and build wave resistant structures. In this way reefs are able to create their own relief. Such a buildup would be called an ecologic reef in the definition of Dunham (1970) or an organic framework reef by Wilson (1975). In this thesis I use the term reef as described above. Other organic buildups which lack the organic framework are called mounds (James, 1992). Mounds are also referred to as organic bank (Wilson, 1975), loose skeletal buildup (Heckel, 1974) or 'stratigraphic reef' as opposed to 'ecologic reef' (Dunham, 1970). A general term for the structures described above is bioherms, or simply carbonate buildups.

Reef builders

Coral reefs are highly complex ecosystems made up by a huge variety of organisms. Not only corals but also, red and green algae, molluscs, bryozoans, sponges, foraminifera, soft corals, tube worms, fishes and many others are a part of the coral reef community. Most of the substrate on a coral reef is created by coral skeletons. The growth of corals allows the construction of carbonate buildups faster than they can be eroded by physical or biological agents. The coral skeletons offer protection and substrate to many other organisms. The framework of a reef is formed by the massive skeletons of reef-building scleractinians. They trap the sediment that is produced by other organisms and prevent it from being washed away. Their resistance to waves, storms and currents make massive corals a key factor in the maintenance of coral reefs. Other reef-building corals such as branching *Acropora sp.* often dominate zones in the reef, but these more fragile branching forms are more easily disturbed by severe storms or hurricanes and turned into coral rubble. The growth of corals keeps the coral reef ecosystem within the zone of light saturation during sea level changes and the fate of a coral reef depends, therefore, largely on the constructive power, i.e. growth potential, of massive head corals.

Because corals form the most important part of the reef structure the environmental controls on reef growth are similar to those for individual coral growth. Everything said in the introduction to part I about the environmental control on coral growth, therefore, applies to coral reef growth.

Reef responses to sea-level

The way in which most geologists view the growth of reefs is relatively simple. A mass of mostly organic, in-situ accumulated carbonate that moves up and down with sea level. Sometimes it drowns sometimes it becomes exposed but generally it stays comfortably close to sea level. I am afraid it really is this simple. Coral reefs grow up to sea level (catch-up) as long as they can match the rate of creation of accommodation space. If there is no more accommodation space they will try to grow oceanward but hey will maintain their top at or near sea level (keep-up). If the rate of creation of accommodation space is greater than the maximum growth rate of the coral reef (i.e. the growth potential) they will either backstep, i.e. migrate shoreward to shallower water, or drown (give-up). If sea level falls, reefs become emerged and the living reef is forced to step down with sea level. During rapid drops or rises of sea-level mostly only a thin veneer of reef is deposited. Periods with relatively stable sea-level position favour the development of extensive reef tracts.

The terms start-up, catch-up, keep-up and give-up have been used to describe the various types of response to the Holocene sea-level rise (Davies and Montaggioni, 1985; Neumann and Macintyre, 1985). The start-up growth phase in which the reef organisms colonize the substrate and establish a foundation from which the reefs can grow, and particularly the duration of this phase (the lag-time for reef initiation), are a key factor in Holocene reef development. Lag periods of up to 2500 years are relatively common after the Holocene transgression and left many reefs stranded in deeper water, unable to catch up with sea level. During the catch-up phase reef growth exceeds the rate of sea-level rise. In

the Holocene catch-up reefs are dominated by massive and branching corals and the highest reef accretion rates are encountered on catch-up reefs. Keep-up reefs are at or near sea level and are often dominated by branching corals. Give-up reefs show a deepening-upward succesion at their top.They commonly fall below the zone of light saturation and are incipiently drowned.

Reef and platform growth and growth potential

The assumption that the growth of corals, particularly massive head corals, is a key factor in reef and thus platform growth is tested by comparing computer simulations with geological observations. The importance of the growth vs. depth relation from part I and the growth potential estimate from the Holocene form the basis of these simulation. The fact that carbonate platforms not only have the potential to grow up vertically but also have the ability to prograde and shed sediment into the adjacent basins is illustrated by computer simulations and a case study of carbonate platform development.

Chapter 5

COMPUTER SIMULATION OF REEF GROWTH

Abstract

Light is one of the major controls on reef growth and carbonate production. The ability of reef-builders to grow depends largely on the amount of light available for photosynthesis. As light decreases with depth, so does reef growth. The computer model presented here builds on this principle by combining two functions, one for photosynthesis and the other for the extinction of light in water. The model is used to simulate the growth of Alacran Reef, Mexico, two reefs of the Great Barrier Reef and the reefs of the windward platform of St. Croix. The model also produces a good simulation of the fore-reef walls in Belize, in agreement with the accretion hypothesis of this feature.

INTRODUCTION

Computer models are used more and more in simulating aspects of carbonate sedimentation (Aigner et al., 1989; Bice, 1988; Bosence and Waltham, 1989; Graus and Macintyre, 1989; Scaturo et al., 1989; among others). These computer simulations help in understanding the interaction of the different controls on carbonate accumulation. However, it remains difficult to separate the role of individual controls - 'The model mimics the geologic record accurately only because we have fixed the variables to do so'(Scaturo et al., 1989, p.75). This statement holds for most of the above mentioned computer simulations.

Without quantification of the individual controls, computer simulation of carbonate deposition will depend on the use of widespread empirical data. The problems involved in this are obvious: these data are derived from different geological and geographical settings and often show variations of orders of magnitude when compared to fossil examples.

The program presented here singles out one factor, light, and its effect on reef accretion.

Light and reef growth

Various authors have stressed the effect of decreasing light levels on reef growth (James and Ginsburg, 1979; Schlager, 1981; among others). However there has been no quantification of this control.

Reef corals grow at depths ranging from the surface down to depths that receive ca. 1% of surface irradiance (Chalker et al., 1988). The 1% surface light level defines the lower limit of the euphotic zone and corresponds to the depth at which primary production equals respiration, i.e. the compensation depth (Jerlov, 1976).

The amount of light penetrating the water column depends on the extinction coefficient (k) of the water. One can characterize different reef settings by the k-value of the reef waters: a value of 0.05 m^{-1} corresponds to a lower limit of coral growth at 90-100 m and maximum reef growth in the upper 40 m (ca. 10% of the surface light level (Chalker, in Done, 1983)), while an extinction coefficient of 0.035 m^{-1} (typical for Pacific atolls) corresponds to a lower limit of coral growth of about 140 m and active reef growth down to 70 m (see Figs. 10 and 11 in introduction to part I). Light not only controls the depth distribution of corals. Figure 5.1 suggests it also affects the decrease of coral growth rates with depth. Light seems such a dominant factor in reef growth that we attempted to model reef growth by taking into account only the decrease of reef growth with depth due to reduced photosynthetic activity.

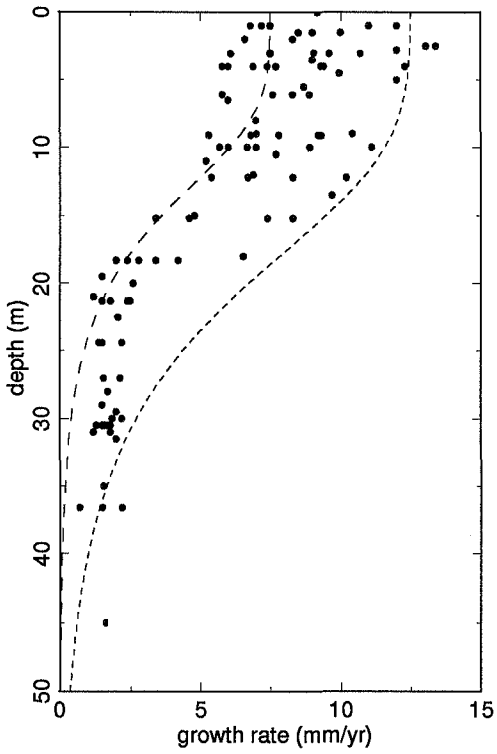

Figure 5.1. Linear growth rates of the main Caribbean reef-building coral *Montastrea annularis* vs. depth (n = 108) compared to production profiles based on the growth function described in this paper (dashed line: G_{max}: 12.5 mm/yr; k: 0.1 m^{-1}; I_0: 2000 µE $m^{-2}s^{-1}$; I_k: 450 µE $m^{-2}s^{-1}$; dotted line: G_m: 7.5 mm/yr; k: 0.15 m^{-1}; I_0: 2000 µE $m^{-2}s^{-1}$; I_k:300 µE m^{-2} s^{-1}). Growth data from: Baker and Weber (1975); Dustan (1975); Gladfelter et al. (1978); Hubbard and Scaturo (1985); Hudson (1981); Huston (1985); Tomascik and Sander (1985). Input values were chosen to produce curves that bracket growth data, but are within reported limits. The similarities between the growth data and the shape of the production curves suggest light determined growth rates.

METHODS

We have developed a program that simulates reef growth by solving a differential equation. This equation is explained in the next section. The program uses procedures for a fourth-order Runge-Kutta method with adaptive stepsize control, as described by Press et al. (1986). The program is written in TurboPascal 4.0 and runs on PC. Results are written to a plotfile and can be modified for various plotting programs.

The simulations presented here build on local data on light conditions, growth rates and reef zonation derived from the literature. When not available, parameter values were chosen for best fit, but within the reported ranges for these geological, biological and oceanographic variables.

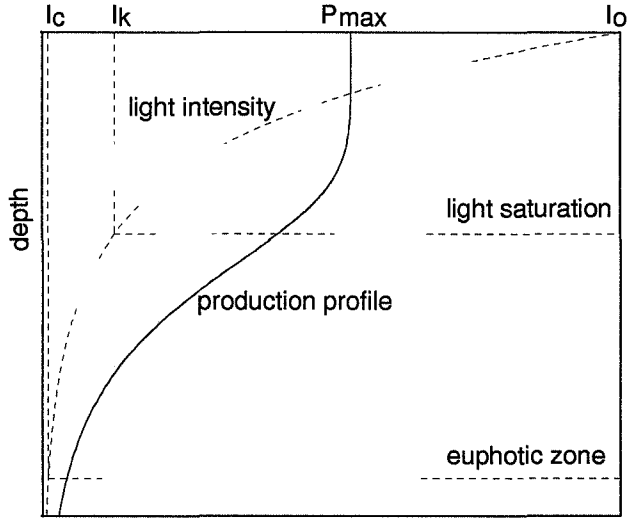

Figure 5.2. Schematic diagram showing the important parameters in calculating carbonate production based on the effect of decreasing photosynthetic activity with decreasing light levels (I_c: light intensity at compensation depth, i.e. lower limit of the euphotic zone;I_k: saturating light intensity; P_{max}: maximum photosynthetic rate; I_0:surface light intensity). I_k is defined as the light intensity at which the *initial* slope (α) of a Photosynthesis vs. Irradiance curve intercepts the horizontal assymptote that defines P_{max}. This causes the decrease of production in the lower part of the zone of light saturation.

A QUANTITATIVE MODEL FOR REEF GROWTH

Parameters

The parameters used in calculating photosynthetic growth of reef building corals (see also Figure 5.2) are:

G_{max} maximum growth rate

The maximum rate of reef growth ranges up to 10-15 mm/yr (Adey, 1978; Davies, 1983; Macintyre et al., 1977).

k extinction coefficient

A measure of the extinction of photosynthetically active radiation (PAR), i.e. light with a wavelength of 400-700 nm. For oceanic waters the value of k ranges from 0.04 to 0.16 m^{-1} (Jerlov, 1976). Reported values for reef waters lie within this range (Brakel, 1979; Chalker 1981; Porter, 1985; Van den Hoek et al., 1975; Weinberg, 1976).

I_0 surface light intensity

The light intensity around solar noon at the water surface in the tropics lies in the range of 2000-2250 $\mu E\ m^{-2}\ s^{-1}$.

I_k saturating light intensity

Light saturating intensities range from 50 to 450 $\mu E\ m^{-2}\ s^{-1}$, depending on species and depth (Chalker, 1981; Wyman et al.1987). Photoadaption of reef-building corals has not been taken into account. More generally light does not become a limiting factor for coral growth until it reaches ca. 10% of its surface value (Chalker, in Done, 1983).

I_z light intensity

The light intensity at depth z is given by Beer-Lambert's law (3).

Functions

According to Chalker (1981) the best function to describe gross photosynthesis by reef-building corals is:

$$P = P_{max} \tanh(I/I_k), \qquad (1)$$

where P is photosynthesis, Pm the maximum photosynthetic rate.

As photosynthesis, calcification rate and skeletal growth are proportional (Chalker et al., 1988), we can replace P by skeletal growth (G):

$$G = G_{max} \tanh(I/I_k) \qquad (2)$$

G is proportional to linear vertical growth if the reef does not change in horizontal area. This seems a reasonable assumption for many reefs during the very rapid Holocene transgresion.

The function that describes the extinction of light in the water column is Beer-Lambert's law:

$$I_z = I_0\, e^{-kz} \qquad (3)$$

I in function (2) can be substituted by this function (3) to give:

$$G = G_{max} \tanh(I_0\, e^{-kz}/I_k) \qquad (4)$$

Depth(z) at any given time(t) can be described as the initial height(h_0) plus the growth increment(h(t)), minus the initial sea-level position (s_0) plus sea-level variations(s(t)). This yields the following differential equation:

$$dh(t)/dt = G_{max} \tanh\left(I_0 \exp(-k((h_0+h(t))-(s_0+s(t))))/I_k\right) \qquad (5)$$

This the equation that is solved by the program.

GEOLOGICAL EXAMPLES

With this model, we have simulated characteristic Holocene growth patterns in order to assess the significance of the light-growth function for reef growth. These applications are described below.

Alacran Reef

The thickest Holocene reef section is recorded in the Isla Perez core hole, Alacran Reef, Mexico (Macintyre et al., 1977). Data from this core, as described by Macintyre et al. (1977; see Fig. 5.3a), are used in a growth curve simulation (G_{max} of 12 mm/yr, corresponds to the maximum accumulation rate given by Macintyre et al.(1977).

The result of this simulation is shown in Figure 5.3b. There is generally good correspondance for the period from the oldest ^{14}C date to present. The difference lies in the timing of initiation of reef growth. In the model presented here, reef growth does not begin until ca. 8000 yrs BP, while in the interpretation of Macintyre et al. (1977), reef growth starts shortly after submergence, between 10,000 and 9,500 yrs BP. Clearly some time is needed before normal marine conditions are well established and allow coral growth. The extinction coefficient we used in these simulations belongs to somewhat turbid reef waters (oceanic water type 3; Jerlov, 1976), a probable result of flooding of the broad insular shelf. It is presently unclear whether reefs need a period of perhaps as much 2500 yrs of virtually zero vertical growth before they are well established and can start vertical growth of the sort presented here, or whether they begin slowly, gradually increase growth rates due to improving environmental conditions and finally catch up with sea level.

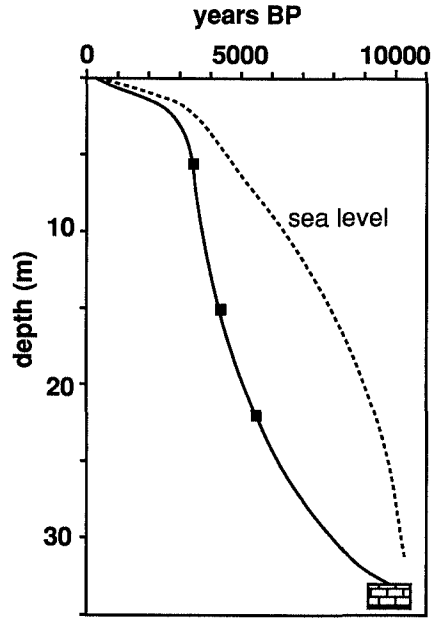

Figure 5.3a. Holocene growth curve and sea-level history of Isla Perez core hole, Alacran Reef, Mexico (after Macintyre et al., 1977). Boxes indicate ^{14}C dates, heavy line - sea level.

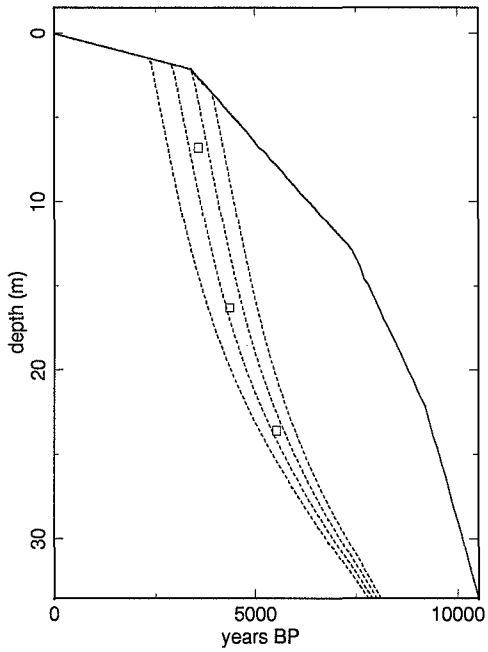

Figure 5.3b. Result of computer simulation of Alacran Reef growth curve. The dashed curves represent four different simulations with reef initiation at 8100 to 7800 yrs. BP (100 yr. intervals). Solid line represents sea-level curve. Boxes indicate ^{14}C dates (G_{max}:12 mm/yr; k: 0.15 m^{-1}; I_0: 2000 $\mu E\, m^{-2} s^{-1}$; I_k: 400 $\mu E\, m^{-2} s^{-1}$). Note good fit to ^{14}C dates.

Examples from St. Croix (Adey, 1978), Florida (Shinn, 1980; Shinn et al., 1989) and the Great Barrier Reef (Davies et al., 1985), show that a time lag between flooding and reef initiation can range anywhere between 500 and 2500 yrs This means that some reefs do not start growing until they are in a water depth of 20 meters (i.e. the lower limit of the zone of light saturation).

St.Croix

The Holocene reef development of the windward platform of St. Croix has been described by Adey (1978). The growth history of the shelf edge reef, the bank barrier reef and the fringing reef of St. Croix is illustrated in Figure 5.4a.

Flooding of the platform, some 9000 yrs ago, killed the fast growing upper portion of the shelf edge reef. Deteriorating water quality, as a result of the flooding of the platform, has been suggested as the cause of the ultimate demise of this shelf edge reef (Adey, 1978). Shallow shelf waters can develop extreme variations of temperature and salinity as well as high turbidity due to soil erosion. Here we simulate the effects of increased turbidity and reduced light levels on the growth and drowning of the shelf edge reefs and the subsequent development of bank barrier and fringing reefs in the shallower parts of the platform.

We set the time lag for initiation of the renewed growth of the shelf edge reef at 2000 yrs. Initiation dates of the growth of the bank barrier reef and the fringing reef were taken from Figure 5.4a. Sea-level input is the same as in the Alacran example. The maximum

growth rate at St. Croix, as reported by Adey (1978) was 10 mm/yr. High water turbidity is represented by a k-value of 0.25 m^{-1}.

Figure 5.4b shows the result of the simulation. The shelf edge reef can not keep up with the rate of sea-level rise and becomes stranded as a deeper water coral community now at a depth of about 20 m. The same turbid waters, however, cannot prevent reefs in the shallower portion of the platform from growing and catching up with sea level, as illustrated by the growth curves for the bank barrier reef and the fringing reef.

This simulation is consistent with the notion that inimical bank water can inhibit reef growth (Ginsburg and Shinn, 1964; Adey, 1978; Neumann and Macintyre, 1985) and that increased turbidity in these bank waters can play a particularly detrimental role in reef development. It should be noted, however, that extreme values of k are required if one assumes, as we did, that turbidity alone caused the demise of the shelf edge reef. An extinction coefficient of k = 0.25 m^{-1} corresponds to a euphotic depth of ca. 20 m and light saturated growth in depths shallower than 10 m. It is questionable however, whether these extreme values were reached during the Holocene transgression. Other detrimental effects of shallow lagoons, such as extreme variations in salinity and temperature, may have contributed to the reef crisis.

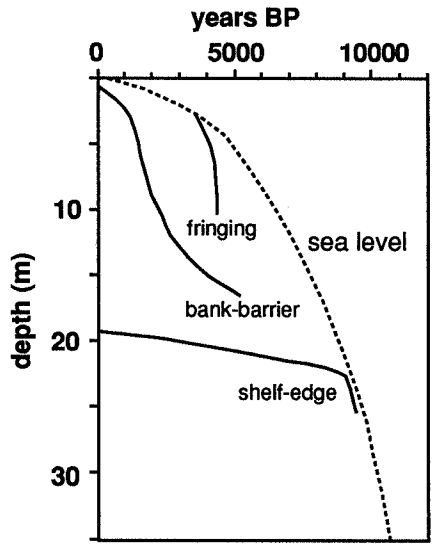

Figure 5.4a. Holocene sea level and growth history of the reefs of the windward platform of St. Croix (after Adey, 1978).

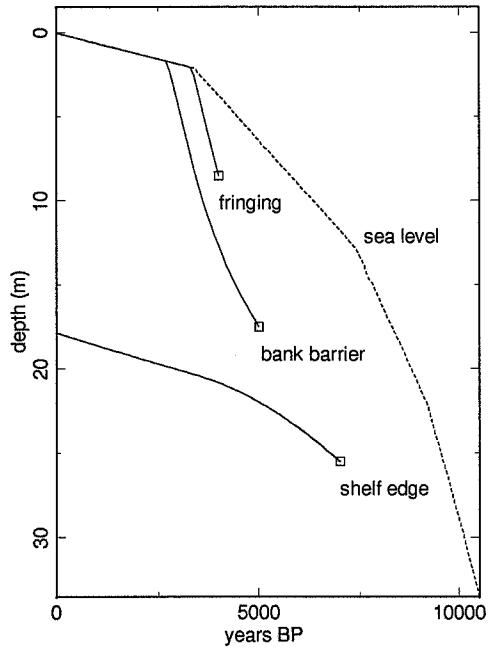

Figure 5.4b. Result of simulation run for St. Croix. Note that high turbidity can cause the demise of the shelf edge reef (G_m: 10 mm/yr ; k: 0.25 m^{-1}; I_0: 2000 µE $m^{-2}s^{-1}$; I_k: 300 µE m^{-2} s^{-1}). Only a slight reduction of turbidity (k: 0.2 - 0.15 m^{-1}) will lead to recovery of the shelf edge reef.

Great Barrier Reef

Davies et al. (1985) describe the Holocene growth history of the Great Barrier Reef based on numerous cores and radiocarbon datings. Data from two outer shelf reefs, Bowl Reef and Myrmidon Reef, were used in a simulation. Bowl Reef started growing around 8630 yrs. BP on a Pleistocene surface 29 m below present sea level and reached sea level between 3500 - 2000 yrs. BP. Maximum water depth above Bowl Reef was 16 - 22 m. Myrmidon reef started growing around 7620 yrs. BP on a Pleistocene surface 24 m below present sea level and reached sea level at approximately the same time as Bowl Reef. Maximum water depth developed on Myrmidon Reef was ca. 20 m. Both Bowl and Myrmidon reef are framework dominated reefs (Davies et al., 1985).

The variation of reef growth rate with depth for the central Great Barrier Reef (Davies et al., 1985: Fig. 5) shows a maximum of 8 mm/yr and a sharp decrease at a depth of ca. 15 m. If we consider this depth to represent the lower limit of light saturation, this would correspond to the following parameter values: G_{max}: 8 mm/yr; k: 0.15 m^{-1}; I_0: 2000 µE m^{-2} s^{-1}; I_k:200 µE m^{-2} s^{-1}.

Figure 5. 5 shows two plots illustrating the simulation of the growth history of both reefs. The growth curves agree with the data presented by Davies et al. (1985). Maximum water depth over both reefs in our simulation was 22.5 and 21 m for Bowl and Myrmidon reef respectively (Fig. 5.5b).

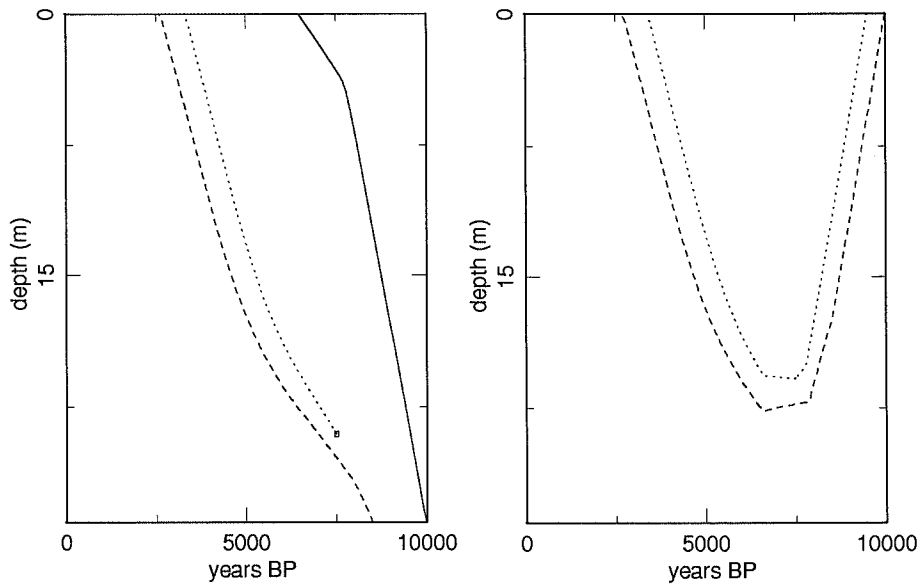

Figure 5.5. Plots illustrating simulation of growth history (left diagram) and paleowaterdepth of Bowl Reef (dashed line) and Myrmidon Reef (dotted line), based on data from Davies et al.(1985). Solid line represents sea-level curve. (G_{max}: 8 mm/yr; k: 0.15 m^{-1}; I_0: 2000 $\mu E\ m^{-2} s^{-1}$; I_k: 200 $\mu E\ m^{-2} s^{-1}$).

We used the examples from the Central Great Barrier Reef to illustrate the effect of changing certain growth parameters such as time lag, maximum growth rate and the light extinction coefficient of the reef waters, on the shape of reef growth curves (Fig. 5.6).

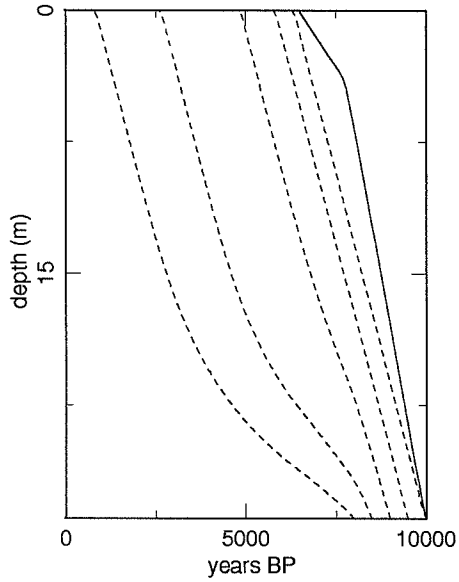

Figure 5.6. Schematic plots illustrating the effect of changing growth parameters on growth curves. Input data similar to Figure 5.5.
Figure 5.6a. Lag time of reef initiation: varied from 0 to 2000 yrs. in 500 yrs. increments (G_{max}: 8 mm/yr; k: 0.15 m^{-1}; I_0: 2000 $\mu E\ m^{-2} s^{-1}$; I_k: 200 $\mu E\ m^{-2} s^{-1}$). Note slow start-up growth with increased lag-time.

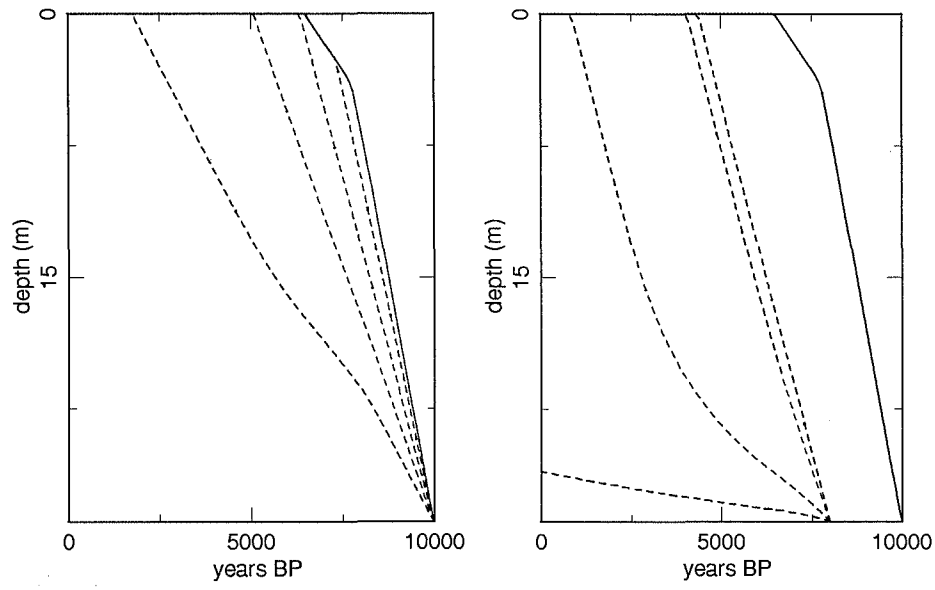

Figure 5.6b (left). Growth rate (G_{max}): varied from 4 to 10 mm/yr in 2 mm/yr increments (k: 0.15 m^{-1}; I_0: 2000 µE m^{-2} s^{-1}; I_k: 200 µE m^{-2} s^{-1};no lag time).
Figure 5.6c (right). Extinction coefficient (k): varied from 0.05 m^{-1} to 0.2 m^{-1} in 0.05 m^{-1} increments (G_{max}: 8 mm/yr; I_0: 2000 µE m^{-2} s^{-1}; I_k: 200 µE m^{-2} s^{-1}; 2000 yrs. time lag). Note that high extinction coefficient leads to near-zero reef growth.

Belize reef margin

James and Ginsburg (1979) proposed the idea that the Belize Reef Margin was formed mainly by accretion during five consecutive Pleistocene sea-level high stands (Fig. 5.7b).

This hypothesis was simulated with our model. A surface dipping 50 degrees and a schematic sea-level curve for the past 80,000 years, similar to that shown by James and Ginsburg (1979:p.171;Fig. 5.7a), served as initial input. In Belize the lower limit of scleractinian coral growth is ca. 90 m and maximum growth occurs down to 40 meters. These values correspond to an extinction coefficient (k) of 0.05 m^{-1} .

The result of the computer simulation is shown in Figure 5.8. It is clearly very similar to the diagram that illustrates the hypothesis of James and Ginsburg (1979; Fig. 5.7b). The reef margin consists of four consecutive, downstepping, shoulders attached to the initial surface, overlain by a Holocene veneer. The model shows that the steps in the Holocene morphology, mentioned by James and Ginsburg (1979: p.171), can be an expression of the underlying morphology, created by different earlier highstands of sea level. The steep wall that can be observed at todays Belize reef margin also appears in the simulation and indicates the ability of reefs to create very steep walls. This phenomenon can be explained by the decrease of growth rates with depth.

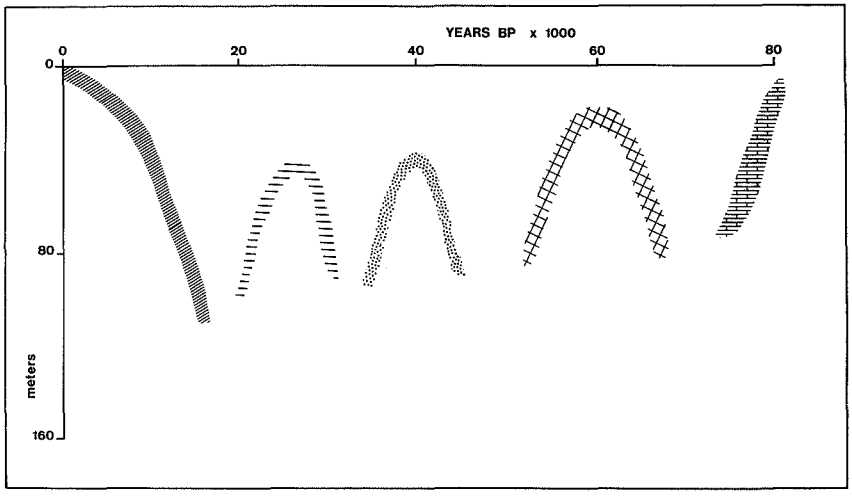

Figure 5.7a. Schematic Pleistocene sea-level curve used by James and Ginsburg (1979) in their model of Belize reef growth. Patterns correspond to Figure 5.7b.

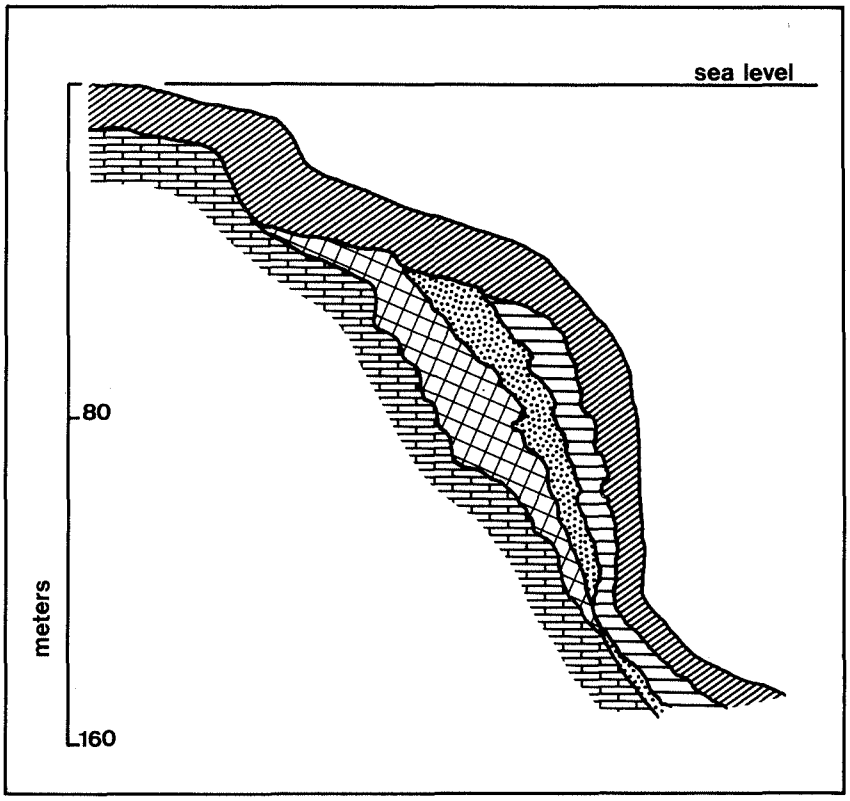

Figure 5.7b. Diagram showing the hypothetical Pleistocene development of the Belize reef margin (after James and Ginsburg, 1979).

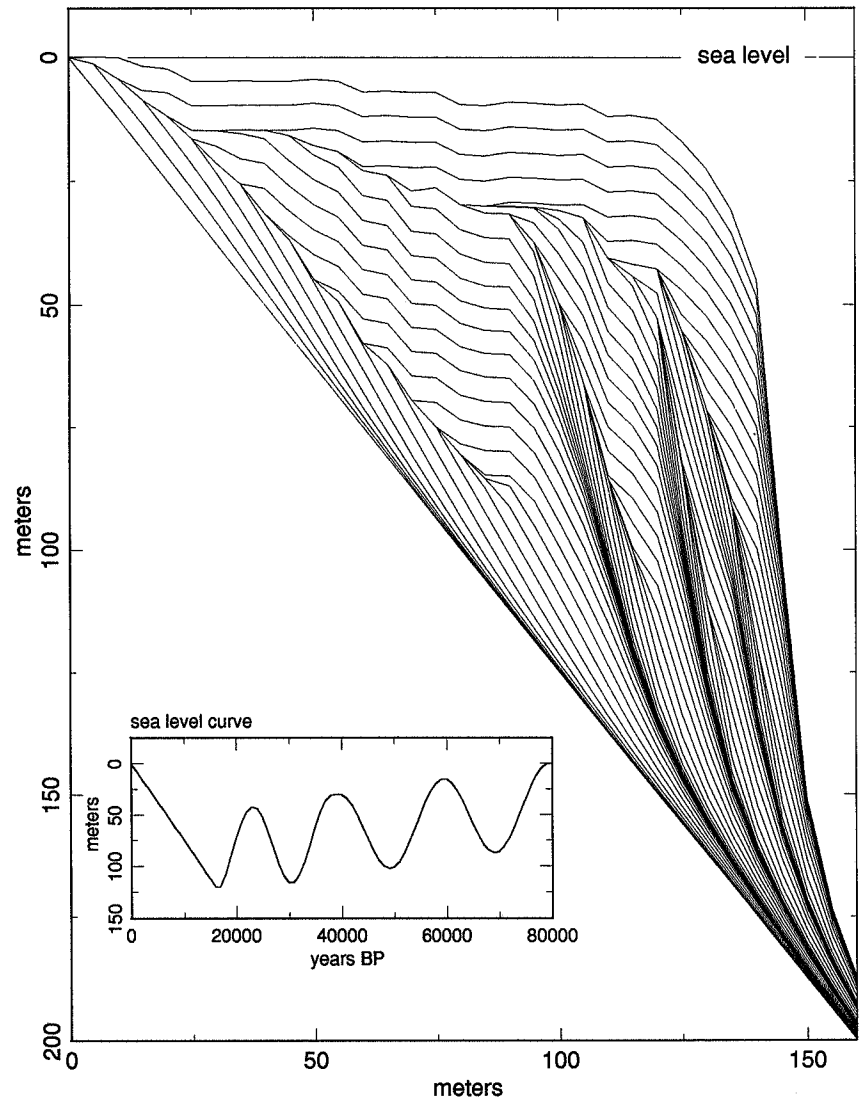

Figure 5.8. Result and sea-level input of computer simulation of the Belize reef margin. Surface plotted every 1000 yrs. (G_{max}: 5 mm/yr; k: 0.05 m^{-1}; I_0: 2000 µE m^{-2} s^{-1}; I_k: 250 µE m^{-2} s^{-1}). Note similarity to Figure 5.7b and the steep fore-reef wall.

Of course our model demonstrates only the possibility of generating a vertical reef wall by depth-dependent growth. We freely admit that a very similar result can be accomplished by cliff erosion during lowstands of sea level. In fact one of us (W.S.) still favors this erosion hypothesis for the origin of the wall (see James and Ginsburg, 1979: p.171).

DISCUSSION

The ability to simulate the above examples by using only a function that relates coral growth and light, indicates the dominant influence of light on reef growth. Other factors such as lateral sediment transport and accumulation are less important in framework-dominated reefs. In Belize, the steep seaward wall allows excess sediment to be shed to greater depths and thus prevents sediment from smothering reef growth. Alacran reef is an isolated reef complex rising above Campeche Bank from depths of 50 m, relatively open to wave and current energy allowing constant removal of sediment. The outer shelf reefs of the Central Great Barrier are framework dominated while detrital sediment becomes more important towards the inner shelf (Davies et al., 1985).

Attempts to simulate reefs that were not dominated by coral framework failed because of important accumulations of back-reef and fore-reef sediments and creation of fore-reef pavements. A comprehensive computer model for carbonate deposition requires an in-depth study and quantification of these additional factors, such as creation of lagoons, wave action, erosion and resedimentation.

The rates of vertical reef growth used in our model range from 5-12 mm/yr. These rates give good simulation results. They are similar to the 10-15 mm/yr range for reef growth given by Adey (1978) and Davies (1983), but they also correspond to the growth rates of reef-building head corals, such as Caribbean *Montastrea annularis* (see Fig. 5.1), and the Pacific coral *Porites lutea* (4-13.5 mm/yr; Buddemeier et al., 1974). This suggests dominant control of large head corals on rates of reef framework construction. Based on our model runs it seems reasonable to consider framebuilding by massive head corals as a measure of reef growth. Growth rates of branching corals such as *Acropora sp.* may exceed growth of massive head corals by an order of magnitude. However, bulk reef growth commensurate with these extreme rates (in excess of 100 mm/yr) has not been found. We assume that most of the skeletal growth of branching corals is turned into sediment that fills the interstices of the framework and nourishes the debris aprons around the reef. The production profile here is very useful in simulation of carbonate deposition and its relation to the biological and physical factors determining reef growth is straightforward.

CONCLUSIONS

This simple numerical model, based on coral growth as a function of light, successfully simulates the growth and demise of framework-dominated Holocene reefs. The same model also simulates the stepwise construction of a fore-reef wall during successive sea-level cycles. These modeling results emphasize the significance of light as the dominant control on reef growth.

Chapter 6

CARBPLAT - A COMPUTER MODEL TO SIMULATE THE DEVELOPMENT OF CARBONATE PLATFORMS

Abstract

This paper presents a computer simulation model for carbonate platforms with two new main components. First, it uses a function for the decrease of carbonate production with depth which combines the photosynthetic growth of carbonate producing organisms and the extinction of light with depth. Platform growth is simulated with a differential equation incorporating sea level. These processes therefore act continuously rather than in steps. Second, it attempts a more realistic approach to carbonate platform slopes by incorporating variation of slope angle with sediment composition. In this model, the angle at which slope sedimentation begins depends on the ratio between sediment produced on the platform interior (mud) and on the platform margin (sand). The shape of the slope is represented by an exponential function that can be changed to accommodate the total amount of slope sediment. The model produces stratigraphic unconformities on the fore-reef slopes due to changing sediment composition.

INTRODUCTION

In the last few years several computer programs for simulating carbonate platforms have been published (Bice, 1988; Bosence and Waltham, 1990; Lerche et al., 1987; Scaturo et al., 1989 ; among others). Each of these models illustrated the interplay of various mechanisms that shape carbonate platforms. It is still, however, a long way to the ultimate model for carbonate platform development. Our purpose is to add to the existing models by presenting a different approach to some of the factors controlling carbonate platform growth. Important additions we make to the current models are a new depth dependent function for carbonate production and variation of the slope angle based on sediment composition.

The production of carbonate decreases with depth. The biologial activity that accounts for most of the shallow water calcification depends on light for its photosynthesis. Production therefore decreases with depth based on the combination of the photosynthetic function (Chalker, 1981) and the exponential decrease of light with depth.

A carbonate platform produces most of its sediment in the upper part of the water column. The carbonate system is limited on the lower side by the decrease of light needed for photosynthesis, and on the upper side by sea level. Sediment produced close to sea level is most likely to be subjected to erosion and removal by waves, tidal currents or storms. This model incorporates a critical depth up to which sediment can accumulate and above which all sediment produced will be removed and shed on the adjacent platform slope.

In this model we describe the shape of the concave carbonate slopes with a simple exponential function. The angle of repose for slope sediments is strongly influenced by sediment cohesion and thus grain size (Kirkby, 1987). Kenter (1990) demonstrated that this rule also applies to large-scale carbonate slopes, where sediment fabric (grain-supported vs. mud-supported) determines the slope angle.

The model assumes that the sediment produced at the platform margin is sand and that produced in the platform interior is mud. We admit that this assumption is not strictly correct. However, there is good evidence that modern platforms such as Florida and the Bahama Banks shed predominantly sand and rubble from the margins while most of the mud is produced in the platform interiors (Neumann and Land, 1975). Sediment composition is used to determine the angle at which sedimentation on the slope can start (given that that point is below the wave base). The shape of the slope is subsequently adjusted to accommodate the total amount of sediment derived from the platform top.

THE PROGRAM

Input consists of production and growth parameters, sea level, and the geometry of the initial platform (see appendix and Fig. 6.1).
The program starts by constructing an initial platform consisting of a row (width) of columns (height). In situ production for each column is then calculated (maximum growth rate depending on the horizontal position on the platform, i.e., interior, back-reef, or margin) by solving a differential equation (eq. 1) for the duration of each time step. Sea level is incorporated into this function and accordingly changed continuously rather than in steps.

Production stops either when time runs out or when the minimum depth for sediment accumulation is reached (1 m in most of our runs) and the surface of the platform is adjusted accordingly. Overproduction in the upper part of the water column is calculated in the same fashion and stored separately. The total amount of overproduced sediment and the ratio between margin and interior sediment (back-reef is assumed to produce equal amounts of both) are calculated, and from this is figured the maximum angle of repose for slope sediments. The program now finds the position on the slope, below the wave base, where this angle is first reached. In an iterative proces the slope coefficient in the function we use to describe the shape of the slope (eq. 2) is then incremented in small steps until all sediment is accommodated. The program continues with production until the total number of time steps is reached.

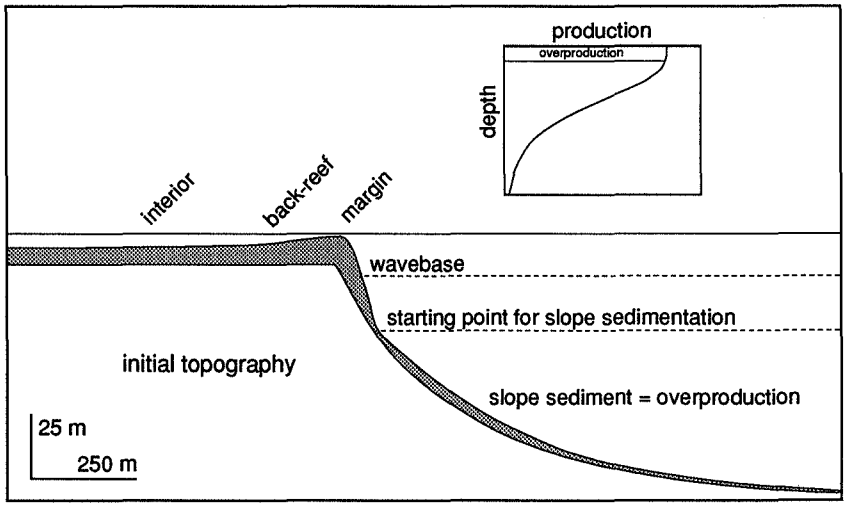

Figure 6.1. Basic platform geometry and important parameters used in CARBPLAT.

Initial Topography

The initial topography underlying a carbonate platform is important in determining the horizontal facies distribution and the position of most prolific reef margin growth on a platform. In most of our runs we used a flat topped platform with an exponential slope as initial input, but other options are possible (e.g., simple dipping surfaces). The height and width of the platform as well as the initial slope angle and shape can be varied.

Platform Growth

Carbonate platforms show a wide variety in facies distribution and growth or production rates. For our model, we constructed a basic platform configuration consisting

of a reef margin and a platform interior separated by a back-reef apron (Figure 6.1). The adjacent platform slope will be discussed in the next section. We use modern reef growth as an analogue for platform margin growth. Maximum rates for reef growth lie within the range of 5 to 15 mm/yr (Schlager, 1981; Davies et al., 1985). Platform interior or lagoonal production rates are well below the rates of platform margin growth as indicated by atolls and elevated reef rims of some platforms, such as the Great Barrier Reef. Reefs can outpace their lagoons up to 3 to 5 times (Davies, 1983; Smith, 1983).

Framebuilding by Scleractinian corals is the most important contributor to reef growth. We therefore used a function for the photosynthetic growth of reef-building corals (Chalker, 1981) combined with the decrease of light with depth to describe platform margin growth (Bosscher and Schlager, 1992a). Production in the platform interior is assumed to decrease in a similar way because it also depends on photosynthesis for calcification.

Depth, the most important factor in determining growth rates, depends on variations in the relative sea-level position. This yields the following simplified differential equation:

$$dh/dt = G_{max} \tanh \{I_0 \exp[-k (s_t-h_t)] / I_k\}, \qquad (1)$$

where G_{max} = maximum growth rate; I_0 = surface light intensity; I_k = saturating light intensity; k = light extinction coefficient; s_t = sea level; h_t = platform height.

This equation is solved for each segment of the platform profile with G_{max} dependent on the horizontal position on the platform (i.e., interior, back-reef, or margin). In our model, production does not elevate the platform surface right up to sea level but rather to a base level, i.e., the depth to which sediments can build and above which sediment will be subject to removal by waves. Production above this point is calculated in the same fashion as in situ production but is stored separately to be distributed on the adjacent slope after each time step.

Considering the time scale and process rates used in our runs, we neglected the effects of subaerial erosion and compaction.

Slope Sedimentation

We use a simple exponential function (eq. 2) to describe carbonate platform slopes. The exponential character of sedimentary slopes has been recognized in prograding deltas (Kenyon and Turcotte, 1985). Several carbonate platforms have been shown to also possess exponential slopes (F.Jacobs and W.Schlager, 1990, personal commun.).

$$h(x) = h_0 \exp(-fx), \qquad (2)$$

where h(x) = height on slope; h_0 = height of slope; x = distance from platform margin; f = slope coefficient.

Carbonate platform flanks are almost exclusively made up of sediments shed by the platform itself. The composition of this platform sediment overproduction determines the angle that the sediments can maintain (Kirkby, 1987; Kenter, 1990). In our model, the ratio between sediment produced by the platform margin (sand) and platform interior (mud) determines this angle (back-reef is assumed to produce equal amounts of both). Muddy sediments will have an angle of repose close to the minimum angle used as initial input. Increasing the amounts of margin material will cause the slope angle to increase towards the maximum angle of repose for non cohesive sand and rubble.

The program calculates the angle between adjacent points on the slope to determine the starting position for slope sedimentation. This is the point where the angle of repose, derived from the sediment composition, is first reached. Because sediment on the slope is subject to removal by waves, the starting point for slope sedimentation has to be below a given wave base. After each time step a certain amount of sediment has to be distributed on the slope from this starting point basinward. This is done in an iterative process in which the slope function is incremented in small steps until all sediment is accommodated.

Sea level

Sea-level variations can be introduced as linear or sinusoidal functions, or as a combination of both. Input consists of initial sea-level position, linear component, sinusoidal frequency, and amplitude. Although the example runs shown here use simple relative sea-level variations, the program allows superposition of longer term trends (e.g., subsidence) on eustatic sea-level variations.

RESULTS

Figure 6.2 shows simulation runs of the program to illustrate the development of a carbonate platform under various sea-level conditions: fast rise, slow rise, stillstand, and fall.

A fast sea-level rise will cause elevation of the rim over the platform interior. Overproduction is nearly zero and limited to the platform margin, resulting in a platform constructed almost exclusively by in situ production (Fig. 6.2a). A reduction of the rate of sea-level rise will result in increased amounts of sediment to be shed on the slope, still dominated by margin and back-reef material. Progradation is relatively fast with a steepening slope (Fig. 6.2b).

A sea-level stillstand will see overproduction of the platform interior resulting in a more gentle slope. The prograding reef margin tends to steepen and slope sediment bypasses the upper slope to form a wedge of sediment on the lower slope (Fig. 6.2c).

A downstepping fringing reef margin with a relatively steep debris apron will develop under regressive conditions (Fig. 6.2d).

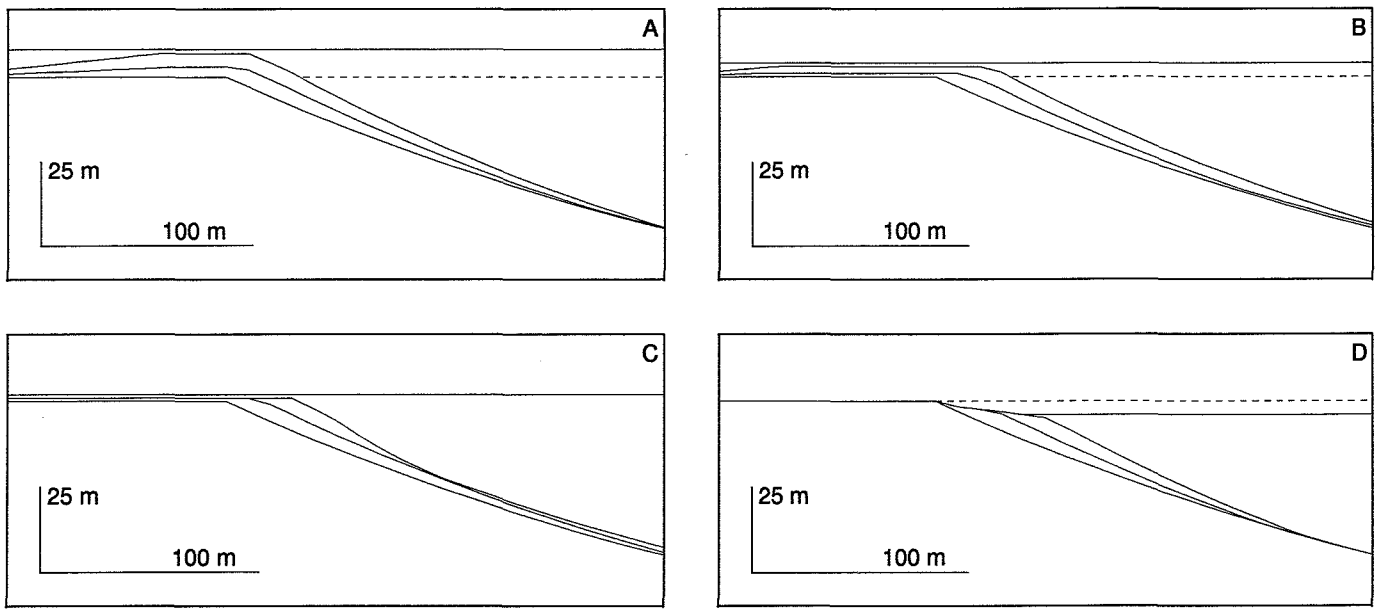

Figure 6.2. CARBPLAT output of one initial platform subjected to four different sea-level regimes. **A**: Sea level rising at a rate of 8000 mm/ka. **B**: Sea level rising at a rate of 4000 mm/ka. **C**: Sealevel remaining constant at 2 m above initial platform top. **D**: Sea level falling at a rate of 4000 mm/ka. Dashed line = initial sea-level position. Solid line = final sea-level position. Other input parameters: run time = 1000 yr;timestep = 100 yr;platform width = 500 m;platform height = 100 m; back-reef width = 100 m;initial angle top of slope = 20 °; margin growth rate = 10000 mm/ka;interior growth rate = 2000 mm/ka; wave base = 10 m; minimum depth of sediment accumulation = 1 m;minimum slope angle;maximum slope angle 35°;light extinction coefficient 0.02 m^{-1};light saturation occurs at 10% of surface light levels. Surface plotted every 500 yr. Plots illustrate only part of calculated sections.

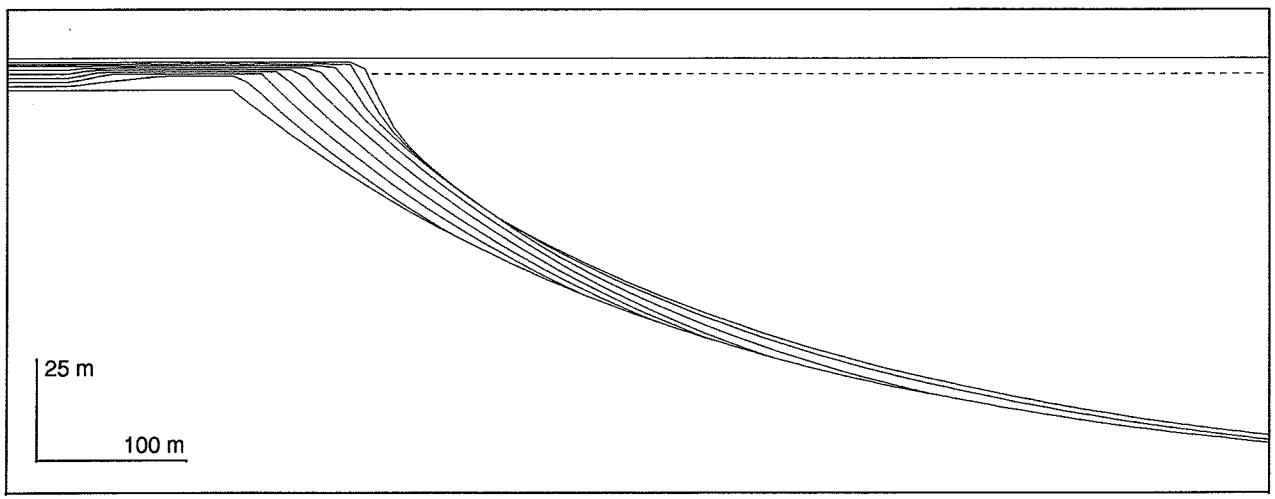

Figure 6.3. CARBPLAT simulation of platform subjected to linear sea-level rise, illustrating effect of variations in textural composition on platform geometry. Change from catch-up to keep-up growth causes overproduction and shedding of sediment onto slope. At first, only sand (reef debris) is being shed, but when platform interior fills up to base level and platform enters keep-up stage, increasing amount of mud reduces angle of repose causing bypassing of steep upper slope and unconformity on lower slope. Dashed line = initial sea-level position. Solid line = final sea-level position. Input parameters: run time 4000 yr;time step 100 yr;platform width = 500 m;platform height = 100 m;sea-level rise = 100 mm/ka. For all other parameters see Figure 6.2. Surface plotted every 500 yr. Plot illustrates only part of calculated section.

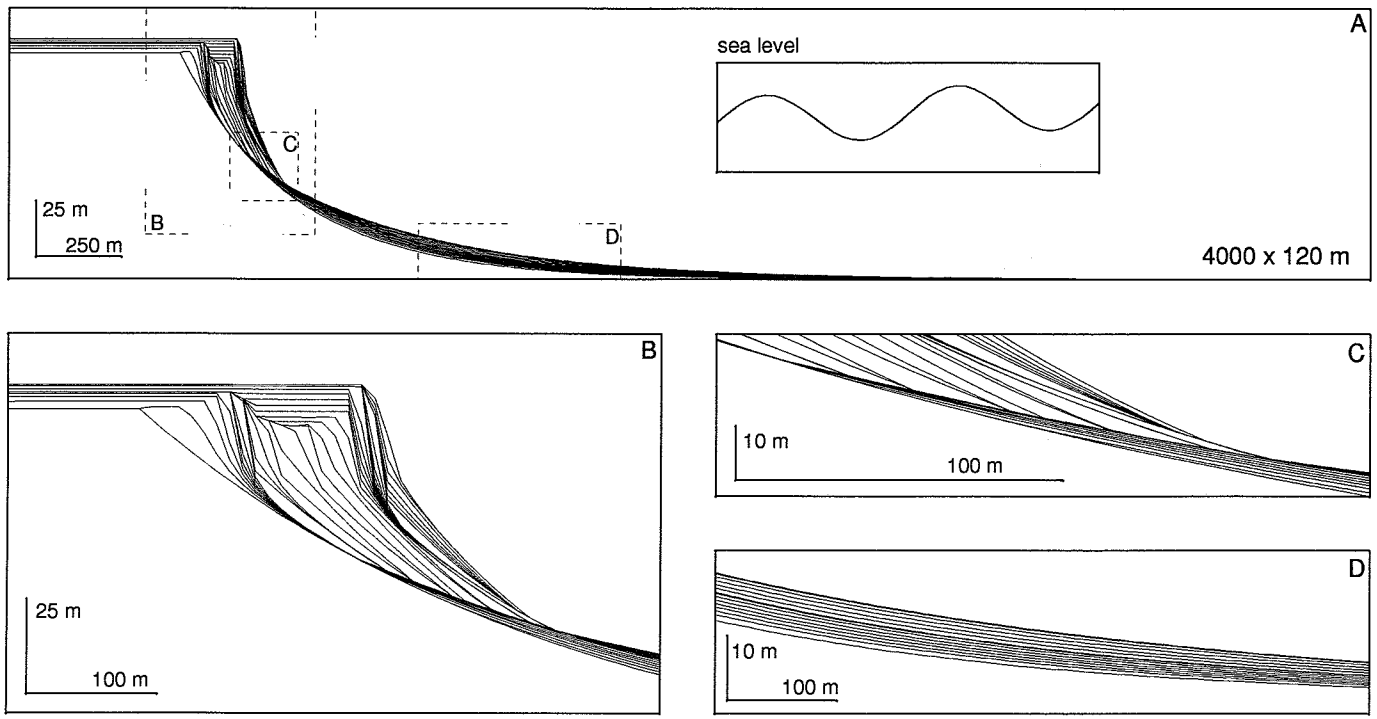

Figure 6.4. CARBPLAT simulation using sinusoidal sea-level rise and the following input parameters (see text for discussion of results): run time = 40000 yr;time step = 1000 yr;platform width = 500 m;platform height = 100 m. Sea-level input: linear rise = 100 mm/ka;sinusoidal frequency = 20 ka;amplitude = 5 m. For all other parameter values see Figure 6.2. **A**: Total calculated section. **B**: Enlarged section of margin geometry. **C**: Downlap of steep, prograding slope onto more gentle, muddy, slope sediments during falling sea level. **D**: Two thinning-upward cycles on lower slope.

Changes in sediment composition and resulting unconformities are not necessarily caused by sea-level fluctuations. This is shown in Figure 3, where a linearly rising sea level induces changes in sediment composition that lead to bypassing of the upper slope and accumulation of muddy sediments on the lower slope.

Figure 6.4a shows a carbonate platform subjected to a sinusoidal sea-level rise. Combinations of the basic responses mentioned above result in a complex progradation geometry with internal unconformities caused by changing sediment composition and slope angles in response to varying sea level (Fig. 6.4b).

Flooding of the initial platform increases the amount of mud to be shed on the slope and thus causes reduction of the slope angle and bypassing of the steep upper slope resulting in a wedge of muddy sediment accumulating on the lower part of the slope. A subsequent sea-level fall shuts off interior production, and a thinning upward cycle is formed on the lower slope (Fig. 6.4d). A fringing reef margin with a sediment apron (consisting of reef debris) downlapping on the more muddy slope sediments follows (Fig. 6.4c). Progradation continues in a similar fashion until the rising sea level starts reflooding (part of) the platform, and slope sedimentation again bypasses the steep upper slope. Figure 6.4 shows two of these sea-level cycles, as illustrated by two thinning upward cycles in the muddy slope sediments (Fig. 6.4d).

DISCUSSION

This model adds new factors that, together with the current carbonate platform models, will improve the understanding of the interplay of the various factors that shape carbonate platforms.

The dependence of the shallow water 'carbonate factory' on biological processes driven by photosynthesis, is represented by the use of a photosynthetic function to construct a depth dependent production function. Although existing models incorporate depth dependent production functions (e.g., Bice, 1988 ; Bosence and Waltham, 1990), the function used here more clearly establishes the link between process and model.

Stratigraphic unconformities, separating strata with different depositional angles, are important features in the sequence stratigrapy of carbonate platforms. Based on the observation that depositional angles depend on textural composition of slope sediments, the model shows that such unconformities can be created in a variety ofways. Not only sea-level fluctuations can cause changes in production of sediment on the platform and produce stratigraphic unconformities (Fig. 6.4). A change in platform size or style of response to sea-level variations, e.g., from catch-up to keep-up will have a similar effect (Fig. 6.3).

Of the numerous factors that determine the development of carbonate platforms, CARBPLAT can illustrate the role and interplay of: platform geometry, carbonate production, slope sedimentation, and sea-level variations (appendix 1).

To allow forward modeling of carbonate platforms, one needs not only to test geological examples but to first of all unravel the underlying controls.

Appendix 6.1. Parameters used in CARBPLAT.

Platform geometry
- platform width
- platfrom height
- back-reef width
- slope coefficient (angle)

Growth and production
- maximum reef growth
- maximum platform interior growth
- surface light intensity
- saturation light intensity
- light extinction coefficient
- minimum depth of sediment accumulation

Slope sedimentation
- wavebase
- minimum angle for carbonate slope sediment
- maximum angle for carbonate slope sediment

Sea level
- initial sea-level position
- linear sea-level variation
- sinusoidal sea-level variation (frequency and amplitude)

Chapter 7

PLIOCENE/PLEISTOCENE PLATFORM FACIES TRANSITION RECORDED IN CALCITURBIDITES (EXUMA SOUND, BAHAMAS)

Abstract

The composition of Pliocene-Pleistocene calciturbidites of ODP Hole 632A (Exuma Sound, Bahamas) has been determined by point-count analysis of thin-sections in order to correlate basin/platform events which influenced sedimentation. Strontium isotope chrono-stratigraphy has been used to correlate basin turbidite compositional variations to the evolution of the platform, as documented by magnesto-stratigraphy. Magnetostratigraphy of Great Bahama Bank cores shows that between 3.4 and 2.5 Ma (Late Pliocene) ooids and peloids became the dominant sediments across the platform. After this period the platform has been subjected to a series of subaerial exposure events. This led to slow accumulation on the platform and starvation of the basin. Around 1 Ma the platform was reflooded, the transgression being followed by an increased production of ooids. There is a change in calciturbidite composition in the earliest Pleistocene coinciding with a regional unconformity. Pleistocene turbidites, containing abundant skeletal material and ooids, overlie Pliocene/early Pleistocene turbidites, rich in mud and skeletal material. The duration of the hiatus, represented by the unconformity, based on $^{87}Sr/^{86}Sr$ dating is 1.0 - 0.7 Ma. Prior to this hiatus sedimentation rates in the basin are an order of magnitude lower than present-day accumulation rates. We conclude that reflooding of the platform around 0.8 Ma led to shedding of both non-skeletal and skeletal sediments. The change of Great Bahama Bank from a Pliocene reef-rimmed skeletal platform to the present-day flat-topped bank, dominated by non-skeletal sediments, can be correlated with the observed change in turbidite composition.

INTRODUCTION

From studies on a series of bore-holes Beach and Ginsburg (1980) made a twofold division in the subsurface bank-interior sediments across Great Bahama Bank: a lower unit of poorly stratified skeletal packstones/wackestones, and an upper unit of poorly stratified packstones and wackestones, containing mainly peloids and ooids. The relatively sharp change from skeletal to non-skeletal limestones was used to define the base of a new formation, the Lucayan limestone (Beach and Ginsburg, 1980). This change in platform facies was interpreted to reflect the transition from an atoll-like platform, in the early Pliocene, to the present-day, flat-topped bank (Fig. 7.1; Beach and Ginsburg, 1980). Subsequent collection and magnetostratigraphic dating, of shallow core borings, and the acquisition of seismic profiles across Great Bahama Bank, has been used to refine this model. These show that the platform had a ramp/shelf geometry rather than a true atoll configuration (Eberli and Ginsburg, 1987; McNeill, 1989).

The present-day facies distribution on the Bahamas shows a platform interior dominated by non-skeletal sediments, with peloidal sands, oolite shoals, mud and occasional patch reefs. This platform interior is surrounded by a 1-10 km wide zone of skeletal sands. Reefs and eolian islands also occur, predominatly on the windward side (Enos, 1974). The Pliocene Bahamas were rimmed by reefs on the windward as well as on the leeward side and had a relatively deep lagoon containing mainly skeletal deposits (Beach and Ginsburg, 1980).

The skeletal to non-skeletal transition took place during the late Pliocene (Beach and Ginsburg, 1980; Williams, 1985; McNeill, 1989), probably as a result of a change in frequency and amplitude of sea-level fluctuations with the onset of glaciation in the northern hemisphere (Shackleton et al., 1984). Based on magnetostratigraphy of Great Bahama Bank cores, it appears that the transition was initiated in the platform interior around 3.4 Ma. Non-skeletal sediment then moved progressively eastward, reaching the margin by about 2.5 Ma (McNeill, 1989). Subsequent subaerial exposure resulted in low sediment accumulation rates and hiatuses in the adjacent basins. Reflooding of the platform, at around 1 Ma, increased rates of production on the platform once again.

We have studied a succession of calciturbidites and periplatform oozes recovered in ODP Core 632A (Exuma Sound, Bahamas) to determine whether the facies transition on the platform was reflected in the composition of the bank-derived turbidites and whether this stratigraphic turning point could be used to correlate from the platform to the basin (Reijmer et al., 1988; Schlager et al., 1990). Because of the lack of reliable biostratigraphic datum levels (Melillo, 1988; Watkins and Verbeek 1988), $^{87}Sr/^{86}Sr$ chronostratigraphy was used to correlate between the platform and basinal turbidites.

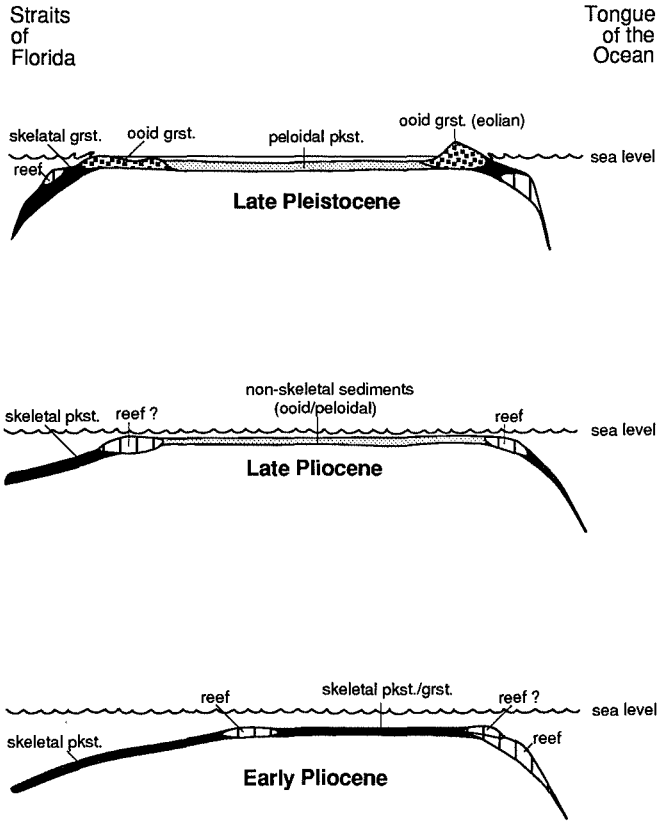

Figure 7.1. Schematic drawings showing the difference in platform geometry and facies distribution between the early Pliocene and late Pleistocene: Reef rimmed platform, skeletal dominated, with a relatively deep lagoon versus a flat topped bank dominated by non-skeletal sediments (late Pleistocene after Schlager and Ginsburg, 1981).

METHODS

Core material and sampling

ODP Hole 632A is situated in Exuma Sound, Bahamas at 23° 50.44' N, 76°26.13' W in a water depth of 1996 m (Fig. 7. 2). Hydraulic piston cores reached a total depth of 141.0 m below sea-floor. Cores 4, 5 and 6 were selected for this study. Identification of turbidites and debris flows was based on the shipboard core descriptions and subsequent descriptions using criteria outlined by Droxler and Schlager (1985). Samples were taken from the coarse-grained intervals. The samples were impregnated with an epoxy resin and thin-sectioned.

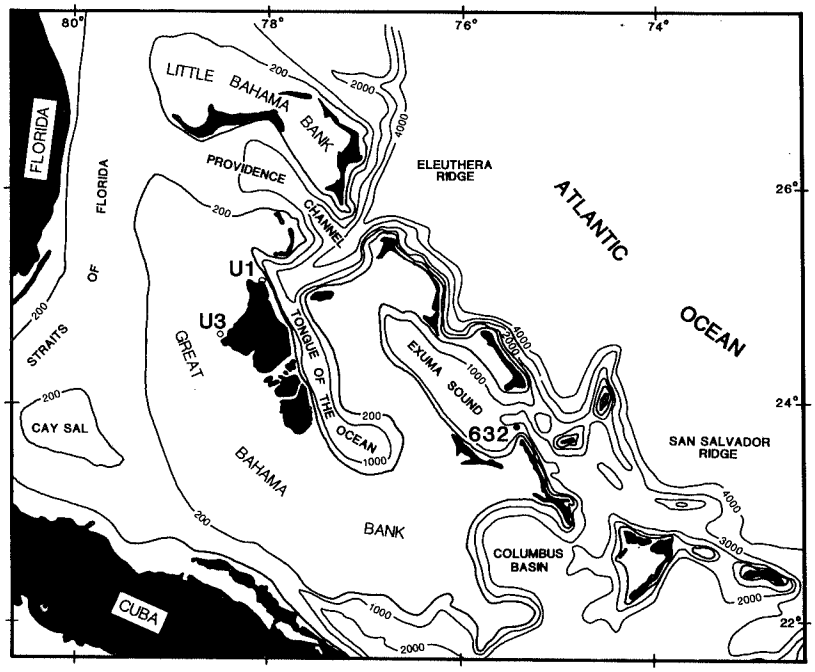

Figure 7.2. Map showing the location of Site 632, ODP leg 101 (Exuma Sound, Bahamas) and platform cores U1 and U3 on Great Bahama Bank. The platform cores have been dated with magnetostratigraphy (McNeill, 1989).

Point-count analysis

The composition of the calciturbidites was determined using the point-count method of Chayes (1956). In every thin section 200 points were counted. In total 66 thin-sections were point-counted using the following categories: 1) ooids/grapestone; 2) mud; 3) pelagic forams, pteropods; 4) peloids; 5) lithoclasts; and 6) neritic skeletal grains. These categories represent the main platform grain types.

Sr-isotope chronostratigraphy

Methods used to separate and collect Sr from $CaCO_3$ are as described in Beets (1991). Bulk samples of approximately 50 mg $CaCO_3$ were dissolved in 500 µl 20% v/v suprapure (quartz-distilled) acetic acid. After 2 hours at room-temperature the solutions were centrifuged and the supernatant liquid was collected, evaporated and subsequently redissolved in 250 µl 1.5 N HCl. 50 µl of sample-solution was used for high-pressure chromatography to separate and concentrate Sr. 1 µg Sr was loaded on double-rhenium

filaments and measured on a Finnigan MAT 261 in static collector, double-jump mode. The measured $^{87}Sr/^{86}Sr$ ratio represents an average of 80 scans at 4 to 6 x 10^{-11} A, corrected for possible Rb interference and normalized to $^{88}Sr/^{86}Sr$ = 8.37521. NBS 987 strontium standard at the CIGO-VU laboratory is routinely measured as 0.710255 ±0.000016 (n=36).

The $^{87}Sr/^{86}Sr$ seawater curve , which is calibrated directly to the Geomagnetic Polarity Time Scale (GPTS) has proven to be useful in dating of marine carbonates (see for instance Ludwig et al., 1988; Quinn et al., 1991). The strong increase in ^{87}Sr during the last 2.4 Ma of 0.000051/Ma (Capo and DePaolo, 1990; Hodell et al., 1991; Beets, 1991) provides a relatively good chronostratigraphic resolution for the Sr isotope method. Theoretically the stratigraphic resolution amounts to 0.19 Ma (Capo and DePaolo, 1990; Hodell et al., 1991) or 0.29 Ma (Beets, 1992) at the 80% confidence interval.

RESULTS

Figure 7.3 shows the stratigraphic position and composition of the turbidites in the studied section of ODP Hole 632A. Several trends are recognizable. There is an overall increase in carbonate mud content in core 6, combined with a reduced input of skeletal grains. At ca. 45 m, the amount of mud drops by approximately 35% and the content of skeletal material increases to over 50%. This change coincides with a regional unconformity and the appearance of ooids in the turbidites. At the top of core/section 4H-5 the content of ooids increases to 30%. Compared to cores 4 and 5, core 6 contains thinner turbidites and more periplatform ooze.

We dated two samples above and two samples below the unconformity that separates cores 5 and 6 (see Fig. 7.3).

Figure 7.4 shows the results of the $^{87}Sr/^{86}Sr$ analyses and the calculated ages based on the age models of Beets (1991), and Capo and DePaolo (1990) combined with Hodell et al. (1991). The sample directly overlying the hiatus, 5cc-189/191, yields an age of 0.71 Ma. This is not distincly different from the age of the sample 3.75m above, 5H-4-137/139, which has an age of 0.79 Ma. The sample directly below the hiatus, 6H-1-005/007 has an age of 1.03 Ma and the age of the sample 3.75 m below, 6H-3-054/056 yields an age of 2.07 Ma. Based on these dates the time-span for the hiatus is 0.3 Ma. These data also show an increased sediment accumulation rate in the Pleistocene by comparison with that of the late Pliocene/earliest Pleistocene (see Fig. 7.5a).

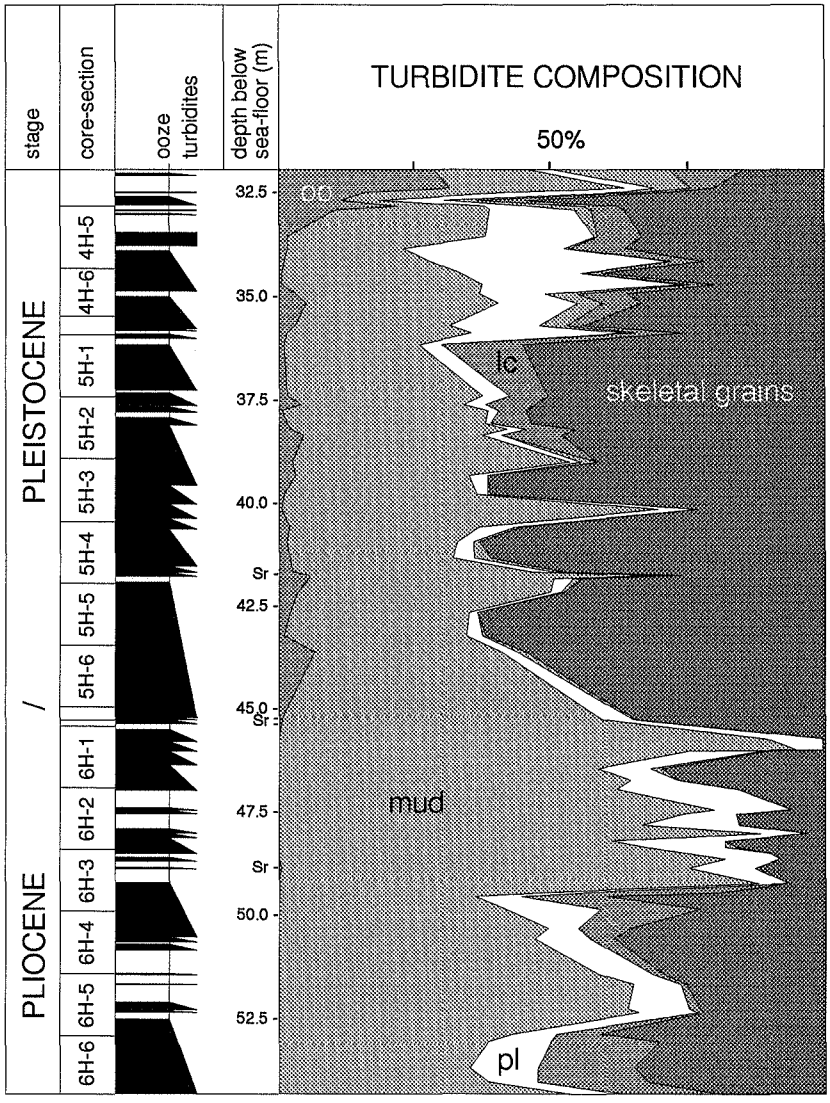

Figure 7.3. Sedimentology and Pliocene-Pleistocene calciturbidite composition of ODP Hole 632A (oo: ooids; pl: planktonics; lc: lithoclasts; minor peloidal material is indicated in between planktonics and lithoclasts). Sr indicates sample points for Sr isotope analysis. Core-section 5H-7 and 5H-cc are located between 5H-6 and 6H-1. For discussion see text.

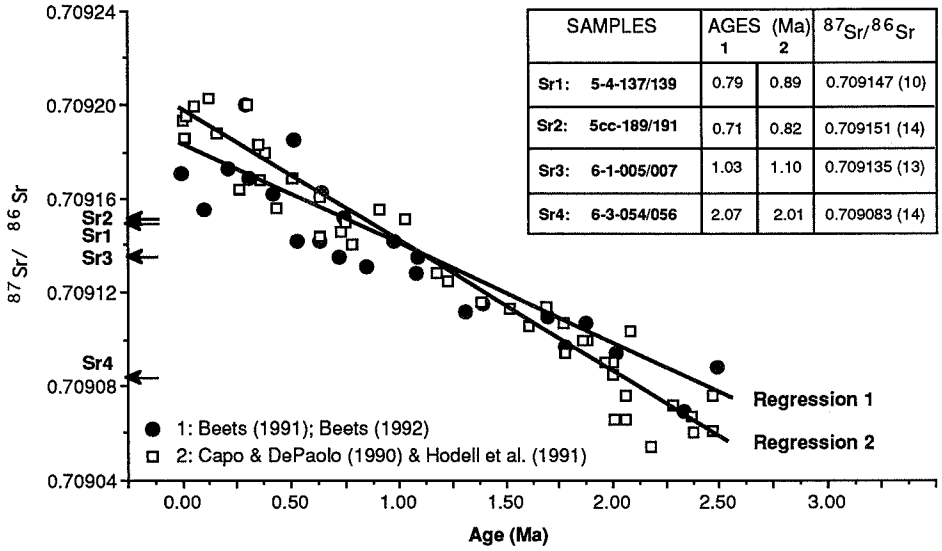

Figure 7.4. The equation for the linear regressions throught the different $^{87}Sr/^{86}Sr$ datasets are:
age(Ma) = 14183.818 - 20000.123*($^{87}Sr/^{86}Sr$) R^2 = 0.847 (1)
age(Ma) = 12386.656 - 17465.723*($^{87}Sr/^{86}Sr$) R^2 = 0.950 (2)
Age (Ma) on the horizontal axis, $^{87}Sr/^{86}Sr$ isotope ratios on the vertical axis. The inferred ages for the samples (core-section-depth in section in cm) derived from the measured $^{87}Sr/^{86}Sr$ isotope ratios are indicated in the upper right corner of the diagram. Uncertainty in ages based on 80% confidence interval (standard error of estimate) are 0.29 Ma and 0.19 Ma for eqs. 1 and 2 respectively.

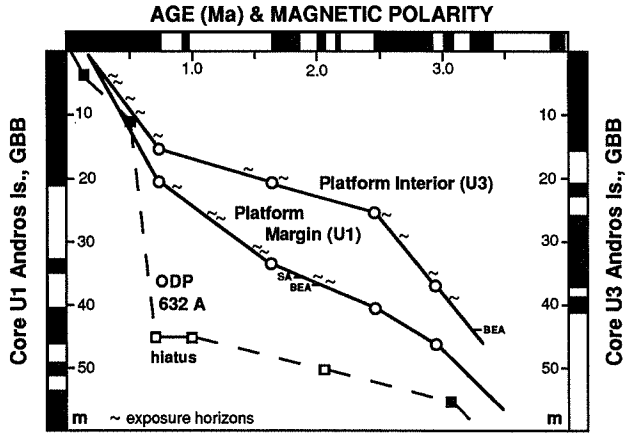

Figure 7.5a. Summary of platform and basin ages. Solid lines depict the approximate age-depth relationship for the platform margin (U1) and a platform interior (U3) core on Great Bahama Bank in the vicinity of Andros Island. Biostratigraphic tie-points are represented by the late Pliocene disappearance of the coral *Stylophora affinis* (SA) and the Bowden Equivalent Assemblages of molluscs (BEA). The magnetostratigraphic age ranges are constrained only to the age of the polarity chron or subchron. The dashed line represents the age-depth accumulation history for ODP Hole 632A, based on Sr isotope dating (open squares) and biostratigraphic dates (black squares) of Reijmer et al. (1988) and Melillo (1988).

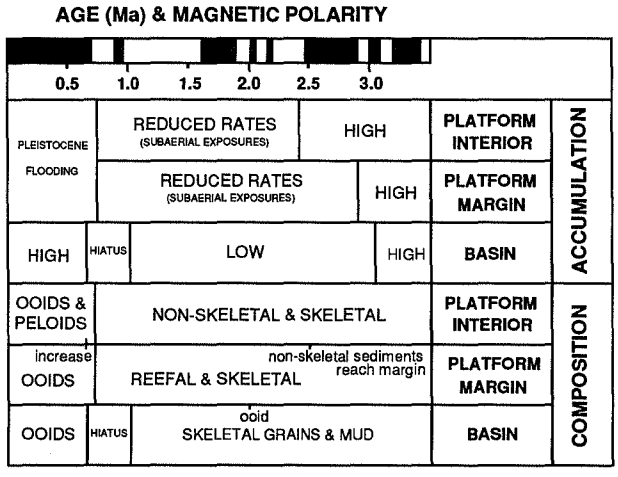

Figure 7.5b. A comparison of events influencing the accumulation rates on the platform and in the basin. In addition, a comparison between the production of sediments on the platform and the response in the basinal calciturbidites is displayed.

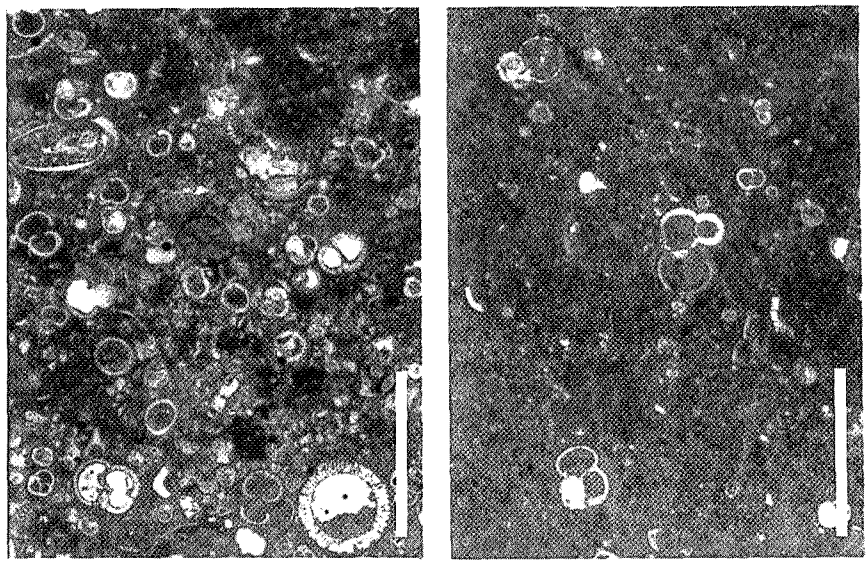

Figure 7.6. Photomicrographs of the main sediment types encountered in the calciturbidites. Scale bars 1 mm. **A** (left): Sample6H-5-093/095: planktonic foraminiferal, skeletal wackestone. **B**: Sample 6H-5-110/121: planktonic foraminifer-bearing mudstone.

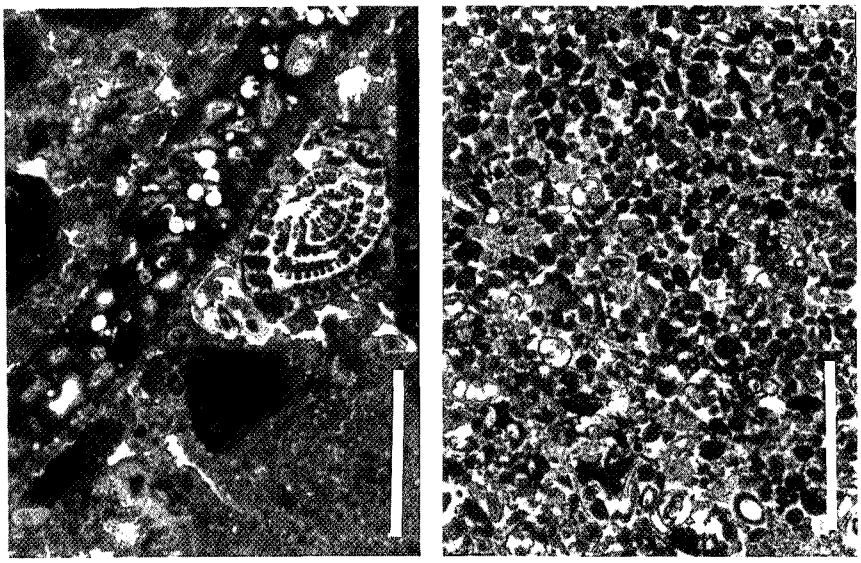

Figure 7.6 (continued). **C** (left): Sample 5H-5-070/072: ooid-bearing, skeletal wackestone-packstone. **D**: Sample 4H-4-73/75: peloidal, ooid grainstone.

DISCUSSION

Age/depth curves of cores U-1 (platform margin) and U-3 (platform interior) show three main phases of accumulation (Fig. 7.5a; McNeill et al., 1988; McNeill, 1989). Relatively rapid accumulation typified the phase prior to 2.4 Ma (late Pliocene) and also that post-dating 0.8 Ma (middle Pleistocene). These phases are separated by a period of reduced accumulation rates. The age/depth curve reconstructed for ODP Hole 632A and all other ODP holes in Bahamian Basins have a similar shape (Leg 101 Scientific Party, 1988; p.470). The sediment accumulation rate for the interval from the first datum-level (sample 6H-3-054/056) to the uncinformity is 3.4 B (m/Ma), nearly an order of magnitude lower than the average rate for Exuma Sound (Reijmer et al., 1988). This period correlates with a stratigraphic interval of closely spaced karst horizons on the platform, indicating a period of prolonged subaerial exposure of Great Bahama Bank (McNeill et al., 1988).
This corresponds to onset of glaciation in the northern hemisphere at around 2.4 Ma (Shackleton et al., 1984) and a corresponding long-term fall of sea-level. The late Pliocene to early Pleistocene turbidites of core 6 are thinner than their counterparts from cores 4 and 5, and separated by relatively thick periplatform ooze deposits.

This period coincides with the aforementioned series of exposure events on the platform, leading to starvation and low sedimentation rates in the basin (Fig. 7.5b). The shedding of platform sediments into the adjacent basin coincides with increased aggradation and prolonged flooding of the platform top, illustrating "highstand shedding" of carbonate platforms.

Changes in the calciturbidite composition seem to have responed to the processes affecting the production on the platform (Fig. 5b). The late Pliocene to Early Pleistocene turbidites of core 6 are rich in mud with some minor skeletal input (Figs. 6a and b). Magnetostratigraphic dates (McNeill, 1989) show that non-skeletal sediments encroached on the eastern margin of Great Bahama Bank by the middle of the late Pliocene, around 2.5 Ma. This was just prior to the period of subaerial exposure that lasted through much of the Late Pliocene and Early Pleistocene (Fig. 5b; McNeill, 1989). During this period two flooding events are recorded from about 2.0 to 1.6 Ma. The trace of ooids in core 6H section 3 dated by Sr isotopes as 2.07 Ma may represent one of these events, and the subsequent shedding of ooids and non-skeletal sediments off the platform.

Another change in turbidite composition occurs at an unconformity within the section spanning the interval from 1.0-0.7 Ma which falls within nannofossil subzone CN14a (Watkins and Verbeek, 1988). The duration of the interval might be shorter as indicated by Sr age dates of the sediments overlying the unconformity, older ages higher up core possibly being due to resedimentation of slope sediments. Following this unconformity, although in low percentages, ooids appear in the turbidites combined with an increase in skeletal material (Fig. 6c). So, the major increase in shedding of ooids and skeletal material occurs in the turbidites from the unconformity upwards, in sediments younger than ca. 0.7 Ma.

We infer that the appearance of ooids in the bank-derived turbidites is coeval with the change in depositional style that defines the base of the Lucayan Limestone on the platform interior. The progressive shallowing of the platform interior allowed the formation of ooids, and shedding of non-skeletal as well as skeletal material from the platforms into the adjacent basins. The significant increase in skeletal material in the calciturbidites might also be related to the renewed development of a relatively broad zone of reefs surrounding the shallow platform (McNeill, 1989).

The major production of ooids on Great Bahama Bank, however, started post 0.73 Ma, with the ooid package along eastern Great Bahama Bank, and for the first time the formation of thick oolitic eolianites (Andros Island) (McNeill, 1989). Higher up in core 4H of Hole 632A ooids appear in the turbidites in vast quantities (Figs.3 and 6d). The initiation of production of these type of grains is detected in the turbidites from the unconformity upwards in sediments, 1 Ma or younger. Higher up in core 4H of Site 632A ooids appear in the turbidites in vast quantities.

From this study it is apparent that production and transport of sediments from carbonate platforms ceases when the platform is exposed, and alternatively the "carbonate factory" will be turned on by reflooding. This highstand shedding mode of sedimentation for carbonate platforms has been documented previously for the Bahamas (Droxler and Schlager, 1985; Reijmer et al., 1988; Haak and Schlager, 1989), and for example in the Maldives Archipelago (Dolan, 1989; Droxler et al., 1990), and the Queensland Shelf (NW Australia; Davies et al., 1989; Davies, Mackenzie et al., 1991).
We have demonstrated here the value of calciturbidites as recorders of platform history. They allow correlation of unconformities and facies changes from the platform into the basin, thus improving the understanding of spatial and temporal stratigraphic relationships.

PART III

ACCUMULATION RATES OF REEFS AND CARBONATE PLATFORMS THROUGH TIME

INTRODUCTION

Phanerozoic reefs and carbonate platforms contain nearly 600 million years of information on the balance between growth potential and relative sea-level. But unlike for the Holocene we do not have the chronostratigraphic resolution for the entire Phanerozoic to directly estimate growth potential from the accumulation rates of carbonate platforms. A compilation of accumulation rates does provide a minimum measure of the gowth potential and allows one to adress changes in shallow water carbonate accumulation (chapter 8). In chapter 9 we discuss the relation between accumulation rates and the interval of observation. This relation provides a basis for evaluating the growth potential of reefs and platforms.

GEOLOGIC HISTORY OF REEFS AND CARBONATE PLATFORMS

Evolution of reef-builders

Throughout the Phanerozoic reefs have been present in the world's oceans. Secretion of calcium carbonate by benthic organisms has allowed the construction of carbonate buildups that ranged from small carbonate mud mounds to impressive barrier reefs, hundreds of kilometres in length. The importance of organisms for the deposition of shallow water carbonate ties the growth and evolution of reefs and carbonate platforms to the evolution of these organisms. From the early Cambrian archeocyathid/algal buildups reef ecosystems have evolved into the present-day reefs dominated by scleractinian corals. During this period various organisms have alternatingly dominated the reef ecosystem. Sponges, algae, stromatoporoids, tabulate and rugose corals, bryozoans, rudist bivalves and many others have played their part in building reefs. The evolution of reef-builders has not been a gradual proces. The geologic history of reefs is punctuated by several mass extinctions of reef-builders. These mass extinctions are usually followed by periods of millions of years of slow recovery or even lack of reef growth. The pioneering and climax stages that follow these periods see the reestablishment of reef ecosystems (Copper, 1988). Several of these successions have been recognized in the geologic record. For thorough reviews see James (1984, 1992) and Copper (1988).

Paleozoic

The first reefs of the Phanerozoic were the *Renalcis* and Archeocyathid/algal build-ups of the early Cambrian. The extinction period that followed is still poorly documented. The resurgence of stromatolites that were important reef-builders before the Phanerozoic marked this period. Skeletal metazoans started to play a role in reef-building again in the middle Ordovician. Middle to early Late Ordovician reefs were dominated by stromato-poroids, corals, bryozoa and calcifying sponges. The end of the Ordovician is characterized by very depauperate reef development. Early Silurian reef development is seen as a pioneering stage that led to the haydays of Paleozoic reefs during late Silurian to late Devonian. In the late Devonian numerous carbonate platforms and reef complexes were present. Some examples are the reef tracts in Alberta, Canada, the impressive barrier reef complex of the Canning Basin in Australia and numerous reefs in western Europe. The dominant reef-building organisms during this period were rugose and tabulate corals and stromatoporoids. The Frasnian-Famennian extinction decimated reef-builders and in the Famenian reefs had nearly vanished In some places reef-builders were replaced by stromatolites (e.g. Canning Basin, Australia). The Frasnian-Famennian crises reduced the global reef area from an estimated five to six milion square kilometres to less than ten thousand (P. Copper, pers. comm. 1992). The Carboniferous has been a period of very depauperate reef development. Climatic and oceanic conditions and the presence of one big landmass (Pangea) reduced the opportunities for reef development. Most Carboniferous reefs were mudmounds inhabited by mainly bryozoans, algae and encrusting foraminifers. Towards the end of the Carboniferous and during the Permian calcisponges, new types of skeletal algae and Tubiphytes appeared and dominated reefs. In the late Permian reef development started to decline and the most dramatic biotic extinction in the Geologic record at the Permo-Triassic Boundary put it to a complete halt.

Mesozoic

No reefs are known from the earliest Triassic (Scythian; Stanley, 1981). The calcite secreting organisms that dominated Paleozoic carbonate buildups were replaced in the Triassic by organims that secrete aragonitic skeletons (scleractinian corals and bivalves) probably due to changes in ocean chemistry. Some of the pre-Mesozoic reef-builders continued in the Triassic such as Tubiphytes, calcisponges and some types of calcareous algae but from the middle Triassic scleractinian corals became significant and by the end of the Triassic dominated the reef ecosystem. Some of the most impressive carbonate buildups from this period are the carbonate platforms that lined the Tethys ocean in the Northern Calcareous Alps in Austria and the Dolomites in Northern Italy. These platforms attained overall thicknesses of up to two kilometres. The Triassic reef communities were a mix of Paleozoic 'survivors' and the new 'truly Mesozoic' reef-builders, of which the scleractinian corals are the most noticable. The end Triassic extinction affected all reef-building organisms but the Paleozoic 'holdovers' never again regained their former role as reef-builders. Early Jurassic reefs are characteristic of a reef community immediately following

an extinction period. They were mounds produced by calcisponges and algae and an impoverished 'Triassic" coral and bryozoa fauna. From this period also bivalve mounds formed by lithiotid and megalodont bivalves are known. Sometime during the Middle Jurassic, reef complexity rose back to the late Triassic level. Complex reefs dominated by scleractinians, calcisponges and stromatoporoids, with an all-time high in coral diversity, are known from many regions, such as the Atlas Mountains in Morocco. The relatively minor extinction event at the Jurassic/Cretaceous boundary did not have a major effect on reef evolution. The coral, algal stromatoporoid buildups from the Jurassic persisted in the early Cretaceous. During the middle and late Cretaceous the major group of reef-building organisms was formed by the Rudist bivalves. They replaced corals and stromatoporoids in many environments. These large sessile organisms adapted to a wide range of environments from high-energy to very restricted. Whether they constructed reefs in a modern sense is still a matter of debate (Kaufmann and Johnson, 1988; Fagerstrom, 1987). It is clear, however, that very few buildups of this period were dominated by corals. The Cretaceous/Tertiary extinction affected all benthic calcareous organisms and Rudist bivalves disappeared completely. Calcisponges and stromatoporoids survived but never fully recuperated.

Cenozoic

Cenozoic reefs are essentially similar to the present-day reefs dominated by scleractinian corals. The few Paleocene reefs that survived were mainly Cretaceous 'left-overs'. The Eocene was marked by the renewed development of hermatypic scleractinians leading to the peak of Cenozoic reef-building in the Oligocene. The final closure of equatorial seaways (Tethys) and the demise of Mediterranean coral reefs due to increased salinity and the final closure of the isthmus of Panama restricted coral reefs to the two major reef provinces of today: the Caribbean and the Indo-Pacific.

Extinction of reef-builders and platform drowning

The discussion that has evolved around the evolutionary trends in reef-builders and particularly the extinction periods has many similarities to the discussion on the K/T boundary. The discussion focusses on the trend (gradual or abrupt) and the cause of the extinction. Obviously these two are related. Meteorite impacts will cause abrupt extinction while climatic changes will produce a more gradual pattern of demise. It becomes even more confusing when one causes the other. Except for the K/T boundary iridium anomalies relating to meteorite impacts have not been found for the other mass extinction events in the Phanerozoic. We therefore have to look for other possible and plausible causes for the extinction of reef-builders. Modern reef development is very much controlled by climatologic and oceanographic parameters (part I). It is therefore easy to envisage the control of these parameters on the evolution of reef-builders. Climatic cooling, accompanied by major regressions of sea-level and reorganization of plate configurations changing ocean currents are often held responsible for the extinctions of Paleozoic reef communities (Copper, 1986; Stanley, 1988). The extinction of reef-builders is generally a stepwise process, corals and other specialized organisms are the first to go, later followed by red algae, green algae and

stromatolites. During Paleozoic extinctions the tropical reef builders suffered more severely than other marine organisms and reef-builders adapted to relatively cool conditions (Stanley, 1988). This pattern is explained by gradual cooling of the climate. The long recovery periods after mass extinction (generally some 10 Ma), even though potential reef-builders are present, are thought to result from prolonged cooling of oceanic waters. Another explanation is provided by Cowen (1988) who, stating that all Phanerozoic reef communities had an underpinning of algal symbiosis, proposed that this delayed renewal is the result of the time needed to re-establish the symbiotic relations of reef organisms.

Extinction of reef-builders will severely reduce the growth potential of reefs and platforms. It is therefore easy to envisage global drowning to occur when a relative sea-level rise follows mass extinction periods.. The Frasnian/ Famennian and Cenomanian/Turonian are possible canditates for the proposed link between drowning and extinction The cause of such extinctions can thus be linked to mechanisms for platform drowning: cooler oceans, nutrient excess, changes in ocean circulation and geochemistry.

Growth potential

Accumulation rates gleaned from the geologic are averaged over many millions of years. The aggradation potential that is relevant to platform drowning is a short term rate measured over intervals of 10^3-10^4 years. For an evaluation of growth potential it is therefore necessary to examine the relation between long-term and short-term rates. Sedimentation is not constant and the stratigraphic record is punctuated by hiatuses. Over longer periods more and longer hiatuses are incorporated in the geologic record. It has been proposed that this relation between sedimentation rate and the duration of the interval over which it is measured has its basis in the fractal distribution of hiatuses (Plotnick, 1986). With increasing stratigraphic resolution these longer hiatuses are progressively omitted from the accumulation rate estimate. Correction for this relation allows the estimation of the growth potential of reefs and platforms from periods with different durations.

Chapter 8

ACCUMULATION RATES OF CARBONATE PLATFORMS

Abstract

The growth potential of carbonate platforms, i.e. the maximum rate at which they can aggrade vertically, is difficult to assess. In an attempt to estimate the growth potential from the conservative side and search for variations with time we have compiled accumulation rates published from the Phanerozoic. Accumulation rates vary through time in a pattern that consists of periods with maximum rates up to 200 B (m/Ma) or more (not corrected for compaction), in the late Devonian, Permian, late Triassic, late Jurassic and mid-Cretaceous, separated by intervals of reduced rates (e.g. Carboniferous, early Jurassic and late Cretaceous). The most dramatic drop occurs at the Permo-Triassic boundary, after which there is no documented platform growth. This pattern resembles the evolutionary rhythm of bloom and demise of reefs and reef-builders. The observed maximum accumulation rate of over 200 B (over time intervals of 10^6-10^7 years), is probably imposed by the maximum rate of long-term relative sea level rise on passive margins, the most favorable site for carbonate platform development. We corrected for the trend of decreasing rates with increasing interval duration by normalizing all the rates to a 1 Ma interval duration. The variations discussed above remain in this corrected data-set. We propose that biological factors can explain much of the observed variations.

INTRODUCTION

The growth potential of reefs and carbonate platforms, i.e. the rate at which they can grow upward and produce sediment, has remained an elusive property of these depositional systems. Schlager (1981) bracketed the value by arguing that it was lower than the maximum Holocene rate of sea level rise (which outpaced most reefs and platforms), and generally higher than the vertical accumulation rate of fossil platforms that built up and prograded at the same time. The first technique is subject to the peculiarities of the short Holocene interval, the second tends to systematically underestimate the growth potential. However, accumulation rates of fossil platforms do provide an important constraint on the growth potential and have the added advantage that they allow one to address the question of the variation of growth potential with time.

Several authors have published comparative accumulation rates for carbonates (Schwab, 1976; Schlager, 1981; Sadler, 1981; Sarg, 1988). These compilations, however, do not consider all stratigraphic intervals and are thus not suitable to search for variations of growth rates through time. This study gives an overview of accumulation rates of most of the extensive carbonate platforms in the Phanerozoic.

The maximum rate at which a carbonate platform can raise its rim or flat top is of key importance to its response to relative rises in sea level. Another measure of the growth potential is the rate at which the system can produce sediment. This measure is particularly important in basin modelling programs that consider not only the rate of upbuilding but also the rate of progradation and basin filling. This rate has not been considered in the present study. The rates given here are therefore conservative estimates of the potential of carbonate platforms to grow vertically.

The difficulty in calculating sediment accumulation rates lies in the determination of the absolute duration of the stratigraphic interval during which these sediments were deposited. We therefore tried only to include references with adequate time control. A tool that might provide better time-control is cyclo-stratigraphy. The recognition of Milankovitch rhythms in platform sediments can give a more accurate determination of the duration of deposition. We included rates calculated in this way derived from well studied examples of cyclicity in carbonate sediments. We compare these rates with those calculated from conventional stratigraphic data.

The growth potential of a carbonate platform is largely controlled by the growth of its organic rim (Schlager, 1981). Thus, platform growth rates may be expected to vary with the evolution of reef/rim builders. To test this notion we compare our data with studies that illustrate the evolution of reef builders through time (Copper, 1988; James, 1984; Raup and Boyajian, 1988).

METHODS

Data used to calculate accumulation rates were obtained from the literature. We used given stratigraphic thicknesses or measured them from cross sections and lithological columns. We calculated accumulation rate by dividing thickness by interval duration. Compaction was not corrected for because in most examples the overburden is not

sufficiently well known. Rates are therefore underestimated. The absolute duration of the stratigraphic intervals was determined from stratigraphic boundaries and the geological time scale by Harland et al. (1982). This time scale was chosen because it covers the entire Phanerozoic and it gives good correlations with regional stratigraphic names often used in the literature. Accumulation rates are given in meters per million years (m/Ma = mm/ka = μm/yr = Bubnoff unit: B; Fischer, 1969).

We have concentrated on pure shallow-water carbonates, rejecting examples with significant intercalations of siliciclastics or deeper water carbonates. However, descriptions are not always detailed enough to be absolutely sure about this point. Only platforms with a life span of millions to tens of millions of years were included. These intervals can be reasonably well dated. Precision in determining the duration of shorter time intervals is generally more speculative.

We corrected for the rule that the duration of the sampling interval is inversely correlated to the accumulation rate (Sadler, 1981; Plotnick, 1986). Linear regression of a rate versus duration plot was used to normalize all rates to an interval duration of 1 Ma. The following equation: $y = -ax + b$, where y = log(corrected rate); a = slope of regression; x = log(interval duration); b = log(uncorrected rate); gives the accumulation rate at log(duration) = 0 (i.e. an interval duration of 1 Ma).

Cyclostratigraphic dating.

Cyclostratigraphy is one technique that does provide a measure of shorter time intervals, comparable to the late Quaternary. Cycles in the Milankovitch frequency band provide equal durations for the sampling intervals and therefore an excellent basis for comparison of the obtained accumulation rates. We included examples from the Jurassic of the Dinaric Alps and the upper Triassic of the Southern Alps. There are unfortunately still too few case studies with well-supported Milankovitch cycles of carbonate platforms to enable us to make a good comparison of these rates for the entire Phanerozoic.

RESULTS

The results of this compilation are shown in Figure 8.1. Table 8.1 lists all the references used in this study. The observed rates range to over 200 B . Most platforms however grow at rates up to 100 B. Rates well over 200 B have been published (Brack, 1991; Sarg, 1988; Schlager, 1981), but mostly they have been measured over short, more speculative, time-intervals. These rates were not incorporated in this study and therefore the maximum rate of around 200 B is a somewhat conservative estimate.

Table 8.1. Accumulation rates of carbonate platforms.

LOCATION/FORMATION	AGE INTERVAL (Ma)	THICKNESS (m)	ACC.RATE (m/Ma)	REFERENCE
CENOZOIC				
French Polynesia	7-0	438	62	Chevalier, 1973
Bombay High Field, India	22.8-15.1	1000	129.9	Rao + Talukdar, 1980
Pearl River mouth basin, S.E.Asia	24-20.7	584	175	Erlich + Barret, 1989
Kais Formation, Irian Jaya	24.6-5.1	1300	66.7	Vincelette + Soeparjadi, 1976
--	14.4-5.1	490	52.7	--
Darai limestone, Papua New Guinea	24.6-5.1	1200	61.5	Pigram et al., 1988
Turks and Caicos, post-Eocene reef	38-0	1800	47.4	Meyerhof + Hatten, 1974
Castelgomberto limestone, Italy	38-32.8	200	38.5	Frost ,1981
Enewetak and Bikini	42-0	1405	33.5	Ladd, 1973
--	42-38	558	139.5	--
Idris 'A' bioherm, Libya	58.4-54.9	366	104.6	Terry + Williams, 1969
Andros Island, Bahamas	65-38	2000	74.1	Goodell + Garman, 1969
--	38-0	670	17.6	--
Long Island, Bahamas	65-0	1220	18.8	Meyerhof + Hatten, 1974
Amapa Formation, Foz Do	65-14.4	4000	79.1	Brouwer + Schwander, 1988
Amazonas Basin, Brazil	42-24.6	1000	57.5	--
Andros Island, Bahamas	65-54.9	1000	99	Paulus, 1972
--	54.9-38	1000	59.2	
CRETACEOUS				
Rocca di Cave, Italy	97.5-91	300	46.2	Carbone + Sirna, 1981
El Abra Formation, Mexico	113-91	1800	81.8	Enos, 1986
Golden Lane Platform, Mexico	113-91	3000	136.4	Wilson, 1975
Glen Rose limest., USA GulfCoast	115-110.5	189	42	Perkins, 1985
Urgonian complex, Spain	119-97.5	4000	186.0	Garcia-Mondejar, 1985
Mosul area, Persian gulf, Iraq	125-97.5	1000	36.4	Wilson, 1975
Cupido Formation, Mexico	125-113	610	50.8	Conklin + Moore, 1977
Barremian, Marseille, France	125-119	350	58.3	Arnaud-Vanneau et al., 1982
Urgonian platform, France	131-119	550	45.8	Masse + Alleman, 1982
Atlantic margin, USA	136-129	--	70	Poag + Schlee, 1984
Bahamas, Cay Sal	138-125	918	70.6	unpublished information
--	125-113	959	79.9	Chevron Oil Co.
Long Island, Bahamas	144-65	4135	52.3	Meyerhof + Hatten, 1974
Andros Island, Bahamas	144-97.5	1196	25.7	Goodell + Garman, 1969
--	97.5-65	579	17.8	--
Shuaiba Formation, Middle East	144-113	666	21.5	Murris, 1980
Florida, Atlantic margin	144-97.5	3000	64.5	Owens, 1983
JURASSIC				
Quintuco Fm., Neuquen Basin	146-136	600	60	Mitchum + Uliana, 1988
Caucasus, USSR	150-144	1000	166.7	Wilson, 1975
Vinales limestone, Cuba	153-147	1000	166.7	Butterlin, 1983
USA Atl.margin, Ft.Pierce Fm.	156-119	3800	102.7	Owens, 1983
Wilmington Platform, USA	156-138	1340	74.4	Meyer, 1989
Abenaki fm, Nova Scotia	163-138	1121	44.8	Eliuk, 1978
Caucasus, USSR	163-144	2000	105.3	Beznosov et al., 1978
Morocco,continental margin	163-144	1700	89.5	Ranke et al., 1982

Table 8.1 (continued). Accumulation rates of carbonate platforms.

North Africa, reef limestone	63-144	1600	84.2	Wilson, 1975
Southern Alps, Italy	163-144	--	45	Winterer + Bosellini, 1981
Slovenia	163-154	600	66.7	Turnsek et al., 1981
Baidoa Fm., Mandera-Lugh basin	169-163	900	150	Nairn, 1978
USA Atlantic margin	181-175	--	35	Poag + Schlee, 1984
--	175-169		70	--
	169-153		85	
	153-148		145	
--	148-144	--	70	--
Apennines, Italy	213-188	800	32	D'Argenio et al., 1975
--	188-144	800	18.2	--
TRIASSIC				
Dachsteinkalk, Alps, Austria	231-213	1730	96.1	Barth, 1968
Hauptdolomit, Alps, Austria	225-213	2000	166.7	Czurda, 1972
Dolomites, Italy	225-213	2100	175	Peloso + Vercesi, 1982
Dachstein limestone, Austria	225-213	2300	191.7	Schwarzacher + Haas, 1986
Hauptdolomit, Austria	225-219	1200	200	Schlager, 1963
Apennines, Italy	231-213	1450	80.6	D'Argenio et al., 1975
Picco di Vallandro, Italy	233.5-227	1500	230.8	Schlager et al., 1991
Wetterstein lst., Austria	238-228	1700	170	Ott, 1972
Wetterstein lst.,	240-229	1730	157.3	Tollmann, 1976
Karwendel and Gramstein	238-229	1300	144.4	--
Latemar buildup, Northern Italy	240-231	--	150	Goldhammer and Harris, 1989
PERMIAN				
Capitan Reef, Permian Basin,USA	253.5-251	350	140	Ross, 1986
Wichita/Albany Fm.	268-251	1585	93.5	Ward et al., 1986
U.Guad.Reef, Permian Basin, USA	268-258	--	107	Saller et al., 1989
Trogkofel Formation,Southern alps	277-263	330	23.6	Flügel, 1981
Urals, reefs, USSR	286-268	1050	58.3	Chuvashov, 1983
--	266-263	300	100	--
Ishimbai and Gorodki, Urals, USSR	286-263	1350	58.7	Nalivkin, 1973
--	268-263	600	120	--
Midland Basin, Texas, USA	286-284	--	60	Mazullo + Reid, 1989
--	284-282	--	90	--
--	268-266-	--	180	
	266-264		75	
CARBONIFEROUS				
Horseshoe reef complex,Texas,USA	296-270	900	34.6	Wilson, 1975
Nena Lucia field, Texas, USA	296-286	305	30.5	Toomey + Winland, 1972
Nansen Fm,Sverdrup Basin, Canada	320-286	2000	58.8	Davies, 1977
Urals, USSR	345-333	900	75	Nalivkin, 1973
Russian Arctic	352-333	1000	52.6	Nalivkin, 1973
Worsaw knoll reef, England	355-340	500	33.3	Parkinson, 1957
Waulsortian reefs, Ireland	356-343	915	70.4	Lees, 1961
Mississippian carbonate shelf,USA	360-345	800	53.3	Rose, 1976
--	345-320	1500	60	--
DEVONIAN				
Nisku Fm, Zeta lake m, Canada	371.5-368	124	35.4	Powder et al., 1980
Golden Spike, Leduc Fm., Canada	373-371	182	91	Walls et al., 1979

Table 8.1 (continued). Accumulation rates of carbonate platforms.

Ancient Wall complex, Canada	374-367	509	72.7	Jull, 1977
Canning Basin, Australia	376-362	2000	142.8	Playford, 1980
Balve and Attendorn complexes,	376-369	1300	185.7	Krebs, 1974
Germany	377-369	959	119.9	--
Ramparts Reef, Mackenzie, Canada	376-372	217	54.3	Muir et al., 1985
Ardennes, Belgium	380-374	500	83.3	Burchette, 1981
--	372-369	600	200	--
Hudson Bay, Kwataboahegan Fm.- Murray Isl.Fm.	387-378	400	44.4	Dimian et al., 1983
Carnian Alps	408-367	1200	29.3	Cantelli et al., 1982
Novaya Zemlya, Arctic USSR	408-387	600	28.6	Nalivkin, 1973
--	374-367	800	114.3	--
	367-360	400	57.1	
SILURIAN				
Douro fm., Somerset Island, Canada	417.5-414	275	78.6	Narbonne + Dixon, 1984
Northern Urals, USSR	421-414	700	100	Nalivkin, 1973
Urals,USSR	424.5-408	2000	121.2	Nalivkin, 1973
Hudson Bay, Severn River Fm. -Attawapiskat Fm.	428-421	500	71.4	Dimian et al., 1983
Niagara Group, Michigan Basin	428-421	183	26.1	Mesolella et al., 1974
Great Basin, Nevada, USA	438-421	1372	80.7	Winterer + Murphy, 1960
Western Arctic, USSR	438-428	500	50	Nalivkin, 1973
ORDOVICIAN				
Hudson Bay, Bad Cache Rapids - Churchill River Fm.	453-438	366	24.4	Dimian et al., 1983
Allen Bay fm., NWT, Canada	448-421	1966	72.8	Sodero + Hobson, 1979
Basin Ranges, USA	470-458	350	29.2	Ross et al., 1989
Cornwallis Island, Canadian Arctic	478-408	3350	47.9	Drummond, 1974
Seward Peninsula, Alaska	505-408	3650	37.6	Drummond, 1974
St.George group, Western Newfoundland, Canada	505-478	490	18.1	Pratt + James, 1982
Arbuckle Group, USA	505-478	1800	66.7	Wilson, 1975
CAMBRIAN				
Whipple Cave Fm.,Nevada, USA	510-505	400	80	Cook + Taylor, 1977
Copper Ridge,Appalachians, USA	525-505	1000	50	Frazier + Schwimmer, 1987
Kicking Horse Rim	540-520	2500	125	Bond + Kominz, 1984
Cambrian platform, Rocky Mts.	540-525	1472	98.1	Aitken, 1978
Western U.S., Eureka	540-525	--	97	Bond et al., 1989
Appalachians, USA	555-478	3750	48.7	Read, 1989
CYCLOSTRATIGRAPHY				
Aptian reefs, Dinaric Alps	0.413	64	155	Grötsch, 1991
Brenta Alta, U.Triassic,	0.413	99	239.7	Purtscheller, 1963
Dolomites, Italy	0.413	97	234.9	
Lofer cyclothems, Dachstein limestone, Austria (200 cycles = 1500 m)	0.041	7.5	187.5	Fischer, 1964
Dachstein limestone	0.021	4.84	230.5	Schwarzacher + Haas, 1986

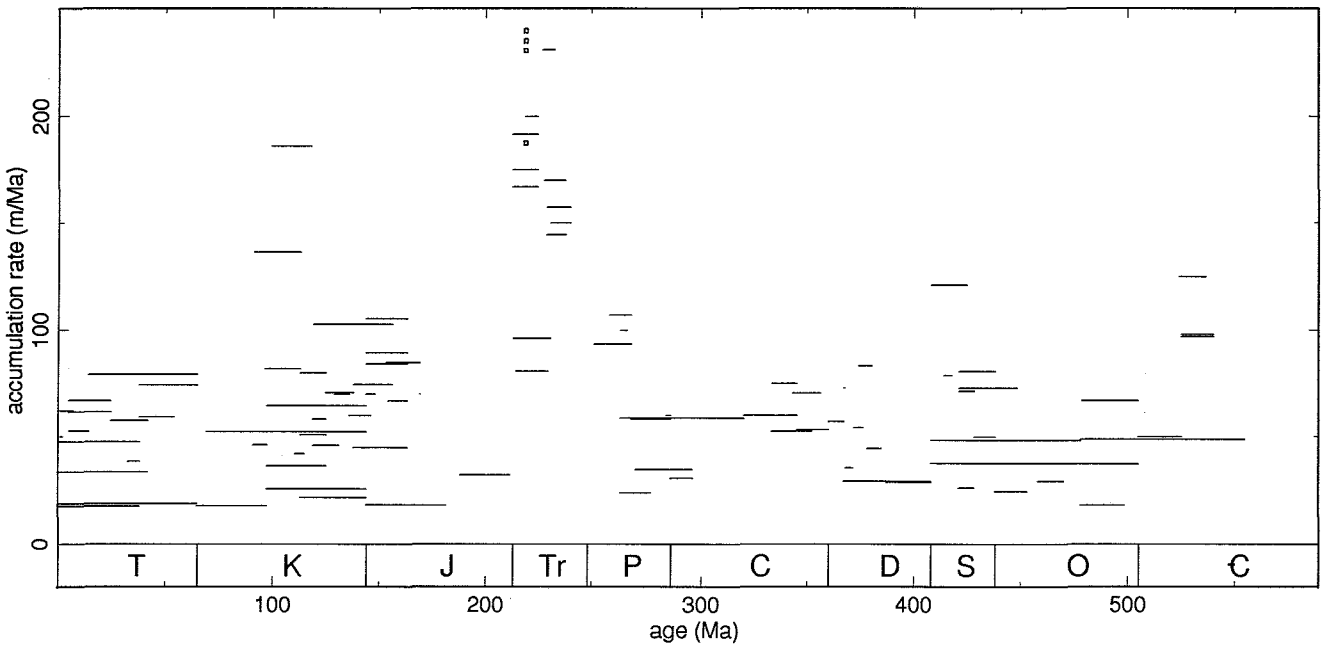

Figure 8.1. Accumulation rates of carbonate platforms (horizontal bars; n = 120). Boxes indicate rates based on cyclostratigraphy (n = 5). Data references in Table 8.1.

There is obvious variation in accumulation rate throughout the Phanerozoic. Periods with rates in the 100-200 B range alternate with longer periods that show maximum accumulation rates below 100 B, or lack platform growth altogether. It is a well-documented fact that accumulation rates tend to decrease with length of the time interval over which they are measured (Sadler, 1981; Plotnick, 1986). The correlation between the length of the sampling interval and accumulation rate is also present in our data. The correlation coefficient R = -0.438 is more than minimaly significant at $\alpha = 0.01$ (n = 119; t = -5.215). The slope of the regression line in Figure 8.2 is similar to that published by Sadler (1981) for reefs and carbonate platforms. We corrected our data for this trend by normalizing to an interval duration of 1 Ma (Fig. 8.3a).

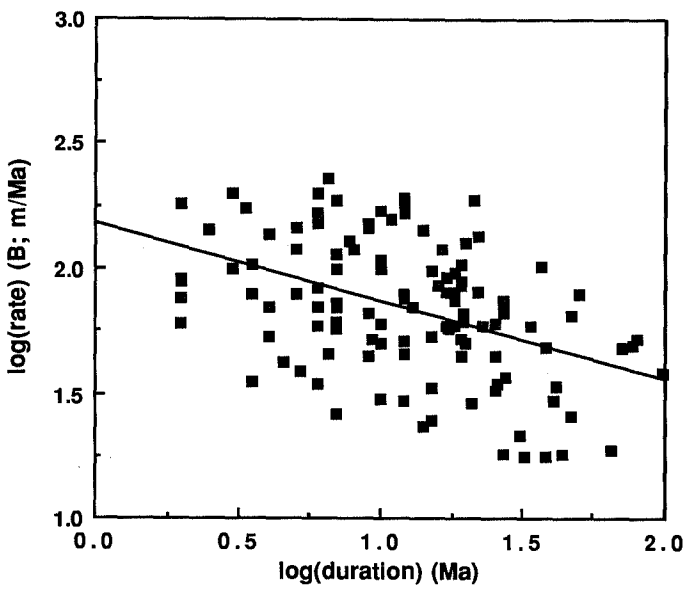

Figure 8.2. Logarithmic plot of the duration of the sampling intervals vs. accumulation rates. Solid line is linear regression (n = 120; R = -0.438). See text for discussion.

In Figure 8.3 the accumulation rates of carbonate platforms are compared with evolutionary trends of reef-builders (Copper, 1988; James, 1984; Raup and Boyajian, 1988). The correspondence between the diagrams combined in Figure 8.3 is not perfect, but there are some striking similarities. Most periods of biotic extinction coincide with minima in accumulation rates. The most pronounced event in both curves is the Permo-Triassic boundary: this most severe biotic crisis coincides with a total lack of documented reefs or carbonate platforms (Stanley, 1981). Similarly biotic extinctions at the Frasnian-Famennian boundary (Devonian) and at the Triassic-Jurassic boundary correlate with a rapid decrease

in carbonate accumulation rates. The trend at the Frasnian-Famennian boundary is obscured only by the relatively high rates during the Famennian of the relict reef province in the Canning Basin, Australia (Copper, 1986). The crisis at the Ordovician-Silurian boundary does not correspond to a drop in accumulation rates. At present we have no explanation for this. Also the extinction event at the K/T boundary does not seem to cause reduced accumulation rates. This is probably the result of the short duration of this event; other extinction events in the Phanerozoic seem to be related to prolonged periods of climatic cooling (Stanley, 1988).

DISCUSSION

Accumulation rate vs. growth potential

We may assume that accumulation rates of platforms shown in Figure 8.1 are significantly lower than the growth potential of platforms. There are several reasons for this. First, the rates are not corrected for compaction. Second, many platforms prograded while growing upward, thus demonstrating that their vertical growth was limited by accomodation rather than the growth potential of the system. Finally, we must consider that the growth potential varies as a function of length of time involved. Accumulation rates corrected for the rule that sedimentation rates decrease with increasing length of the time interval (Fig. 8.2; Sadler 1981) are shown in Figure 8.3a. We normalized all rates to an interval duration of 1 Ma, based on the regression from Figure 8.2. Because we used only intervals > 1 Ma, all normalized rates are greater than those from the uncorrected data-set.

The growth potential of a carbonate platform determines whether it can keep up with the creation of accomodation space or has to give-up and eventually drown. Platform drowning is a relatively short-term process. Optimum growth is restricted to the top 20 - 40 m of the euphotic zone; at a subsidence rate of 200 B, a platform will traverse this zone in 100 - 200 ka. The rates for the time domain relevant to this process will definitely be higher than the maximum rates presented here. These extrapolated higher rates are close to the growth potential as inferred from the Holocene rates

Time measured by cyclostratigraphy vs. conventional stratigraphy

There are only few examples of accumulation rates determined from the duration of orbital cycles (cyclostratigraphy; see Table 8.1). We found generally good correspondence between these rates and those based on conventional biostratigraphy tied to a chronologic time scale (Fig. 8.1). At first, this is surprising, because Milankovitch cycles measure accumulation over 10^4-10^5 years, whereas the biostratigraphic intervals used were one or two orders of magnitude longer. We believe, however, that the good agreement between these different approaches is explained by the techniques used in cyclostratigraphy. All the studies cited by us used spectral analysis in search of Milankovitch rhythms and made a simple transformation from space rhythm to time rhythm by assuming that bed thickness (i.e. the measured variable) was proportional to time. This approach will produce convincing

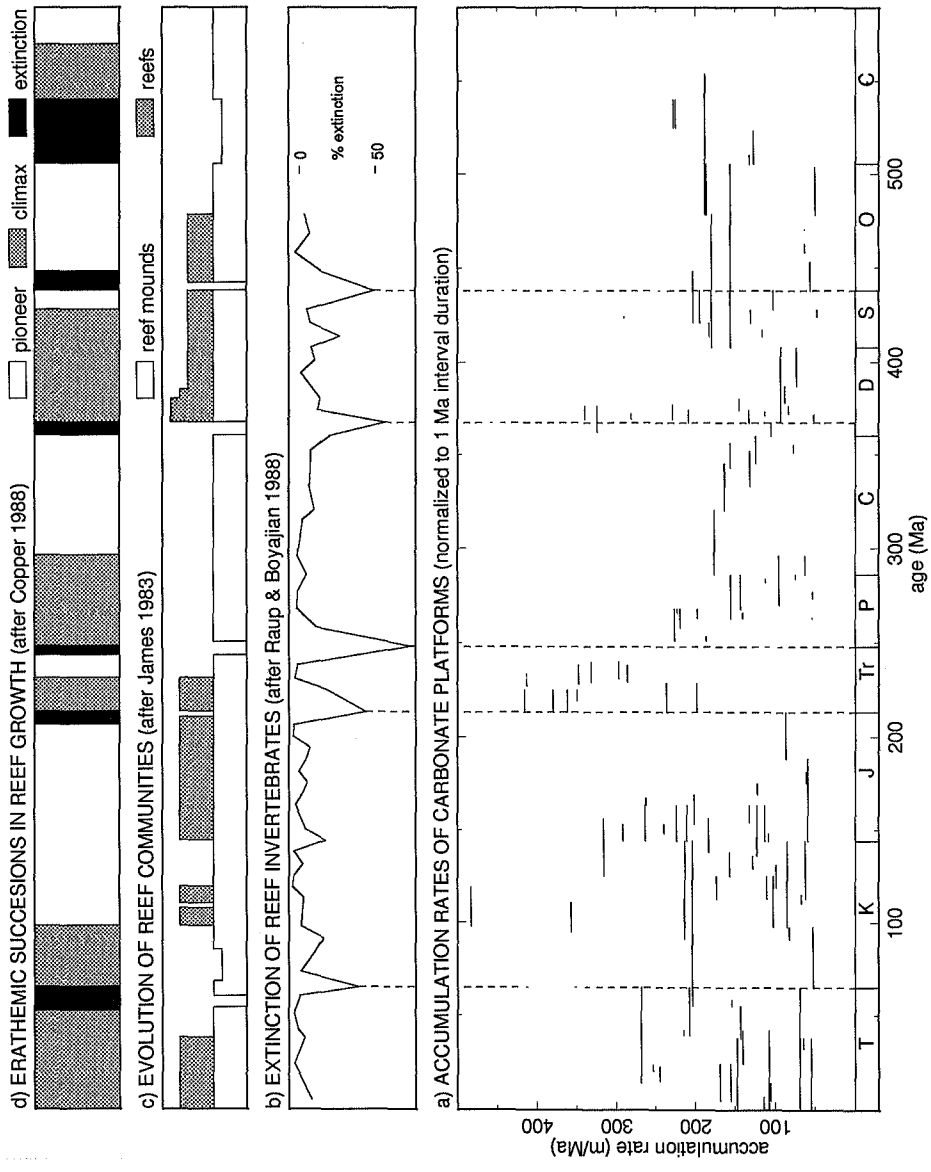

Figure 8.3. **A**: Accumulation rates of carbonate platforms normalized to an interval duration of 1 Ma. Based on regression from Figure 8.2. **B**: Extinction of reef invertebrates in percentage less median (after Raup and Boyajian, 1988). **C**: Evolution of reef communities, divided into reefs and reef mounds (modified after James, 1984). **D**: Pioneering, climax and extinction phases in reef growth (modified after Copper, 1988)(See text for discussion).

arguments for orbital rhythms only in sections with long-term, steady accumulation, i.e. sections where short-term and long-term accumulation rates are similar.

Possible causes of variation in accumulation rate

The rate at which carbonate platforms build up is determined by two factors - the rate of relative rise of sea-level and the growth potential of the systems, that is the maximum rate at which the platform can grow upward if not limited by accommodation space. We believe that for rates of over 25 B sustained over 10^6 - 10^7 years the effect of eustatic fluctuations is small and that the relative sea level rise recorded by carbonate platforms is dominated by the effects of subsidence by cooling of the crust and loading by sediment. It has already been pointed out that the observed sedimentation rates do not reflect the short-term growth potential of the system. The possibility remains, however, that our curve reflects the long-term growth potential of platforms in one way or another. Alternatively, the rate could be limited by tectonic setting - there may be times when there is no fast-subsiding crust suitable for platform growth. We will briefly review the arguments for either cause.

Biotic control

The strongest argument for variations in long-term growth potential is the correlation of decreased accumulation rates with high rates of biotic extinction and reduction of reef builders as described by Copper (1988), James (1984) and Raup and Boyajian (1988). Considering the dominant influence of the reef margins on the platform as a whole, it seems very plausible that reef crises will reduce the growth potential of the entire platform. However, there is no indication that periods of decreasing sedimentation rates coincide with drowning events. In fact, the mid-Cretaceous drownings, probably the most extensive ones in the Phanerozoic, coincide with a high in platform accumulation rates (Fig. 8.3; Schlager, 1989).

Tectonic control

Tectonic control of the observed sedimentation rates is suggested, among others, by the magnitude of these rates. They range from ca. 20 B to over 200 B. These are common subsidence rates on passive margins and ocean crust, the most favorable settings for long-term growth of carbonate platforms. In active margins, collision zones and strike-slip settings, carbonate platform growth is easily disturbed and replaced by siliciclastic deposition owing to high relief and rapid erosion.

There is good evidence that world-wide averages of subsidence rates in basins and continental margins have fluctuated during earth history. Young, rapidly subsiding passive margins were created in episodic pulses (e.g. Watts, 1982, for the past 200 Ma) and global averages of tectonic subsidence have varied significantly throughout the Phanerozoic (Guidish et al., 1984;Ronov et al., 1980). Data compiled by Ronov et al. (1980) on average

subsidence rates and relative frequency of carbonate rocks and relative intensity of reef-building are compared by Kuznetsov (1990). These data show that variations in global subsidence do not resemble the variations in relative frequency of carbonate rocks and relative intensity of reef-building, nor do they correlate with the fluctuating accumulation rates presented in this paper. The most striking example is the total absence of reefs or platforms at the Permo-Triassic boundary: global subsidence rates are relatively high (Guidish et al., 1984) or increasing (Ronov et al., 1980), while there is a dramatic drop in platform accumulation rates corresponding to the most pronounced faunal extinction in the Phanerozoic (Raup and Boyajian, 1988). The same holds for the incision at the Triassic-Jurassic boundary. Thus, tectonic control on these variations does not seem likely. Furthermore, the variations in global subsidence found by Guidish et al. (1984) and Ronov et al. (1980) are one or two orders of magnitude too small to significantly influence sedimentation rates on platforms.

CONCLUSIONS

This paper gives a good overview of the accumulation rates of carbonate platforms throughout the Phanerozoic. However, the picture of variations of Phanerozoic accumulation rates is too fragmentary to identify the various controls. In particular, we are unable to decide whether the observed minima in accumulation rates are caused by (biologically regulated) reductions of growth potential or by global variations in tectonic subsidence. Our data indicate that tectonic and biotic controls may well act in tandem. The observed rates seem to be limited on the high side by subsidence, whereas the lows may represent true, biologically controlled minima in the long-term growth potential of reefs and platforms. Tectonic control provides space to accommodate platforms and reefs, but biological control decides whether they really take this opportunity.

Chapter 9

PLATFORM DROWNING AND SCALING OF SEDIMENTATION RATES

Abstract

Sedimentation rates in carbonates, like in other depositional systems decrease with increasing time span of observation. We have quantified this trend over eight orders of magnitude by combining accumulation rates from the geologic record with Holocene data and measurements of annual coral growth. A very consistent picture emerges that confirms several earlier estimates. It indicates that platforms that aggraded at 20 - 200 B (m/Ma), as commonly observed in the 10^6 - 10^7 year domain, were able to grow at an average of 1000 B and up to 10000 B in the 10^4 year domain. This short-term growth potential is most relevant for drowning of reefs and platforms The euphotic zone is 30 - 150 m thick and the light-saturated zone of maximum production only 10 - 20 m. Drowning, therefore is likely to be a short-term process. The short-term growth potential estimated from the scaling law of sedimentation rates (and from independent estimates in the Holocene) is so high that it seriously limits the number of possible causes of drowning of reefs and platforms. It completely eliminates sea-level rise from increased sea-floor spreading as a cause of drowning; thermal subsidence matches this growth potential only during the first 0 - 0.1 Ma and is therefore largely ineffective in platform drowning. The same holds for sea-level cycles in the million-year range postulated from sequence stratigraphy ("third-order cycles"). Most likely causes of drowning are changes in the environment that reduce the growth potential and sea-level pulses related to tectonic processes that are themselves governed by power laws and therefore subject to scaling. A likely candidate in the second category is episodic subsidence by intraplate deformation.

INTRODUCTION

For many depositional environments it is well established that sedimentation rates decrease as the time span of measurement increases (Sadler, 1981; Plotnick, 1986). Also widely accepted is the cause of this trend: the fact that the stratigraphic record is perforated by hiatuses on almost all time scales. Long-term averages of sedimentation include many, long hiatuses; as the time span of observation is reduced, these hiatuses are progressively recognized and excluded from the sedimentation rate estimates. A very attractive model to illustrate the stratigraphic record is that of a self-similar Cantor set as proposed by Plotnick (1986; see also Fig.10.4). This model is most applicable to deposits from environments where conditions vary from rapid deposition on the one extreme to intensive erosion on the other. The shoalwater carbonates considered here fall in this category as do shallow marine and fluviatile siliciclastics as well as deepwater sediments controlled by turbidity and contour currents. To what extent the model can be applied to fine-grained pelagic sediments is open to debate; however, this question is not relevant for our line of argument.

Independently, Enos (1991) and (Bosscher and Schlager, 1992b) have recently compiled sedimentation rates of Phanerozoic reefs and carbonate platforms. The two data sets, consisting of individually listed and referenced rates, provide an update of the more extensive, but older and not individually listed compilation of Sadler (1981). In this report, we examine the rate-time span relationship for those data and discuss the implications of this trend for the process of drowning of reefs and platforms.

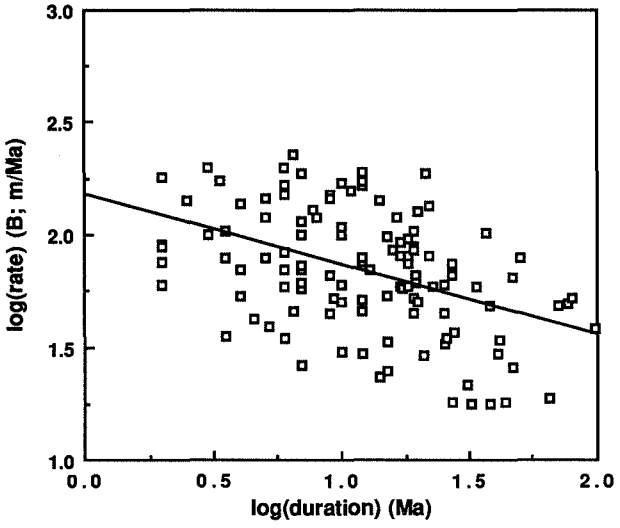

Figure 9.1. Accumulation rates of Phanerozoic shoalwater carbonates plotted against the length of the time span over which the rate was averaged. Only rates over ca. 20 B have been considered. Least-square regression indicates decrease of rates with increasing time span. R = -0.44, significant at $\alpha = 0.01$ (n = 119; t = -5.215). After Bosscher and Schlager (1992b).

Accumulation rates vs. time span in carbonate deposits

Figure 9.1 shows a compilation of accumulation rates in Phanerozoic shoalwater carbonate deposits, plotted against the length of the time interval in which the rates were observed. There is considerable scatter but the decrease in accumulation rate with increasing time span is obvious. The least-squares regression gives a trend very similar to the one found by Sadler (1981) for a totally different data set (Fig. 9.2).

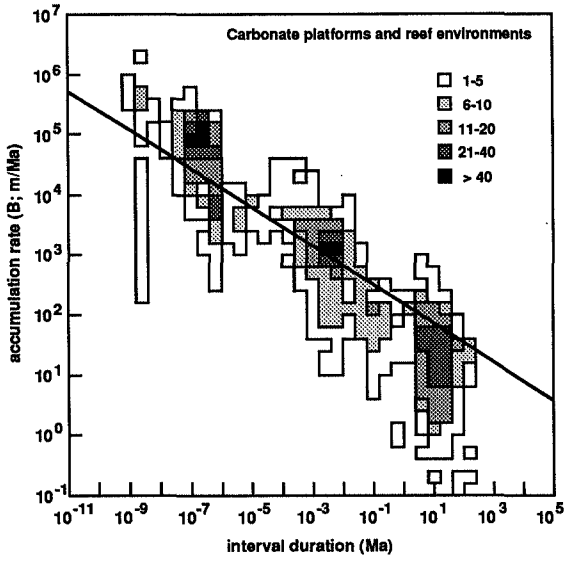

Figure 9.2. Accumulation rates of reefs and carbonate platforms versus timespan of observation (after Sadler, 1981). Solid line is linear regression from Figure 9.1.

Figure 9.3 shows that short-term rates observed on reefs and platforms fit the trend remarkably well. Reef growth and carbonate accumulation in the Holocene transgression have been well constrained by radiocarbon dating. These rates were determined in the range of 10^3- 10^4 years. Time spans of years to hundreds of years are covered by growth rates of massive head corals, the key element in modern reef frameworks. They, too, follow the trend predicted by the regression equation of Figure 9.1.

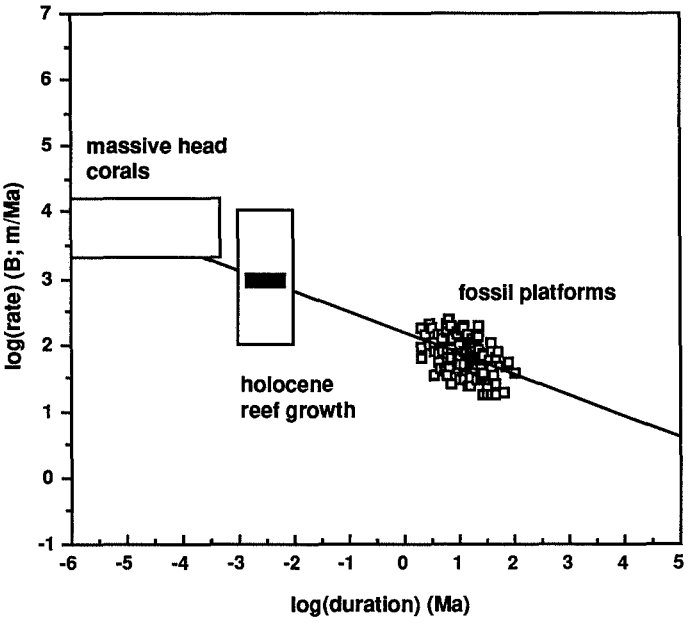

Figure 9.3. Comparison of carbonate accumulation rates in the geologic domain (millions of years), with rates in the Holocene (10^3 - 10^4 years) and in modern environments (10^{-1} - 10^2 years). Note that the regression line derived from the million-year domain also applies to the short-term record. Black square represents growth potential estimate from Schlager (1981). Data from: chapter 2; Enos (1991); Schlager (1981).

The appearance of coral colonies in this trend warrants a comment. Coral growth, like that of trees, is guided by astronomical and biological clocks. Consequently, growth is distinctly periodic up to the annual cycle and beyond that rather steady over the life span of an individual. Therefore, we imagine that in framework-dominated reefs the pattern of stop-and-go sedimentation ends with the individual coral colony. In detrital deposition, such as storm layers in supratidal flats, the trend of increasing rates with decreasing time span has been shown to continue to the realm of days and hours. We expect it to break down at time spans required for the deposition of individual grains.

A recent compilation of shallow water carbonate sedimentation rates by Enos (1991) which includes various carbonate depositional environments is show in Figure 9.4. There is a very good correspondance between this data set and those presented in Figure 9.1. The slope of the trend in carbonates is very similar to the one found by Sadler (1981). It is significantly flatter than the trend in siliciclastics (Sadler, 1981). We speculate that this difference reflects the strong tendency of carbonates to fill available submarine accommodation and to resist mechanical surface erosion through organic frame-building and early cementation.

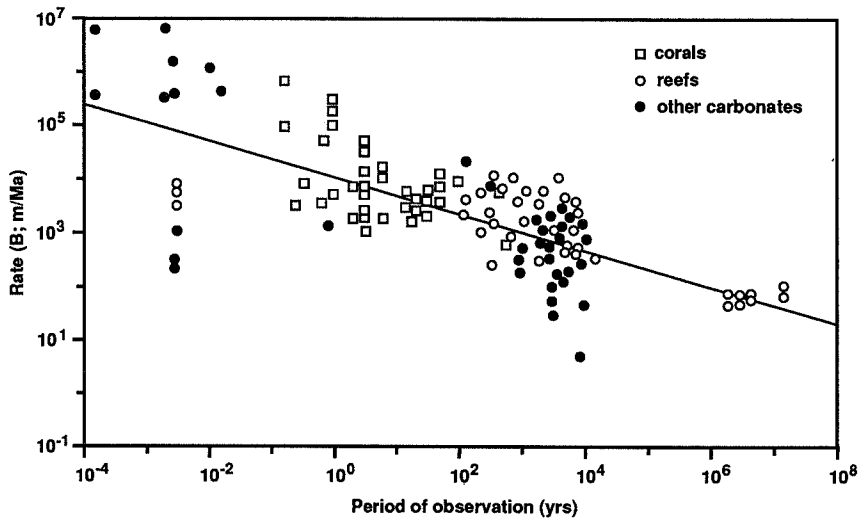

Figure. 9.4. Accumulation and growth rates of corals, reefs, and other shallow water carbonates versus period of observation from Enos (1991). Solid line is linear regression from Figure 9.1. Note overall similarity to Figures 9.2 and 9.3.

Viewed overall, the trend of decreasing rates with increasing time span extends over eight orders of magnitude and seems to be a rather fundamental property of shoalwater carbonate accumulations. It also sheds new light on the problem of drowning of reefs and platforms. Before examining these implications we will briefly discuss the validity of the rate-time trend observed in Figures 9.3 and 9.4.

Validity of the trend

Anders et al. (1987) pointed out that plots of accumulation rates vs. length of observation span may produce spurious negative correlations because of built-in limitations of the natural data set. For very short time intervals, determination of accumulation rates is limited by the precision with which sediment thickness and/or the associated time interval can be measured. Consequently, the lower left of plots like Figures 9.3 and 9.4 may be empty not because appropriate rates do not occur but because they cannot be measured. This "limit of precision" of Anders et al. (1987) has an analogue in the "limit of thickness" in the upper right field of the rate-time plot. There, high rates maintained over long intervals are increasingly difficult to observe for want of undisturbed field sections and adequate deep drilling data.

We believe that the objections of Anders et al. (1987) are principally correct. However, the effects mentioned do not significantly disturb our analysis for the following reasons:

Anders et al. (1987) argue that the effects of the limit of precision disappear when median accumulation rates are calculated for constant ranges of thickness rather than time. For our data set, the trend remains virtually unchanged, suggesting that is is genuine and not induced by the limits of precision and thickness in the sense of Anders et al. (1987).

Our compilation reduces the effect of the limit of precision by employing more precise measuring techniques in the short-term range. Standard techniques of (bio)-stratigraphy and thickness measurement in the field are used in the 1-100 Ma range only. We estimate that these data have a precision of ±10% in both time and thickness domains. Holocene rates in the 1000-year range, rely on radiocarbon dating of individual, in-situ corals. These dates, measured near the half-life point of the decaying isotope, typically are quoted with an error of a few percents. Thicknesses refer to distance between individual corals and therefore are not subject to lateral variations of beds; their precision is certainly ± 5% or better. Finally, annual rates are determined from growth bands of individual corals. The annual nature of these bands has been widely established (Knutson et al., 1972; Hudson et al., 1976; among others). The exact timing of the deposition of these bands may vary (Barnes et al., 1992), but we estimate the precision in time for average growth rates measured over periods of several years to be ±10% or better. The precision in thickness of the annual growth band is about ± 5%. In summary, we believe that the precision of Holocene accumulation rates and annual growth rates of corals is equal to or better than that of geological formations measured in the million-year domain.

The limit of thickness of Anders et al. (1987) should not seriously affect our data because we applied a high cut at 100 Ma.This is considerably shorter than the growth period of long-lived platforms such as the Bahams and the southern Apennines that extended over 150-180 Ma (Meyerhoff and Hatten, 1974; D'Argenio et al.1975). With the high cut at 100 Ma, the maximum thicknesses entered in the calculations of Figure 9.2 are in the range of 4000-6000 m. This is high, but not even close to the maximum thicknesses measured and dated by sedimentary geologists. Field geologist have gleaned time-thickness data from accumulations at least three times as thick and numerous boreholes in sedimentary basins penetrate 6000 m or more of stratigraphic thickness.

Finally, Anders et al. (1987) direct their comment specifically to pelagic sediments whereas this discussion revolves around shoalwater sediments. Rate-time trends in shoalwater sediments differ from those of deepwater deposits: the trend in shoalwater deposits is more distinctly linear and lacks the rapid upturn of median values in the short-term rates (compare our Fig. 9.1 and Fig. 3 of Sadler (1981), with Fig. 5 of Sadler (1981), and Fig. 2 of Anders et al. (1987)). It is the rapid change in short-term rates that is so elegantly explained by the notion of a limit of precision. The central tendency in the medium time range is only marginally affected by the modifications applied by Anders et al. (1987).

Another source of uncertainty with plots of sedimentation rates vs. time is the fact that time appears once as a simple variable and once in the composite variable of accumulation rates. Plots such as Figure 9.1 therefore face the mathematical problem of plotting a variable against its inverse. Two arguments support our contention that the

observed trend has a strong natural (as opposed to spurious) component. First the slope of the regression line differs significantly from the value of -1 that would be expected for totally spurious correlations of x vs. x^{-1} (Kenney, 1982). Second, the slopes in siliciclastics, shoalwater carbonates and deep-sea sediments differ considerably with deep-sea sediments having the flattest slope, in agreement with the notion that the deep-sea record is the most complete (Sadler, 1981; Anders et al., 1987).

Implications for platform drowning

Unlike siliciclastics, carbonate platforms can be drowned, i.e. submerged to water depths from which they cannot grow back to sea level. Drowning requires a relative rise of sea level that exceeds the aggradation potential of the platform; the process depends, therefore, on the balance between growth and relative sea level rise rather than sea level alone.

The race between relative sea level and platform growth goes over a short distance - the thickness of the euphotic zone where nearly all carbonate production takes place. In fact, the most crucial distance is even less, namely the light-saturated zone in the top 10-20 m of the water column (Bosscher and Schlager, 1992a; chapter 2). Thus, drowning or survival of reefs and platforms critically depends on their aggradation potential in the 10^3-10^4 year range. The regression equation from Figure 9.1 predicts that the Phanerozoic platforms whose rates we measured in the million-year domain should have aggraded at average rates of 1000 B in the thousand-year domain. This can be taken as a lower limit for their aggradation potential in this time range and agrees surprisingly well with an earlier estimate by Schlager (1981; Fig. 9.3), who deduced a conservativegrowth potential of 1000 B for reefs and platforms during the Holocene transgression. The maximum rate of reef accretion during the Holocene transgression was ca. 12000 B (Figs. 9.3 and 9.4; see also Table 10.2). These maximum rates have been observed only rarely and only for short periods under optimal conditions. The extended sea-level rise of 10000 - 12000 B during the early part of the Holocene transgression (Fairbanks, 1989; Grigg and Epp, 1989) drowned most coral reefs that were established during the last glacial maximum. At rates of ca. 1000 B, commonly experienced during the past 5000 years, reefs in the tropics generally kept pace with sea level and many even expanded their area. Reefs near the norther and southern limits of reef growth have not yet coalesced to continuous barriers and are still trailing sea-level. From this pattern we conclude that 1000 B is a reasonable estimate of the average aggradation potential of modern reefs.

This short-term aggradation potential is so high that it severely limits the options for drowning of reefs of platforms. A growth potential of over 1000 B immediately eliminates sea-level rise by increased sea-floor spreading as a cause of platform drowning. The maximum rates of change by this mechanism is ca. 12 B, the long term average of the last 70 Ma is 5 B (Table 9.1;Pitman and Golovchenko, 1983). Furthermore, the high growth potential severly reduces the significance of thermal subsidence as a drowning agent. This

process can be viewed as steady and not subject to scaling laws such as those governing accumulation. Table 9.2 presents the rates of thermal subsidence based on the empirical formula of Parsons and Sclater (1977). It matches the aggradation potential of platforms only during the first 0.1 Ma of the subsidence history. Thereafter, thermal subsidence is too slow to outpace healthy reefs and platforms.

Table 9.1. Mechanisms and rates of sea-level rise.

mechanism	magnitude (m)	maximum rate (m/Ma)	reference
glacio-eustasy	100-150	up to 20000	Fairbanks, 1989
intraplate stress	100	10-100	Cloetingh, 1988
MOR volume	350-500	7.5-12	Pitman and Golovchenko, 1983
sediment recycling	60-85	0.8-1.4	Pitman and Golovchenko, 1983

Table 9.2. Thermal subsidence rates.

interval (Ma)	subsidence rate (m/Ma)
0-0.1	1107
0-0.2	783
0-0.5	495
0-1.0	350
0-2.0	247

Based on empirical formula for thermal subsidence from Parsons and Sclater (1977)

Similarly, the sea-level cycles proposed by Haq et al. (1987) are an extremely unlikely cause of platform drowning even if one assumes a conservative short-term aggradation potential of 1000 B. Rates of rise of these cycles are typically in the range of 10 - 100 B. Pulses that exceed 100 B are preceded by equally large and rapid falls of sea level. Thus, platforms will first be exposed by the rapid fall and will remain high and dry during most of the subsequent rise. This renders the rapid sea-level pulses of the curve by Haq et al. (1987) ineffective for platform drowning (Schlager, 1991).

Glacio-eustatic pulses such as those of the past 0.5 Ma can easily outpace reefs and platforms. the early part of the Holocene transgression is a case in point as mentioned above. Between 12000 and 6000 yrs BP rates of sea-level rise averaged 10000 to 12000 B, exceeding the estimated aggradation potential by one order of magnitude. Fairbanks et al. (1992) estimate that the most rapid pulses of deglaciation caused sea level to rise at rates of 45000 B. However, large glaciations capable of generating sea-level cycles with amplitudes that approach the thickness of the euphotic zone have been rare in earth history. Furthermore, glacio-eustatic fluctuations tend to be distinctly cyclic with rises followed by equally rapid falls. This exposes the platform and allows the system to resume growth at a lower elevation. Drowning by glacio-eustatic cycles is effective only if: (a) a very assymetric rise is produced by superposition of different cycles; or, (b) the reef growth is so disturbed by the rapid alternation of exposure and flooding that it can no longer compensate for the effects of long-term subsidence or long-term sea-level rise ("stepwise drowning" of Hine and Steinmetz, 1984); or, (c) subsidence is so rapid that the bank top is removed below the point of the next sea-level lowstand (Schlager, 1981); Ludwig et al. (1991) have shown that sea-level pulses related to glacio-eustasy have been able to drown reefs with the help of continued subsidence.

Desiccation of ocean basins creates another type of eustatic pulses that may easily exceed the aggradation potential of reefs and platforms. The limitations are the relatively small amplitude - 15 m for the desiccation of the Mediterranean (Pitman and Golovchenko, 1983). Much like glacio-eustasy, desiccation of ocean basins is likely to be cyclic and thus dependent on subsidence or other long-term rises of sea level to complete drowning

The short-term growth potential derived from the combination of geological observation and scaling laws leaves two major areas in search for causes of drowning: environmental changes that reduce the aggradation potential and pulses of relative sea level linked to processes that are themselves self-similar and governed by power laws. Drowning by environmental change may be effective because carbonate systems, particularly reefs, are made up of highly specialized communities that are intimately tied to the ocean environment. Slight changes in this environment may cause the entire system to collapse. Schlager (1991) reviewed the arguments for environmental control of global drowning events in particular.

Drowning by relative sea-level pulses (other than glacio-eustasy and basin dessication mentioned above) largely depends on tectonics as a driving force. Tectonic processes are not uniform in this respect. Plate motion itself is rather steady such that rates of plate motion determined from the geologic record agree well with rates obtained from space geodesy over a few years (Gordon and Stein, 1992). Fault movements, on the other hand, are distinctly episodic, reflecting the gradual build-up and abrupt release of stress. It is widely accepted that timing and magnitude of fault movements and associated earthquakes obey a power-law and produce self-similar patterns (e.g. Turcotte, 1992). We consider it very likely that large strike-slip systems generate pulses of subsidence that exceed the growth potential of carbonate systems and drown them. However, belts of strike-slip tectonics are not a

preferred setting for reefs and carbonate platforms. Faulting and rapid subsidence at plate margins due to rifting or related to intraplate stress may be another candidate. It is of considerable importance for the present discussion that intraplate deformation has also been shown to fall in the category of non-steady tectonic processes (Cloetingh, 1988). It is largely discontinuous and pulsating and provides a potential mechanism for regional drowning events in the carbonate record. A particular advantage of sea-level pulses related to intraplate deformation is that they may be acyclic. The cyclic nature of, for instance, glacio-eustatic fluctuations reduces their potential for drowning because the drowned system is easily brought back into the photic zone by the next fall in sea level.

Conclusions

Accumulation rates of shoalwater carbonates consistently increase with decreasing time span - a trend generally observed in sediments. Regression equations from several data sets indicate that the commonly observed rates of 20 - 200 B (m/Ma) in the geologic record correspond to rates of 1000 to 10000 B in the 10^3-10^4 year domain.

This short-term growth potential has important implications for drowning of reefs and platform. The rate is so high that it completely eliminates sea-level rise from increased sea-floor spreading as a cause of drowning; Rates of thermal subsidence match this growth potential only during the first 0.1 Ma and are therefore largely ineffective in platform drowning. The same holds for sea-level cycles in the million-year range postulated from sequence stratigraphy ("third-order cycles").

Potential causes for platform drowning are environmental changes that reduce the growth potential and sea-level pulses generated by processes that are themselves self-similar and governed by power laws. Pulses of subsidence related to intraplate deformation may be particularly important in this category.

Chapter 10

DISCUSSION AND CONCLUSIONS

DEPTH RELATED CHANGES IN CORAL GROWTH

The role of light in coral growth has been acknowledged for a long time. The depth of the euphotic zone is accepted as the lower limit of coral growth and below that depth reefs are considered drowned. Few people have tried to relate the geologically important measures of coral growth to the decrease of light with depth (James and Ginsburg, 1979; Graus and Macintyre, 1982; Hubbard and Scaturo, 1985). Yet this relation is one of the basics of carbonate sedimentology. The results presented in parts I and II of this thesis are a first attempt to quantify this relationship.

The growth rate of corals, the density of their skeleton, and thus their rate of calcification decrease with depth in a manner that seems to be dictated by the decreasing amounts of light. Figure 10.1 shows a compilation of the studies on the skeletal growth of the reef-building coral *Montastrea annularis* presented in Part I of this thesis. Light saturated growth occurs to a depth of ca. 15 m. This depth of 15 m occurs frequently in the literature as the depth at which major changes in the skeletal growth of *M. annularis* take place throughout the Caribbean. The light saturation depth of ca. 15 m seems to be a characteristic of Caribbean reefs obviously related to the similar light conditions on these reefs (see also Fig. 10 in the introduction to part I).

From the study on the carbon isotopic composition of the skeletons of these coral it is apparent that gross photosynthesis decreases more rapidly than would be expected from the observations on other skeletal growth parameters. I propose that photoadaptive strategies employed by corals to optimize the use of available light are responsible for this. Photoadaption can extend the depth of light saturation and increase the P/R ratio. The pattern of decreasing skeletal growth with depth is the final product of these adaptions to lowering light levels. The difference between the gross photosynthetic rate and skeletal growth seems thus a result of photoadaption. The light saturation depth of ca. 15 m reported here for the growth rate of *M. annularis* from Curaçao is twice as deep as the saturation depth for gross photosynythesis based on the $\delta^{13}C$ of the skeleton.

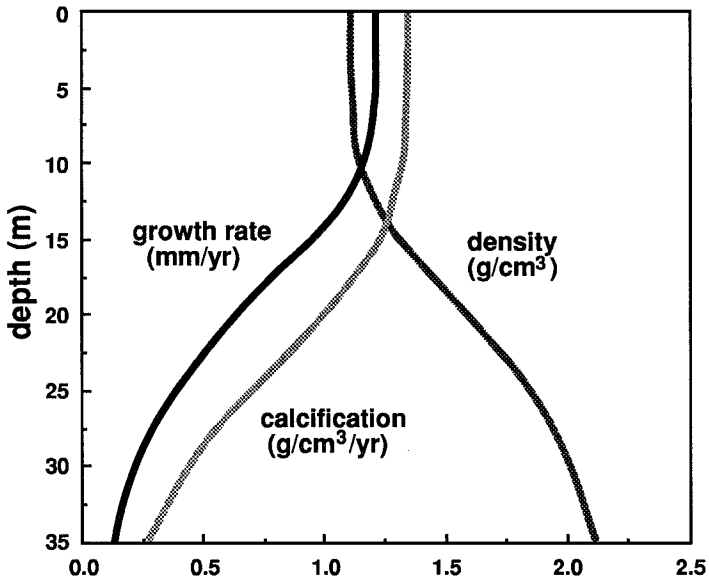

Figure 10.1. Skeletal growth of *Montastrea annularis* vs. water depth. Growth rate and skeletal density based on fitted curves from chapters 2 and 3. Calcification rate calculated from growth rate and skeletal density.

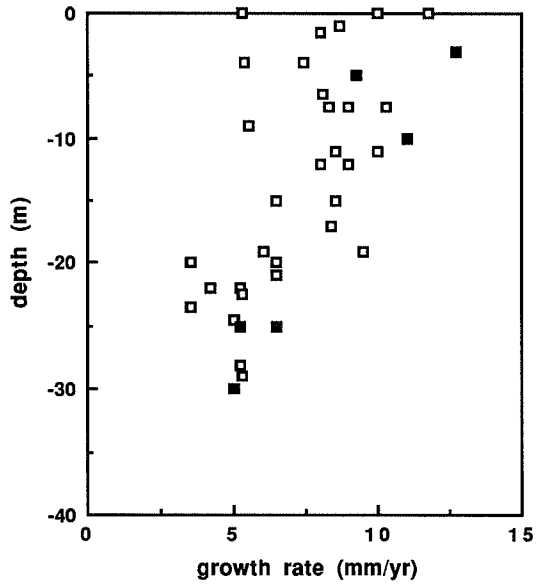

Figure 10.2. Growth rate of the Pacific reef-building coral *Porites lutea*, from Enewetak Atoll (data from: Buddemeier et al., 1974;Highsmith, 1979).

The maximum reported growth rate of *M. annularis* ranges from 10-16 mm/yr (see chapter 2 and 3). The average maximum growth rate for *M. annularis* from Curaçao is ca.12 mm/yr. This rate compares very well with maximum growth rates of their Pacific counterpart, the massive head coral *Porites lutea* of ca. 13.5 mm/yr. The decrease of growth rate with depth for *P. lutea* from Enewetak atoll is shown in Figure 10.2. The decrease of growth rate with depth is obvious, but more gradual than that reported for *M. annularis*. This is probably the result of the high transparency of Enewetak reef waters. In Figures 10 and 11 in the introduction to Part I it is shown that the depth of the euphotic zone in the waters surrounding Enewetak Atoll is ca. 140 m as opposed to 90-100 m in the Caribbean. This increased light penetration results in a greater depth of light saturation and a more gradual decrease of growth rates.

THE ROLE OF CORALS IN REEF GROWTH

What do the growth rates of reef-building corals tell us about the growth rate of entire coral reefs. Can one simply extrapolate coral growth rates to reef growth rates? Is it valid to assume that the pattern of decreasing growth rates of corals with depth will be mimicked by the patterns af accretion in the reefs on which they live? Corals are by far the most important group in terms of carbonate production. Hubbard et al. (1990) have shown that of the total carbonate production of fringing reefs of St. Croix corals account for nearly 95 %. The construction of wave-resistant framework by corals occurs at various rates for different coral species (Table 10.1). Construction of reef framework determines the ability of reefs to grow upward. Some branching reef-building corals can grow over 100 mm/yr, but their role in building wave resistant framwork is relatively minor (Hubbard et al., 1990). The agreement between growth rates of massive head corals such as *Montastrea annularis* and *Porites sp.* and Holocene reef accretion rates (Table 10.2), suggests that these head corals set an upper limit to the growth rates of coral reefs. Computer simulations of Holocene reef growth based on the assumption that the growth rate of massive head corals determines reef growth, support this notion (chapter 5). In the introduction to part II it is shown that the green alga Halimeda has similar depth limits as hermatypic corals. The relation between light and photosynthesis for Halimeda is similar to the light response of hermatypic scleractinians as shown in the introduction to part I (Abel and Drew, 1985). Furthermore coralline algae are completely autotrophic and have depth limits comparable to those of reef-building corals. We can therefore safely assume that carbonate production by these other important sediment producers decreases with depth in a way similar to that of reef-building corals.

Table 10.1. Growth rates of reef-building corals.

	growth rate * (mm/yr)	references
CARIBBEAN		
Acropora palmata	50-100	Bak, 1976; Gladfelter et al., 1978
Acropora cervicornis	45-130	Shinn, 1966; Gladfelter et al.,1978
Montastrea annularis	2-16	Bosscher and Meesters, 1992
INDO-PACIFIC		
Porites lutea	4-13.5	Buddemeier et al., 1976
Porites lobata	2-15	Grigg, 1982
Acropora sp.	100-200	Davies, 1983
Pocillopora damicornis	6-72	Glynn and Stewart, 1973
Platygra sp.	5-12	Weber and White, 1974

Table 10.2. Holocene reef growth rates.

	rate (mm/yr) (based on ^{14}C dates)	references
CARIBBEAN		
St.Croix	1-12	Adey, 1978
Alacran, Mexico	1.25-12	Macintyre et al., 1977
Florida	3.6-10.7	Lighty et al., 1978
Panama	1.6-10.8	Macintyre and Glynn, 1976
Curaçao	1-4	Focke, 1978
INDO-PACIFIC		
Enewetak Atoll	up to 10	Davies, 1983
Tarawa Atoll	5-8.2	Marshall and Jacobson, 1985
Hawaii	1-10	Grigg, 1982
Great Barrier Reef	up to 8	Davies, 1983
Reunion	up to 10.2	Montaggioni, 1977
Maldives	up to 6	Woodroffe, 1992

THE GROWTH OF CARBONATE PLATORMS

Tropical platforms rimmed by reefs produce most of their sediment when they are flooded by the sea (Schlager, 1992). Although the upward growth of entire platforms is determined by the growth of the rim, the ability of platforms to produce sediment depends largely on the platform interior 'carbonate factory' (Schlager 1992). Carbonate production rates for platform margins are higher than for the platform interior, but the relative size of the interior production area makes it a significant producer of sediment. The assumption that carbonates build up to a certain base-level and only start shedding sediment when this level is reached, forms the basis of the simulation model CARBPLAT (chapter 6). The assumed difference in grainsize of sediment produced by the platform margin and the platform interior and the consequently different angle of repose for these sediment types, may cause unconformities that are not necessarily related to sea-level. In CARBPLAT simulations large amounts of mud are exported from the platform during flooding of the platform. These muds onlap the more steeply dipping slopes of sand and rubble shed by fringing reefs during sea-level lowstands. Figure 6.3 shows that on carbonate platforms subjected to a linear sea-level rise unconformities can be created as a result of changes in the exported sediment types after flooding. This CARBPLAT simulation corresponds to observations on the deposition of a Holocene mud wedge after flooding of the Bahamas carbonate platforms (Grammer, 1991; Schlager, 1992).

The basic assumptions incorporated in CARBPLAT are depth dependent production (see part I), slope angle dependent on sediment composition (Kenter, 1990), and highstand shedding of carbonate platforms. Highstand shedding by carbonate platforms is illustrated by changes in composition and accumulation rates of calciturbidites in Exuma Sound, Bahamas (chapter 7). Accumulation rates ofthese calciturbidites vary with flooding of the platform. When the platform top was exposed in the late Pliocene to Pleistocene , as i ndicated by several subaerial exposure horizons, accumulation rates were low. When the platform topwas flooded during the Pleistocene, large amounts of sediment were exported from the platform top, containing abundant ooids.

Computer simulations are by definition a simplification of the 'real world'. But the assumptions that underlie CARBPLAT are well constrained and illustrated in parts I and II of this thesis. The simulation results shown in chapters 5 and 6 show that depth-dependent production and highstand shedding are important principles of carbonate sedimentation.

GROWTH POTENTIAL

The maximum growth rate of coral reefs and carbonate platforms during the Holocene transgression was ca. 12000 B (m/Ma; Table 10.2). This rate was measured over intervals in which the reefs were in a catch-up growth phase. I therefore assume that this rate is a reasonable estimate of the maximum growth potential of coral reefs . From studies on Pacific reef growth Grigg and Epp (1989) arrived at a similar figure for maximum reef accretion. Average reef accretion rates during the Holocene have been in the range of 1000 to 10000 B (Davies, 1983; Grigg and Epp, 1989). Comparison with accumulation rates of reefs and platforms from the Phanerozoic suggests that during most of the geologic history reefs and carbonate platforms were able to grow at rates of 1000 B for thousands of years.

Some remarks on scaling laws

With decreasing time span the number and size of observed hiatuses in a stratigraphic section increases (chapter 9; Sadler, 1981; Plotnick 1986). Schematically the stratigraphic record can be described by a Cantor bar (Plotnick, 1986; Fig. 10.3). The distribution of hiatuses is scale invariant and hence has a fractal distribution obeying power laws. If the size and number of hiatuses increases with the time span of observation then the average sedimentation rate should decrease with inreasing timespan of observation. With improved chronostratigraphic resolution hiatuses are progressively omitted from the calculated accumulation rates. This fractal distribution of hiatuses reflects the cumulative effects of many factors that make sedimentation and erosion episodic or pulsating. Recognition of this trend in stratigraphic records allows extrapolation of short term accumulation rates from longer term records.

Extrapolation of accumulation rates of fossil carbonate platforms that grew for many millions of years to intervals of 10^1-10^4 years (Holocene coral and reef growth rates) shows that these agree surprisingly well (chapter 9). This observation supports the assumptions on the fractal distribution of hiatuses mentioned in the previous paragraph. It also suggests that during most of the Phanerozoic, the growth rates of coral reefs and carbonate platforms have been of the same order of magnitude as those observed during the Holocene and Pleistocene. This does not hold for the periods following extinction events. During these periods the growth potential must have been severely reduced as is apparent from the lack or paucity of reefs and platforms in these periods (Copper, 1988; James, 1992).

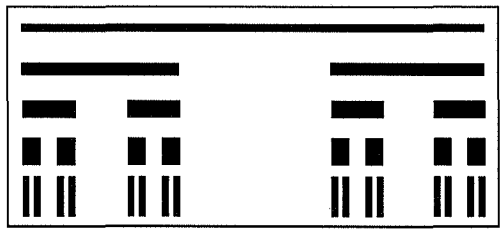

Figure 10.3. Cantor bar, illustrating the fractal distribution of hiatuses in the stratigraphic record. The pattern is created by removing the middle third of each bar for each step. The length of the bar represents time, the area of the bar theamount of sediment. With increased chronostratigraphic resolution the number of recognized hiatus increases and the accumulation rate (height of the bar) increases.

DROWNING OF REEFS AND CARBONATE PLATFORMS

Drowning of reefs and carbonate platforms, i.e. submergence below the euphotic zone, has occured throughout the geologic record. Drowning of reefs and platforms requires that the rate of creation of accommodation space (relative sea-level rise) exceeds the growth potential. A platform will drown if this rapid rise lasts long enough to traverse the thickness of the euphotic zone. So there are basically two options to drown reefs, either by a rapid relative sea-level rise or by reduction of growth potential (Schlager, 1981, p.204-205).

Rapid rates of sea-level rise, as observed during the Pleistocene/Holocene glacio-eustatic sea-level cycles, are able to drown coral reefs. During the Holocene transgression most reefs were outpaced by sea-level (Schlager 1981; Ludwig et al, 1991; among others). The average rate of sea-level rise during the first half of this transgression was ca. 12000 B, with a maximum in the order of 20000 B (Grigg and Epp, 1989). Most Holocene reefs only established themselves when the rate of sea-level rise slowed down ca. 9000 years ago , mostly on antecedent Pleistocene foundations. The cyclic nature of such sea-level variations however renders them incapable of permanently drowning reefs. If subjected to rapid sea-level rises reefs will try to 'backstep' and reestablish when rates of sea-level rise drop below their maximum growth rate or during the next sea-level fall. Sea level on its own can not permanently drown reefs and platforms. In areas with rapid tectonic subsidence, superimposed on cyclic sea-level variations, however, relative sea-level rises are a possible cause for drowning.

The other option to drown reefs and platforms is a reduction of the growth potential. The sensitivity of reef-building communities to environmental factors (see introduction to Part I) offers a wide range of possible causes for reef and platform drowning. Changes in temperature, salinity, nutrients, increased terrigenous runoff, changes in ocean chemistry and ocean circulation, can all cause the demise of coral reefs and carbonate platforms. Many of these factors are related or have a common cause. For example during the Holocene sea-level rise the bank-barrier reefs of St. Croix drowned probably as a result of inimical bank waters after flooding of the shelf (Adey, 1978). Large-scale geologic processes such as increased seafloor spreading or changes in ocean hypsometry and plate configuration can affect sea-level variations, change climatic conditions, cause upwelling of cold nutrient-rich water, change the area available for carbonate platform development or move platforms outside the favourable belt of tropical reef development. It is obvious that it is often difficult to assign one single cause to reef and platform demise. Changes in environmental conditions can occur extremely rapid on a geologic time scale. We often lack the chronostratigraphic resolution to assess the exact cause of drowning. The drowning of reefs and carbonate platforms has been called a paradox by Schlager (1981). This was based on the observation that the growth potential, derived from Holocene reef growth rates and progradation of ancient platforms is higher than long term rates of relative sea-level rise. From the above I agree with Schlager (1981) that a reduction of growth potential is a plausible answer to this paradox.

Drowning periods in geologic history

After drowning shallow water carbonates will be covered by progressively deeper water pelagic sediments (see for example Campbell, 1992). Some of these drowning periods coincide with periods of extinction of reef-builders (see chapter 8). Drowning during these periods is obviously related to the cause of the extinction of reef-builders. Extinction of reef-building organisms will reduce growth potential. Most of the Paleozoic extinctions seem to be related to cooler oceans (Copper, 1986; Stanley, 1988). Cooler, nutrient-rich waters, will be detrimental to reef development. Hallock and Schlager (1986) proposed that drowning in the late Devonian, early Jurasic and Cretaceous may be caused by eutrophication during open ocean overturn in anoxic periods. The late Devonian drowning coincided with a large extinction of reef-builders and has often been related to cooler oceans (Copper, 1986; Stanley, 1985). The possible role played here by nutrient excess is illustrated by the near disappearance of the probably symbiont-bearing tabulate corals (Cowen, 1988) whereas the non-symbiotic rugose corals suffered much less. The algal symbiosis makes coral reef ecosystems largely autotrophic and thus vulnerable to competition from heterotrophic organisms in high-nutrient environments (see introduction to part I).

SHALLOW WATER CARBONATES IN THE GLOBAL CARBON BUDGET

Long term trends in carbonate deposition

Through the incorporation of carbon in skeletal $CaCO_3$ and organic matter coral reefs and carbonate platforms constitute an important sink for carbon. As is shown in chapter 8, accumulation rates of shallow water carbonates have fluctuated during geologic history. When periods with little shallow water carbonate deposition alternate with periods that show a global coral reef area of many millions of square kilometres this should have a noticable effect on the saturation of the oceans wirh respect to $CaCO_3$ and the CO_2 content of the atmosphere. Figure 10.4 gives the mass vs. age for Phanerozoic carbonate rocks. The total carbonate reservoir in sedimentary rocks is ca. 9000×10^{20} g $CaCO_3$ (Hay, 1985). This is the equivalent of ca. 1100×10^{20} g C or 25000 times the present carbon reservoir in ocean water. On a geologic timescale shoalwater carbonates (as opposed to pelagic carbonates) form the most important sink for carbon. A relationship between the amount of carbon deposited in carbonate rock and the PCO_2 of the atmosphere has been proposed by several authors: Berger (1982), Mackenzie and Morse (1992); among others. According to Mackenzie and Morse (1992) high levels of atmospheric CO_2 and hence higher temperatures during the Devonian and Cretaceous, led to increased carbonate depositional rates.

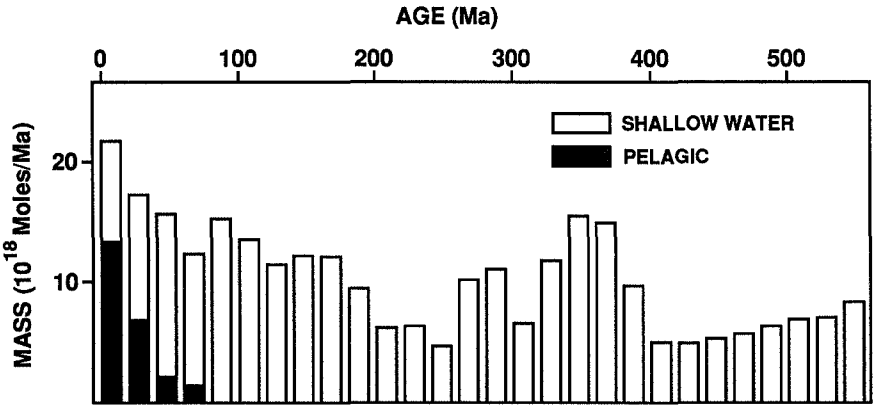

Figure 10.4. Mass versus age for carbonate rocks divided into shallow water and pelagic environments (modified after Boss and Wilkinson, 1991).

A possible implication of the mass age trend shown in Figure 10.4 could be the near-cessation of shallow water limestone deposition within the next 100 Ma. That is, if the "calcite-pull" scenario (Wilkinson and Walker, 1989) is the underlying mechanism for this trend. This means that with the rise of planktonic foraminifers and calcitic nannoplankton in the early Mesozoic and their rapid expansion since the middle Cretaceous carbonate deposition gradually shifted from cratonic to pelagic environments. The pelagic reservoir now accounts for ca. 60% of the total carbonate deposition whereas it only constitutes 7% of the total Phanerozoic carbonate mass (Wilkinson and Walker, 1989). If the evolution of planktonic calcifiers is the cause for this trend and the pelagic reservoir keeps increasing at the expense of the cratonic reservoir, shallow water carbonate deposition will cease to exist within 100 Ma (Wilkinson and Walker, 1989). This cessation will be preceded by a gradual decrease in growth potential. An alternative explanation for the observed trend is the partitioning between the cratonic and pelagic reservoirs by sea-level. Surface area available for shallow water carbonate deposition will be greater when sea level is high. This means that when sea-level is falling, which has been the case since the late Mesozoic, cratonic carbonate deposition will be limited and favour the increase of the pelagic reservoir. The good fits between model trends based on global sea-level variations and the mass age trend shown in Figure 10.4 show that this scenario, too, agrees well with the available data (Wilkinson and Walker, 1989). It has so far been impossible to determine which of the mechanisms underlies the geological observations (Boss and Wilkinson, 1991).

The pelagic carbonate reservoir has increased since the late Mesozoic and, because the global carbonate flux is finite, this has been at the expense of shallow water carbonates. Coral reefs precipitate ca 900×10^9 kg $CaCO_3$ per year and predictions are this rate will increase with rising sea-level (Kinsey and Hopley, 1991). It should be noted that the short term effect of carbonate production by coral reefs is a contribution of CO_2 to the atmosphere (Kinsey and Hopley, 1991). An amount of 900×10^9 kg $CaCO_3$ per year corresponds to ca. 3.7×10^{20} gCa per million year This agrees with the extrapolation of the mass age trend for

the cratonic reservoir shown in Figure 9. If an extrapolation from present-day values to periods of millions of years is at all valid this would suggest that the predicted cessation of shallow water carbonate deposition is questionable. The variation in accumulation rates of carbonate platforms throughout the Phanerozoic reported in chapter 8 suggests that during certain periods of geologic history cratonic carbonate accumulation may have been markedly lower. If the flux of carbonate to the oceans has been constant throughout the Phanerozoic as suggested by Boss and Wilkinson (1991) and Mackenzie and Morse (1992), then this must have had a profound effect on the carbonate saturation level of the oceans. The role of shallow water carbonates as sinks for carbon, therefore must have varied during the Phanerozoic. According to Mackenzie and Morse (1992) much of the variation observed in carbonate mass age trends tracks the first order sea-level variations. This would agree with the 'calcite-push' model of Wilkinson and Walker (1989). During periods of high sea-level the fluxes of carbonate and also carbonate depositional rates are high. The 'push' of carbonate to greater depths results from reduced carbonate fluxes that accompany a low sea level. The lack of well preserved pre-Mesozoic oceanic crust and pelagic sediments makes it difficult to assess the validity of this 'calcite-push' model. There are occurences of Paleozoic deep water limestones (Boss and Wilkinson, 1991) and perhaps the partitioning of carbonate to deeper water during lower sea level resulted in a deepened CCD to maintain steady state with respect to the influx of Ca^{2+} and dissolved inorganic carbon (Mackenzie and Morse, 1992)

The prediction that with rising sea-level carbonate production will increase (Kinsey and Hopley, 1991) supports sea-level ('calcite-push' model of Wilkinson and Walker (1989)) as the mechanism behind the partitioning of carbonates between the continental and oceanic reservoirs. Obviously the evolution of planktonic calcifiers during the Mesozoic played a role in the partitioning of carbonates. The observation that the growth potential of shallow water carbonates has varied during the Phanerozoic (chapter 8) suggests that a simple sea-level partitioning model is an oversimplification. First order sea-level changes can not explain the variations in carbonate accumulation rates for the Phanerozoic (Figure 8.3). This suggests that evolutionary trends and long-term sea-level changes act in tandem, a fact readily accepted for the Cenozoic partitioning of carbonate to the pelagic reservoir.

CONCLUSIONS

The decrease of skeletal growth with depth of the main reef-building coral in the Caribbean, *Montastrea annularis*, is dominated by the decrease of light. The decrease of photosynthesis with depth can be described using a function that combines the relation between light and photosynthesis and the exponential decay of light in the water column. The decrease of coral growth rates with depth can similarly be described using such a function. In the shallow zone of light saturation coral growth rates remain relatively constant. Below the light saturation depth growth rates decrease rapidly. Considering the importance of photosynthesis for carbonate production by reef organisms it is assumed that this growth depth relation holds for nearly all reef-builders and thus also for reef growth.

The growth of massive head corals can be considered as a measure of the growth potential of Holocene coral reefs. The maximum growth rates of these corals are commensurate with the observed maximum Holocene accretion rates. Computer simulations of reef growth have shown that Holocene reef accretion curves are in agreement with the response of the growth rate of corals to changing depth (i.e. sea level).

Drowning of reefs can occur by a variety of mechanisms: rapid rise of sea-level, increased turbidity, nutrients, changing oceanographic conditions etc.
Considering the growth potential of coral reefs and carbonate platforms large drowning events must have resulted from a reduction of the growth potential through environmental crises. Rapid tectonic subsidence can result in drowning on a more regional scale.

Two depths are critical for the drowning of coral reefs and carbonate platforms: the base of the euphotic zone, below which platforms cannot rebound, and the base of the zone of light saturation, below which the rates of carbonate production decline rapidly.

The simulation model CARBPLAT shows carbonate platforms as 'highstand-shedders'. That means that only if the platform is flooded and has built up to sea level large amounts of sediment can be exported. If the assumptions that underlie this model are valid, then unconformities on platform slopes and in adjacent basins can be caused by changes in sea level as well as changes in sediment composition on the platform. The creation of hiatuses and changes in sediment accumulation rates in basins adjacent to carbonate platforms illustrate this.

Accumulation rates of Phanerozoic carbonate platforms measured over intervals of millions of years have been generally in the range of 20 to over 200 B (m/Ma). Extrapolation of these rates to the time domain relevant for drowning (10^3-10^4 years), using scaling laws, suggests that these platforms had a growth potential of approximately 1000 B.

REFERENCES

Abel. K.M., and Drew, E.A., 1985. Response of *Halimeda* metabolism to various environmental parameters. Proceedings 5th International Coral Reef Symposium, v.5, p.21-26.

Acevedo, R., Morelock, J., and Olivieri, R.A., 1989. Modification of coral reef zonation by terrigenous sediment stress. Palaios, v.4, p.92-100.

Adey, W.H., 1978. Coral reef morphogenesis: a multidimensional model. Science, v.202, p.831-837.

Adey, W.H., 1986. Coralline algae as indicators of sea-level. *in* Van der Plassche, O. (ed.), Sea-level research: a manual for the collection and evaluation of data. Geo Books, Norwich, p.229-281.

Aharon, P., 1991. Recorders of reef environment histories: stable isotopes in corals, giant clams, and calcareous algae. Coral Reefs, v.10, p.71-90.

Aigner, T, Doyle, M., Lawrence, D., Epting, M., and Van Vliet, A., 1989. Quantitative modeling of carbonate platforms: some examples. *in* Crevello, P., Wilson, J.L, Sarg, J.F., and Read, J.F, (eds.), Controls on carbonate platform and basin development. Society of Economic Paleontologists and Mineralogists Special Publication 44, p.27-37.

Aitken, J.D., 1978. Revised model for depositional grand cycles, Cambrian of the southern Rocky Mountains. Canada. Bulletin of Canadian Petroleum Geology, v.26, p.515-542.

Aller, R.C., and Dodge, R.E., 1974. Animal-sediment relations in a tropical lagoon, Discovery Bay, Jamaica. Journal of Marine Research, v.32, p.209-232.

Anders, M.H., Krueger, S.W., and Sadler, P.M., 1987. A new look at sedimentation rates and the completeness of the stratigraphic record. Journal of Geology, v.95, p.1-14.

Arnaud-Vanneau, A., Arnaud, H., Cotillon, P., Ferry, S., and Masse, J.P., 1982. Caractères et évolution des plates-formes carbonatées périvocontiennes au Crétacé Inférieur (France Sud-Est). Cretaceous Research, v.3, p.3-18.

Bak, R.P.M., 1974. Available light and other factors influencing growth of stony corals through the year in Curaçao. Proceedings 2nd International Coral Reef Symposium, v.2, p.229-233.

Bak, R.P.M., 1977. Coral reefs and their zonation in Netherlands Antilles. The American Association of Petroleum Geologists, Studies in Geology 4, p.3-16.

Baker, P.A., and Weber, J.N., 1975. Coral growth rate: variation with depth. Earth and Planetary Science Letters, v.27, p.57-61.

Barnes, D.J., Taylor, D.L., 1973. In situ studies of calcification and photosynthetic carbon fixation in the coral *Montastrea annularis*. Helgoland wissenschaftliche Meeresuntersuchungen, v.24, p.284-291.

Barnes, D.J., Lough, J.M., and Taylor, R.B., 1992, Coral density banding - the mist is clearing. 7th International Coral Reef Symposium, p.7 (abstract).

Barth, W., 1968, Die geologie der Hochkalter-Gruppe in den Berchtesgadener Alpen, Neues Jahrbuch Geologisch-Paläontologische Abhandlungen, v.131, p.119-177.

Beach, D.K., and Ginsburg, R.N., 1980. Facies succession of Pliocene-Pleistocene carbonates, northwestern Great Bahama Bank. American Association of Petroleum Geologists Bulletin, v. 64, p.1634-1642.

Beets, C.J., 1991. The Late Neogene $^{87}Sr/^{86}Sr$ isotopic record in the western Arabian Sea, Site 722. *in*: Prell, W.L., Niitsuma, N., et al. (eds.), Proceedings of the Ocean Drilling Program, Scientific Results, v.117, Part B: College Station, Texas (Ocean Drilling Program), p.459-463.

Beets, C.J., 1992. Calibration of late Cenozoic marine strontium variations and its chronostratigraphic and geochemical applications. Ph.D. thesis, Vrije Universiteit, Amsterdam, 133p.

Berger, W.H., 1982. Increase of carbon dioxide in the atmosphere during deglaciation: the coral reef hypothesis. Naturwissenschaften, v.69, p.87-88.

Berggren, W.A., Kent, D.V., Flynn, J.J., and Van Couvering, J.A., 1985. Cenozoic Geochronology. Geological Society of America Bulletin, v.96, p.1407-1418.

Beznosov, N.V., Gorbatchik, T.N., Mikhailova, I.A., and Pergament, M.A., 1978. Soviet Union. *in* Moullade, M., and Nairn, A.E.M., (eds.), The Phanerozoic geology of the world I, The Mesozoic, A. Elsevier, Amsterdam, 529 p.

Bice, D., 1988. Synthetic stratigraphy of carbonate platform and basin systems. Geology, v.16, p.703-706.

Bond, G.C., and Kominz, M.A., 1984. Construction of tectonic subsidence curves for the Early Paleozoic miogeocline, southern Canadian Rocky Mountains: Implications for subsidence mechanisms, age of brakeup and crustal thinning. Geological Society of America Bulletin, v.95, p.155-173.

Bond, G.C., Kominz, M.A.,, Steckler, M.S., and Grotzinger, J.P., 1989. Role of thermal subsidence, flexure, and eustacy in evolution of early Paleozoic passive margin carbonate platforms. *in* Crevello, P., Wilson, J.L, Sarg, J.F., and Read, J.F, (eds.), Controls on carbonate platform and basin development. Society of Economic Paleontologists and Mineralogists Special Publication 44, p.39-61.

Bosence, D., and Waltham, D., 1990. Computer modeling the internal architecture of carbonate platforms. Geology, v.18, p.26-30.

Boss, S.K., and Wilkinson, B.,H., 1991. Planktogenic/eustatic control on cratonic/oceanic carbonate accumulation. Journal of Geology, v.99, p.497-513.

Bosscher, H., and Meesters, E.H., 1992, Depth related changes in the growth of *Montastrea annularis*. Proceedings 7th International Coral Reef Symposium, p.11 (abstract).

Bosscher, H., and Schlager, W., 1992a. Computer simulation of reef growth. Sedimentology, v.39, p.503-512

Bosscher, H., and Schlager, W., 1992b. Accumulation rates of carbonate platforms. Journal of Geology (in press).

Brack, P, 1991. Large-scale and small-scale geometries of carbonate platforms and basins: a comparison of biostratigraphically constrained examples from the South Alpine Triassic. Dolomieu Conference on Carbonate Platforms and Dolomitization, Ortisei, Italy, p.38-39 (abstract).

Brakel, W.H. ,1979. Small-scale spatial variation in light available to coral reef benthos: quantum irradiance measurements from a Jamaican reef. Bulletin of Marine Science, v.29, p.406-413.

Brouwer, M.J.N., and Schwander, M.M., 1988. Cenozoic carbonate banks, Foz do Amazonas, northeast Brazil. *in* Bally, A.W., (ed.), Atlas of seismic stratigraphy. American Association of Petroleum Geologists, Studies in Geology 27, v.2, p.174-178.

Buddemeier, R.W., 1974. Environmental control over annual and lunar monthly cycles in hermatypic coral calcification. Proceedings 2nd International Coral Reef Symposium, v.2, p.259-267.

Buddemeier, R.W., Maragos, J.E., and Knutson, D.W., 1974. Radiographic studies of reef coral exoskeletons: rates and patterns of coral growth. Journal of Experimental Marine Biology and Ecology, v.14, p.179-200.

Buddemeier, R.W., and Kinzie, R.A., 1976. Coral growth. Oceanography and Marine Biology Annual Review, v.14, p.183-225.

Burchette, T.P., 1981. European Devonian reefs: a review of current concepts and models. *in* Toomey, D.F., (ed.), European fossil reef models. Society of Economic Paleontologists and Mineralogists Special Publication 30, p.85-142.

Butterlin, J., 1983, The Caribbean region. *in* Moullade, M., and Nairn, A.E.M., (eds.), The Phanerozoic Geology of the world II, The Mesozoic, B. Elsevier, Amsterdam, p.89-119.

Campbell, A.E., 1992. Unconformities in seismic records and outcrop. Ph.D. Thesis, Vrije Universiteit, Amsterdam, 187p.

Cantelli, C., Spalletta, C., Vai, G.B., and Venturini, C., 1982, Sommersione delle piattaforme e rifting devono-dinantiano e namuriano nella geologia del Passo M. Croce Carnico. *in* Castellarin, A., and Vai, G.B., Guida alla Geologia del Sudalpino Centro-Orientale: Bologna. Societa Geologica Italiana, p.293-303.

Capo, R.C., and DePaolo, D.J., 1990. Seawater strontium isotope variations from 2.5 million years ago to the Present. Science, v.249, p.51-55.

Carbone, F., and Sirna, G., 1981, Upper Cretaceous reef models from Rocca di Cave and adjacent areas in Latium, central Italy. *in* Toomey, D.F., (ed.), European fossil reef models. Society of Economic Paleontologists and Mineralogists Special Publication 30, p.427-445.

Chalker, B.E., 1981. Simulating light-saturation curves for photosynthesis and calcification by reef-building corals. Marine Biology, v.63, p.135-141.

Chalker, B.E., 1983. Calcification by corals and other animals on the reef. *in* Barnes, D.J.,(ed.), Perspectives on coral reefs. Australian Institute of Marine Science Contribution 200, p.29-45.

Chalker. B.E., Barnes. D.J., and, Isdale, P., 1985. Calibration of X-ray densitometry for the measurement of coral skeletal density. Coral Reefs, v.4, p.95-100.

Chalker, B.E., Barnes, D.J., Dunlap, W.C., and Jokiel, P.L., 1988. Light and reef-building corals. Interdisciplinary Science Reviews, v.13, p.222-237.

Chalker, B.E., and, Barnes, D.J., 1990. Gamma densitometry for the measurement of skeletal density. Coral Reefs, v.9, p.11-23.

Chappell, J., 1980. Coral morphology, diversity and reef growth. Nature, v.286, p.249-252.

Chayes, F., 1956. Petrographic modal analysis. J. Wiley & Sons, New York, 113 p.

Chevalier, J.P., 1973. Geomorphology and geology of coral reefs in French Polynesia. *in* Jones, O.A., and Endean, R., (eds.), Biology and Geology of Coral Reefs, Academic Press, New York, v.1, p.113-141.

Chuvashov, B.I., 1983. Permian reefs of the Urals. Facies, v.8, p.191-212.

Clausen, C.D., and Roth, A.A., 1975. Effect of temperature and temperature adaption on calcification rate in the hermatypic coral *Pocillopora damicornis*. Marine Biology, v.33, p.93-100.

Cloetingh, S., 1988. Intraplate stresses: a new element in basin analysis. *in* Kleinspehn, K.L., and Paola, C., (eds.),New perspectives in basin analysis. Springer-Verlag, New York, p.205-230.

Coles, S.L., and Jokiel, P.L., 1977. Effects of temperature on photosynthesis and respiration in hermatypic corals. Marine Biology, v.43, p.209-216.

Coles, S.L., and Jokiel, P.L., 1978. Synergistic effects of temperature, salinity and light on the hermatypic coral *Montipora verrucosa*. Marine Biology, v.49, p.187-195.

Conklin, J., and Moore, C., 1977. Paleoenvironmental analysis of the Lower Cretaceous Cupido Formation, northeast Mexico. *in* Bebout, D.G., and Loucks, R.G., (eds.), Cretaceous carbonates of Texas and Mexico. Bureau of Economic Geology, Report of Investigations 89, p.302-323.

Cook, H.E., and Taylor, M.E., 1977. Comparison of continental slope and shelf environments in the Upper Cambrian and Lowest Ordovician of Nevada. *in* Cook, H.E., and Enos, P., (eds.), Deep water carbonate environments. Society of Economic Paleontologists and Mineralogists Special Publication 25, p.51-81.

Copper, P., 1986. Frasnian/Famennian mass extinction and cold-water oceans. Geology, v.14, p.835-839.

Copper, P., 1988. Ecological succession in Phanerozoic reef ecosystems: is it real? Palaios, v.3, p.136-152.

Cortés, J.N., and, Risk, M.J., 1985. A reef under siltation stress: Cahuita, Costa Rica. Bulletin of Marine Science, v.36, p.339-356.

Cowen, R., 1988. The role of algal symbiosis in reefs through time. Palaios, v.3, p.221-227.

Czurda, K., 1972. Parameter und Prozesse der Bildung bituminöser Karbonate (Bituminöser Hauptdolomit). Mitteilungen der Gesellschaft der Geologie- und Bergbaustudenten in Österreich, v.21, p.235-250.

D'Argenio, B., Pescatore, T., and Scandone, P., 1975. Structural pattern of the Campania-Lucania Apennines. Quaderni de 'La ricerca scientifica', v.90, p.313-327.

Darwin, C.R., 1842. The structure and distribution of coral reefs. University of Arizona Press, 1984 edition, 214p.

Davies, G.R., 1977. Turbidites, Debris sheets and truncation structures in Upper Paleozoic deep-water carbonates of the Sverdrup Basin, Arctic Archipelago. *in* Cook, H.E., and Enos, P, (eds.), Deep water carbonate environments. Society of Economic Paleontologists and Mineralogists Special Publication 25, p.221-247.

Davies, P.J., 1977. Modern reef growth - Great Barrier Reef. Proceedings 3rd International Coral Reef Symposium, v.2, p.325-330.

Davies, P.J., 1983. Reef Growth. *in* Barnes, D.J., (ed.), Perspectives on coral reefs. Australian Institute of Marine Science Contribution, 200, p.69-106.

Davies, P.J., and Montaggioni, L., 1985. Reef growth and sea-level change: the environmental signature. Proceedings 5th International Coral Reef Symposium, v.3, p.477-515.

Davies, P.J., Marshall, J.F., and Hopley, D., 1985. Relationships between reef growth and sea level in the Great Barrier Reef. Proceedings 5th International Coral Reef Symposium, v.3, p.95-103.

Davies, P.J., Symonds, P.A., Feary, D.A., and Pigram, C.J., 1989. The evolution of the carbonate platforms of northeast Australia. *in* Wilgus, C.K., Hastings, B.S., Kendal, C.G.St.C., Posamentier, H.W., Ross, C.A., and Van Wagoner, J.C. (eds.), Sea-level changes: an integrated approach. Society of Economic Paleontologists and Mineralogists Special Publication 42, p.233-258.

Davies, P.J., Mackenzie, J.A., et al., 1991. Proceedings Ocean Drilling Program, Initial Reports. v.133, 1485p.

Dimian, M.V., Gray, R., Stout, J., and Wood, B., 1983. Hudson Bay Basin. *in* Bally, A.W., (ed.), Seismic expression of structural styles. American Association of Petroleum Geologist, Studies in Geology 15, v.2, p.2.2.4-1 - 2.2.4-8.

Dodge, R.E., 1980. Preparation of coral skeletons for growth studies. *in* Rhoads, D.C., and Lutz, R.A., (eds.), Skeletal growth of aquatic organisms, Plenum Press, New York, v.1, p.615-618.

Dodge, R.E., and, Thompson, J., 1974. The natural radiochemical and growth records in contemporary hermatypic corals from the Atlantic and Caribbean. Earth and Planetary Science Letters, v.23, p.313-322.

Dodge, R.E., and, Brass, G.W., 1984. Skeletal extension, density and calcification of the reef coral, *Montastrea annularis*: St.Croix, U.S. Virgin Islands. Bulletin of Marine Science, v.34, p.288-307.

Dodge, R.E., Garcia, R., Szmant, A.M., Swart, P.K., Leder, J.J., and Forester, A., 1992. Skeletal structural basis of density banding in the reef coral *Montastrea annularis*. 7th International Coral Reef Symposium, p.24 (abstract).

Dolan, J.F., 1989. Eustatic and tectonic controls on deposition of hybrid siliciclastic/carbonate basinal cycles: discussion with examples. American Association of Petroleum Geologists Bulletin, v.73, p.1233-1246.

Done, T.J., 1983. Coral zonation: its nature and significance. *in* Barnes, D.J. (ed.), Perspectives on coral reefs. Australian Institute of Marine Science contribution 200, p.107-147.

Droxler, A.W., and Schlager, W., 1985. Glacial versus interglacial sedimentation rates and turbidite frequency in the Bahamas. Geology, v.13, p.799-802.

Droxler, A.W., Haddad, G.A., Mucciarone, D.A., and Cullen, J.L., 1990. Pliocene/Pleistocene aragonite cyclic variations in holes 714A and 716B (The Maldives) compared with Hole 633A (The Bahamas): records of climate induced $CaCO_3$ preservation at intermediate waterdepth. Proceedings Ocean Drilling Program, Scientific Results, v.115B, p.539-577.

Drummond, K.J., 1974. The ancient continental margin of Alaska. *in* Burk, C.A., and Drake C.L., (eds.), The Geology of continental margins. Springer-Verlag, New York, p.797-810.

Dubinsky, Z., 1992. The ratio of energy and nutrient fluxes regulates the symbiosis between zooxanthellae and corals. 7th International Coral Reef Symposium, p.26 (abstract).

Dustan, P., 1975. Growth and form in the reef-building coral *Montastrea annularis*. Marine Biology, v.33, p.101-107.

Dustan, P., 1979. Distribution of zooxanthellae and photosynthetic chloroplast pigments of the reef-building coral *Montastrea annularis* Ellis and Solander in relation to depth on a West-Indian coral reef. Bulletin of Marine Science, v.29, p.79-95.

Dustan, P., 1982. Depth-dependent photoadaption by zooxanthellae of the reef coral *Montastrea annularis*. Marine Biology, v.68, p.253-264.

Eberli, G.P., and Ginsburg, R.N., 1987. Segmentation and coalescence of Cenozoic carbonate platforms in northwestern Great Bahama Bank. Geology, v.15, p.75-79.

Eberli, G.P., Ginsburg, R.N., Swart, P.K., McNeill, D.F., and Kenter, J.A.M., 1991. Preliminary correlations of lithology and seismic reflectors in prograding Neogene carbonate of Great Bahama Bank. American Association of Petroleum Geologists Bulletin, v.75, p.567 (abstract).

Eliuk, L.S., 1978. The Abenaki formation, Nova Scotia shelf, Canada - A depositional and diagenetic model for a Mesozoic carbonate platform. Bulletin of Canadian Petroleum Geology, v.26, p.424-514.

Emiliani, C., Hudson, J.H., Shinn, E.A., and George, R.Y., 1978. Oxygen and carbon isotopic growth record in a reef coral from the Florida Keys and a deep-sea coral form Blake Plateau. Science, v.202, p.627-629.

Enos, P., 1974. Map of surface sediment facies of the Florida-Bahamas Plateau. Geological Society of America, Map Series MC-5, 4 p.

Enos, P., 1986. Diagenesis of Mid-Cretaceous Rudist reefs, Valles Platform, Mexico. *in* Schroeder, J.H., and Purser, B.H., (eds.), Reef Diagenesis. Springer-Verlag, Berlin, p.160-185.

Enos, P., 1991. Sedimentary parameters for computer modeling. *in* Franseen, E.K., Watney, W.L., Kendall, C.G.St.C., and Ross, W., (eds.), Sedimentary modeling: computer simulations and methods for improved parameter definition. Kansas Geological Survey Bulletin, v.233, p.63-99.

Erlich, R.N., Barret, F.S., and Ju, G.B., 1990. Seismic and geologic characteristics of drowning events on carbonate platforms. American Association of Petroleum Geologists Bulletin, v.74, p.1523-1537.

Fagerstrom, J.A., 1987. The evolution of reef communities. J. Wiley & Sons, New York, 600p.

Fairbanks, R.G., and Dodge, R.E., 1979. Annual periodicity of the $^{18}O/^{16}O$ and $^{13}C/^{12}C$ ratios in the reef-building coral *Montastrea annularis*. Geochimica et Cosmochimica Acta , v.43, p.1009-1020.

Fairbanks, R.G., 1989. A 17.000-year glacio-eustatic sea level record: influence of glacial melting rates on the Younger Dryas event and deep-ocean circulation. Nature, v.342, p.637-642.

Fairbanks, R.G., Guilderson, T., Rubenstone, J., and Lao, Y., 1992. Magnitude and rates of sea level change during the Pleistocene. 29th International Geological Congress, Kyoto, Japan, v.1, p.93 (abstract).

Fischer, A.G., 1964. The Lofer cyclothems of the Alpine Triassic. Kansas Geological Survey Bulletin, v.169/1, p.107-150.

Fischer, A.G., 1969. Geological time-distance rates: the Bubnoff unit. Geological Society of America Bulletin, v.80, p.549-552.

Flügel, E., 1981. Lower Permian Tubiphytes/Archeolithopora buildups in the Southern Alps (Austria and Italy), *in* Toomey, D.F., (ed.), European fossil reef models. Society of Economic Paleontologists and Mineralogists Special Publication 30, p.143-160.

Focke, J.W., 1978. Holocene development of coral fringing reefs, leeward off Curaçao and Bonaire (Netherlands Antilles). Marine Geology, v.28, p.M31-M41.

Frazier, W.J., and Schwimmer, D.R., 1987. Regional stratigraphy of North America. Plenum Press, New York, 719 p.

Frost, S.H., 1981. Oligocene reef coral biofacies of the Vicentin area, northeast Italy. *in* Toomey, D.F., (ed.), European fossil reef models. Society of Economic Paleontologists and Mineralogists Special Publication 30, p.483-539.

Fricke, H., and Meisschner, D., 1985. Depth limits of Bermudan scleractinian corals: a submersible survey. Marine Biology, v.88, p.175-187.

Garcia-Mondejar, J., 1985. Aptian and Albian reefs (Urgonian) in the Ason-Soba area. *in* Mila, M.D., and Rosell, J., (eds.), 6th European Regional Meeting of Sedimentology, excursion guidebook, Lleida, Spain, p.329-351.

Geister, J., 1977. The influence of wave exposure on the ecological zonation of Caribbean coral reefs. Proceedings 2nd International Coral Reef Symposium, v.1, p.23-30.

Ginsburg, R.N., and Shinn, E.A., 1964. Distribution of reef-building communities in Florida and the Bahamas. Bulletin of the America Association of Petroleum Geologists, v.48, p.527 (abstract).

Ginsburg, R.N., McNeill, D.F., Eberli, G.P., Swart, P.K., and Kenter, J.A.M., 1991. Transformation of morphology and facies of Great Bahama Bank by Plio-Pleistocene progradation. Dolomieu Conference on Carbonate platforms and Dolomitization, Ortisei, Italy. v.1, p.88-89 (abstract).

Gladfelter, E.H., Monahan, R.K., and Gladfelter, W.B.,1978. Growth rates of five reef-building corals in the northeastern Caribbean. Bulletin of Marine Science, v.28, p.728-734.

Gladfelter, E.H., and Kinsey, D.W., 1985. Metabolism, calcification and carbon production. Proceedings 5th International Coral Reef Symposium, v.4, p.503-542.

Goldhammer, R.K., and Harris, M.T., 1989. Eustatic controls on the stratigraphy and geometry of the Latemar buildup (Middle Triassic), the Dolomites of Northern Italy. *in* Crevello, P., Wilson, J.L, Sarg, J.F., and Read, J.F., (eds.), Controls on carbonate platform and basin development. Society of Economic Paleontologists and Mineralogists Special Publication 44, p.323-338.

Goodell, H.G., and Garman, R.K., 1969. Carbonate geochemistry of Superior deep test well, Andros Island, Bahamas. American Association of Petroleum Geologists Bulletin, v.53, p.513-536.

Gordon, R.G., and Stein, S., 1992. Global tectonics and space geodesy. Science, v.256, p.339-342

Goreau, T.F. ,1959. The physiology of skeleton formation in corals. I. A method for measuring the rate of calcium deposition by corals under different conditions. Biological Bulletin, v.116, p.59-75.

Goreau, T.J., 1977. Carbon metabolism in calcifying and photosynthetic organisms: theoretical models based on stable isotope data. Proceedings 3rd International Coral Reef Symposium, v.2, p.395-401.

Goreau, T.F., Goreau, N.I., and Goreau, T.J., 1979. Corals and coral reefs. Scientific American, v.241, p.110-120.

Grammer, G.M., 1991. Formation and evolution of Quaternary carbonate foreslopes, Tongue of the Ocean, Bahamas. Ph.D. Thesis, University of Miami, 314p.

Graus, R.R., and, Macintyre, I.G., 1982. Variation in growth forms of the reef coral *Montastrea annularis* (Ellis and Solander): A quantitative evaluation of growth response to light distribution using computer simulation. *in* Rützler, K., and, MacIntyre, I.G. (eds.), The Atlantic barrier reef ecosystem at Carrie Bow Cay, Belize. Scientific Reports 1, Smithsonian Contributions to the Marine Sciences no 12, Smithsonian Institution Press, Washington DC, p.441-464

Graus, R.R., and Macintyre, I.G., 1989. The zonation patterns of Caribbean coral reefs as controlled by wave and light energy input, bathymetric setting and reef morphology: computer simulation experiments. Coral Reefs, v.8, p.9-18.

Grigg, R.W., 1982. Darwin Point: a threshold for atoll formation. Coral Reefs, v.1, p.29-34.

Grigg, R.W., and Epp, D., 1989. Critical depth for the survival of coral islands: effects on the Hawaiian Archipelago. Science, v.243, p.638-641.

Grötsch, J., 1992. Guilds, cycles and episodic vertical aggradation of a reef (Upper Barremian to Lower Aptian, Dinaric Carbonate Platform NW Yugoslavia). *in* De Boer, P.L., and Smith, D.G., (eds.), Orbital forcing and cyclic events. International Association of Sedimentologists Special Publication, Oxford, (in press).

Guidish, T.M., Lerche, I., Kendall, C.G.St.C., and O'Brien, J.J., 1984. Relationship between eustatic sea level changes and basement subsidence. American Association of Petroleum Geologists Bulletin, v.68, p.164-177.

Gundersen, K.R., Corbin, J.S., Hanson, C.L., Hanson, M.L., Hanson, R.B., Russell, Stollar, A., and Yamada, O., 1976. Structure and biological dynamics of the oligotrophic ocean photic zone off the Hawaiian islands. Pacific Science, v.30/1, p.45-68.

Haak, A.B, and Schlager, W., 1989. Compositional variations in calciturbidites due to sea-level fluctuations, late Quaternary, Bahamas. Geologische Rundschau, v.78, p.477-486.

Hallock, P., 1981. Algal symbiosis: a mathematical analysis. Marine Biology, v.62, p.249-255.

Hallock, P., and Schlager, W., 1986. Nutrient excess and the demise of coral reefs and carbonate platforms. Palaios, v.1, p.389-398.

Haq, B.U., Hardenbol, J., and Vail, P.R., 1987. Chronology of fluctuating sealevels since the Triassic. Science, v.235, p.1156-1166.

Harland, W.B., Cox, A.V., Llewellyn, P.G., Pickton, C.A.G., and Walters, 1982. A Geologic time scale. Cambridge University Press, Cambridge, 131 p.

Harmelin-Vivien, M., 1985. Atoll de Tihea, Archipel des Tuamota. Proceedings 5th International Coral Reef Symposium, v.1, p.213-266.

Haubitz, B., Prokop, M., Döhring, W., Ostrom, J.W., and Wellnhofer, P., 1988. Computed tomography of *Archeopteryx*. Paleobiology v.14, p.206-213.

Hay, W.W., 1985. Potential errors in estimates of carbonate rock accumulating through geologic time. *in* Sundquist, E.T., and Broecker, W.S., 1985. The carbon cycle and atmospheric CO_2: Natural variations Archean to Present. p.573-585.

Highsmith, R.C., 1979. Coral growth rates and environmental control of density banding. Journal of Experimental Marine Biology and Ecology, v.37, p.105-125.

Hine, A.C., and Steinmetz, J.C., 1984. Cay Sal Bank, Bahamas - a partially drowned carbonate platform. Marine Geology, v.59, p.135-164.

Hillis-Collinvaux, L., 1986. Halimeda growth and diversity on the deep fore-reef of Enewetak Atoll. Coral Reefs, v.5, p.19-21

Hodell, D.A., Mueller, P.A., and Garrido, J.R., 1991. Variations in the strontium isotopic composition of seawater during the Neogene. Geology, v.19, p.24-27.

Hounsfield, N.G., 1973. Computerized transverse axial scanning tomography. British Journal of Radiology, v.46, p.1016.

Hubbard, D.K., and Scaturo, D., 1985. Growth rates of seven species of Scleractinean corals from Cane Bay and Salt River, St. Croix, U.S.V.I. Bulletin of Marine Science, v.36, p.325-338.

Hubbard, D.K., Miller, I.A.,and Scaturo, D., 1990. Production and cycling of calcium carbonate in a shelf-

edge reef system (St. Croix, U.S. Virgin Islands): applications to the nature of reef systems in the fossil record. Journal of Sedimentary Petrology, v.60/3, p.335-360.
Hudson, J.H., Shinn, E.A., Halley, R.B., and Lidz, B., 1976. Sclerochronology: a tool for interpreting past environments. Geology, v.4, p.361-364.
Hudson, J.H., 1981. Growth rates in *Montastrea annularis*: a record of environmental change in Key Largo coral reef marine sanctuary, Florida. Bulletin of Marine Science, v.31, p.444-459.
Hughes, T.P., 1987. Skeletal density and growth form of corals. Marine Ecology Progress Series, v.35, p.259-266.
Huston, M., 1985. Variation in coral growth rates with depth at Discovery Bay, Jamaica. Coral Reefs, v.4, p.19-25.
James, N.P., and Ginsburg, R.N., 1979. The seaward margin of Belize barrier and atoll reefs. Special Publication of the International Association of Sedimentologists 3, Blackwell, Oxford, 191 p.
James, N.P., 1984. Reefs, *in* Walker, R.G., (ed.), Facies Models. Geoscience Canada Reprint Series 1, p.229-244.
James, N.P., and Bourque, P.A., 1992. Reefs and mounds. *in* Walker, R.G., and James, N.P., (eds.), Facies Models. Geological Association of Canada, p.323-347.
Jerlov, N.G., 1976. Marine Optics. Elsevier, Amsterdam, 231 p.
Jull, R.K., 1977. The distribution of corals near the margin of an Upper Devonian carbonate complex in western Canada. Mémoires du Bureau de Recherches Géologiques et Minières, v.89, p.160-166.
Kaufmann, E.G., and Johnson, C.C., 1988. The morphological and ecological evolution of middle and upper Cretaceous reef-building rudistids. Palaios, v.3, p.194-216.
Kenney, B.C., Beware of spurious self-correlations! Water Resources Research, v.18, p.1041-1048.
Kenter, J.A.M., 1989. Applications of Computerized Tomography in sedimentology. Marine Geotechnology v.8, p.201-211.
Kenter, J.A.M., 1990. Carbonate platform flanks: slope angle and sediment fabric. Sedimentology, v.37, p.777-794.
Kenyon, P.M., and Turcotte, D.L., 1985. Morphology of a delta prograding by bulk sediment transport. Geological Society of America Bulletin, v.96, p.1457-1465.
Kinsey, D.W., and Hopley, D., 1991. The significance of coral reefs as global carbon sinks - response to Greenhouse. Palaeogeography, Palaeoclimatology, Palaeoecology, v.89, p.363-377.
Kinsman, D.J.J., 1964. Reef coral tolerance of high temperatures and salinities. Nature, v.202, p.1280-1282.
Kirk, J.T.O., 1983. Light and photosynthesis in aquatic ecosystems. Cambridge University Press, Cambridge, 401 p.
Kirkby, M.J., 1987. General models of long-term slope evolution through mass-movements. *in* Anderson, M.G., and Richards, K.S., (eds.), Slope stability. J. Wiley & Sons, Chichester, England, p.359-380.
Knowlton, N., Weil, E., Weigt, L.A., and Guzman, H.M., 1992. Sibling species in *Montastrea annularis*, coral bleaching, and the coral climate record. Science, v.255, p.330-333.
Knutson, D.W., Buddemeier, R.W., and Smith, S.V., 1972. Coral chronometers: seasonal growth bands in reef corals. Science, v.177, p.270-272.
Krebs, W., 1974. Devonian carbonate complexes of central Europe. *in* Laporte, L.F., (ed.), Reefs in time and space. Society of Economic Paleontologists and Mineralogists Special Publication 18, p.155-208.
Kuznetsov, V., 1990. The evolution of reef structures through time: importance of tectonic and biological controls. Facies, v.22, p.159-168.
Ladd, H.S., 1973. Bikini and Eniwetok atolls. *in* Jones, O.A., and Endean, R.,(eds.), Biology and Geology of Coral Reefs. Academic Press, New York, v.1, p.93-112.
Land, L.S., Lang, J.C. and Smith, B.N., 1975. Preliminary observations on the carbon isotopic composition of some reef coral tissues and symbiotic zooxanthellae. Limnology Oceanography, v.20, p.283-287.
Leder, J.J., Szmant, A.M. and Swart, P.K., 1991. The effect of prolonged "bleaching" on skeletal banding and stable isotopic composition in *Montastrea annularis*. Coral Reefs, v.10, p.19-27.
Lees, A, 1961. The Waulsortian 'reefs' of Eire: a carbonate mudbank complex of Lower Carboniferous age. Journal of Geology, v.69, p.101-109.
Leg 101 Scientific Party, 1988. Cruise synthesis. *in* Austin, J. A., Schlager W., et al. (eds.), Proceedings Ocean

Drilling Program, Scientific Results, v.101, p.455-472.

Lerche, I., Dromgoole, E., Kendall, C.G.St.C., Walter, L.M., and Scaturo, D., 1987. Geometry of carbonate bodies: A quantitative investigation of factors influencing their evolution. Carbonates and Evaporites, v.2, p.15-42.

Liddel, W.D., and Ohlhorst, S.L., 1988. Hard substrata community patterns, 1 - 120 m, North Jamaica. Palaios, v.3, p.413-423.

Lighty, R.G., Macintyre, I.G., and Stuckenrath, R., 1978. Submerged early Holocene barrier reef south-east Florida shelf. Nature, v.275, p.59-60.

Logan, A., and Anderson, I.H., 1991. Skeletal extension growth rate assessment in corals, using CT scan imagery. Bulletin of Marine Science, v.49, p.847-850.

Ludwig, K.R., Halley, R.B., Simmons, K.R., and Peterman, Z.E., 1988. Strontium-isotope stratigraphy of Enewetak Atoll. Geology, v.16, p.173-177.

Ludwig, K.R., Szabo, B.J., Moore, J.G., and Simmons, K.R., 1991. Crustal subsidence rate off Hawaii determined from $^{234}U/^{238}U$ ages of drowned coral reefs. Geology, v.17, p.171-174.

Macintyre, I.G., and Glynn, P.W., 1976. Evolution of modern Caribbean fringing reef, Galeta Point, Panama. American Association of Petroleum Geologists Bulletin, v.60/7, p.1054-1072.

Macintyre, I.G., Burke, R.B., and Stuckenrath, R., 1977. Thickest recorded Holocene reef section, Isla Peréz core hole, Alacran Reef, Mexico. Geology, v.5, p.749-754.

Mackenzie, F.T., and Morse, J.W., 1992. Sedimentary carbonates through Phanerozoic time. Geochimica et Cosmochimica Acta, v.56, p.3281-3295.

Maragos, J.E., Evans, C., and Holthuis, P., 1985. Reef corals in Kaneohe Bay six years before and after terminateion of sewage discharge. Proceedings 5th International Coral Reef Symposium, v.4, p.189-194.

Marcus, J., and Thorhaug, A., 1981. Pacific vs. Atlantic responses of the subtropical hermatypic coral *Porites spp.* to temperature and salinity effects. Proceedings 4th International Coral Reef Symposium, v.2, p.16-20.

Marshal, J.F., and Jacobson, G., 1985. Holocene reef growth of a mid-Pacific atoll: Tarawa, Kiribati. Coral Reefs, v.4, p.11-17.

Masse, J.P., and Alleman, J., 1982. Relations entres les séries carbonatées de plate-forme Provençale et Sarde au Crétacé Inférieur. Cretaceous Research, v.3, p.19-33.

Mazullo, S.J., and Reid, A.M., 1989. Lower Permian platform and basin depositional systems, northern Midland Basin. *in* Crevello, P., Wilson, J.L, Sarg, J.F., and Read, J.F., (eds.), Controls on carbonate platform and basin development. Society of Economic Paleontologists and Mineralogists Special Publication 44, p.305-320.

McConnaughey, T., 1989. ^{13}C and ^{18}O isotopic disequilibrium in biological carbonates: I. Patterns. Geochimica et Cosmochimica Acta, v.53, p.151-162.

McNeil, D.F., Ginsburg, R.N., Chang, S-B.R., and Kirschvink, J.L., 1988. Magnetostratigraphic dating of shallow-water carbonates from San Salvador, Bahamas, Geology, v.16, p.8-12.

McNeill, D.F., 1989. Magnetostratigraphic dating and magnetization of Cenozoic platform carbonates from the Bahamas. Ph.D. Thesis, University of Miami, 210p.

McNeill, D.F., Swart, P.K., and Vahrenkamp, V.C., 1991. Magnetostratigraphic dating: insights to Late Cenozoic deposition and dolomitization of Little Bahama Bank. American Association of Petroleum Geologists Bulletin, v.75, p.633 (abstract).

Melillo, A.J., 1988. Neogene planktonic foraminifer biostratigraphy, Leg 101, Bahamas. *in* Austin, J. A., Schlager W., et al. (eds.), Proceedings of the Ocean Drilling Program, Scientific Results, Volume 101, Part B. College Station, Texas (Ocean Drilling Program), p.3-46.

Mesolella, K.J., Robinson, J.D., McCormik, L.M., and Ormiston, A.R., 1974. Cyclic deposition of Silurian carbonates and evaporites in Michigan Basin. American Association of Petroleum Geologists Bulletin, v.58, p.34-62.

Meyer, F.O., 1989. Siliciclastic influence on Mesozoic platform development: Baltimore Canyon trough, western Atlantic. *in* Crevello, P.D., Wilson, J.L., Sarg, J.F., and Read, J.F., (eds.), Controls on carbonate platform and basin development, Society of Economic Paleontologists and Mineralogists Special

Publication 44, p.213-232.
Meyerhof, A.A., and Hatten, C.W., 1974. Bahamas salient of North America. *in* Burk, C.A., and Drake, C.L., (eds.), The Geology of continental margins. Springer-Verlag, New York, p.429-446.
Mitchum, R.M., and Uliana, M.A., 1988. Regional seismic stratigraphic analysis of Upper Jurassic-Lower Cretaceous carbonate depositional sequences, Neuquen Basin, Argentina, in Bally, A.W., (ed.), Atlas of seismic stratigraphy. American Association of Petroleum Geologists, Studies in Geology 27, v.2, p.174-178.
Montaggioni, L., 1977. Structure interne d'un récif corallien holocène (île de la Réunion, Océan Indien). Mémoires du Bureau de Recherches Géologiques et Minières 89, p.456-466.
Muir, I., Wong, P., and Wendte, J., 1985. Devonian Hare Indian-Ramparts (Kee Scarp) evolution, Mackenzie Mountains and subsurface Norman Wells, N.W.T.: Basin-fill and platform-reef development. *in* Longman, M.W., Shanley, K.W., Lindsay, R.F., and Eby, D.E, (eds.), Rocky Mountain carbonate reservoirs - a core workshop. Society of Economic Paleontologists and Mineralogists Core Workshop 7, p.311-341.
Murris, R.J., 1980. Middle East: stratigraphic evolution and oil habitat. American Association of Petroleum Geologists Bulletin, v.64, p.597-618.
Muscatine, L., Porter, J.W., and Kaplan, I.R., 1989. Resource partitioning by reef corals as determined from stable isotopic composition I. $\delta^{13}C$ of zooxanthellae and animal tissue vs depth. Marine Biology, v.100, p.185-193.
Naim, A.E.M., 1978. Northern and eastern Africa. *in* Moullade, M., and Naim, A.E.M., (eds.), The Phanerozoic geology of the world I, Mesozoic, A. Elsevier, Amsterdam, p.329-370.
Nalivkin, D.V., 1973. Geology of the U.S.S.R.. Oliver and Boyd, Edingburgh, 855 p.
Narbonne, G.M., and Dixon, O.A., 1984. Upper Silurian lithistid sponge reefs on Somerset Island, Arctic Canada. Sedimentology, v.31, p.25-50.
Neumann, A.C., and Macintyre, I.G., 1985. Reef response to sea level rise: keep-up, catch-up or give-up. Proceedings 5th International Coral Reef Symposium, v.3, p.105-110.
Neumann, C.A., and Land L.S, 1975. Lime mud deposition and calcareous algae in the Bight of Abaco: A budget. Journal of Sedimentary Petrology, v.40, p.763-786.
Ott, E., 1972. Mitteltriadische Riffe der Nordlichen Kalkalpen und altersgleiche Bildungen auf Karaburun und Chios (Agäis). Mitteilungen der Gesellschaft der Geologie- und Bergbaustudenten in Österreich, v.21, p.251-276.
Owens, J.P., 1983. The northwestern Atlantic Ocean margin. *in* Moullade, M., and Naim, A.E.M., (eds.), The Phanerozoic Geology of the world II, The Mesozoic, B. Elsevier, Amsterdam, p.33-60.
Parkinson, D., 1957. Lower Carboniferous reefs of Northern Ireland. American Association of Petroleum Geologists Bulletin, v.41, p.511-537.
Parsons, B., and Sclater, J.G., 1977. An analysis of the variation of ocean floor bathymetry and heat flow with age. Journal of Geophysical Research, v.82, p.803-827.
Patterson, M.R., Sebens, K.P., and Olson, R.R., 1991. In situ measurements of flow effects on primary production and dark respiration in reef corals. Limnology and Oceanography ,v.36, p.936-948.
Pätzold, J., 1984. Growth rhythms recorded in stable isotopes and density bands in the reef coral *Porites lobata* (Cebu, Phlippines). Coral Reefs, v.3, p.87-90.
Paulus, F.J., 1972. The Geology of site 98 and the Bahama Platform. *in* Hollister, C.D., and Ewing, J.I., (eds.), Initial Reports of the Deep Sea Drilling Project XI: Washington, D.C., U.S.Government Printing Office, p.877-897.
Peloso, G.F., and Vercesi, P.L., 1982. Geologia della zona a NE di Tione di Trento. *in* Castellarin, A., and Vai, G.B., (eds.), Guida alla Geologia del Sudalpino Centro-Orientale: Bologna. Societa Geologica Italiana, p.115-121.
Perkins, B.F., 1985. Caprinid reefs and related facies in the Comanche Cretaceous Glen Rose limestone of central Texas. *in* Bebout, D.G., and Ratcliff, D., (eds.), Lower Cretaceous depositional environments from shoreline to slope - a core Workshop. GCAGS - GCS/SEPM Annual Meeting, p.129-140.
Pigram, C.J., Davies, P.J., Feary, D.A., and Symonds, P.A., 1989. Tectonic controls on carbonate platform evolution in southern Papua New Guinea: Passive margin to foreland basin. Geology, v.17, p.199-202.

Pitman, III, W.C., and Golovchenko, X., 1983. The effect of sea level change on the shelfedge and slope of passive margins. *in* Stanley, D.J., and Moore, G.T., (eds.), The shelfbreak: critical interface on continental margins. Society of Economic Paleontologists and Mineralogists Special Publication 33, p.41-58.

Playford, P.E., 1980. Devonian 'Great Barrier Reef' of Canning Basin, western Australia. American Association of Petroleum geologists Bulletin, v.64, p.814-840.

Plotnick, R.E., 1986. A fractal model for the distribution of stratigraphic hiatuses. Journal of Geology, v.94, p.885-890.

Poag, C.W., and Schlee, J.S., 1984. Depositional sequences and stratigraphic gaps on submerged United States Atlantic margin. In Schlee, J.S., (ed.), Interregional unconformities and hydrocarbon accumulation. American Association of Petroleum Geologists Memoir 36, p.165-182.

Porter, J.W .,(1985) The maritime weather of Jamaica: its effect on annual carbon budgets of the massive reef-building coral *Montastrea annularis*. Proceedings 5th International Coral Reef Symposium, v.6, p.363-379.

Powder, D.A., Venour, E.R., and Tremblay, L., 1980. Pinnacle reef reservoirs, Zeta Lake member, Nisku formation (Upper Devonian), west Pembina area, Alberta, *in* Halley, R.B., and Loucks, R.G., (eds.), Carbonate reservoir rocks: Society of Economic Paleontologists and Mineralogists Core Workshop 1, p.64-78.

Pratt, B.R., and James, N.P., 1982. Cryptalgal-metazoan bioherms of Early Ordovician age in the St.George Group, western Newfoundland. Sedimentology, v.29, p.543-569.

Press, W.H., Flannery, B.P., Teukolsky, S.A., and Vetterling, W.T., 1986. Numerical recipes: the art of scientific computing. Cambridge University Press, Cambridge, 818 p.

Purtscheller, P., 1962. Sedimentpetrographische Untersuchuchungen am Hauptdolomit der Brentagruppe. Tschermaks Mineralogische und Petrographische Mitteilungen, v.8, p.167-217.

Quinn, T.M., Lohmann, K.C., and Halliday, A.N., 1991. Sr isotopic variation in shallow water carbonate sequences: stratigraphic, chronostratigraphic, and eustatic implications of the record at Enewetak Atoll. Paleoceanography, v.6/3, p.371-385.

Ranke, U., von Rad, U., and Wissmann, G., 1982. Stratigraphy, facies and tectonic development of the on- and offshore Aaiun-Tarfaya basin - a review. *in* von Rad, U., Hinz, K.,Sarnthein, M. and Seibold, E., (eds.), Geology of the northwest African continental margin. Springer-Verlag, Berlin, p.86-105.

Rao, R.P., and Talukdar, S.N., 1980. Petroleum geology of Bombay High Field, India. *in* Halbouty, M.T., (ed.), Giant oil and gas fields of the decade 1968-1978. American Association of Petroleum Geologists Memoir 30, p.487-506.

Raup, D.M., and Boyajian, G.E., 1988. Patterns of generic extinction in the fossil record. Paleobiology, v.14, p.109-125.

Read, J.F., 1989. Controls on evolution of Cambrian-Ordovician passive margin, U.S.Appalachians. *in* Crevello, P., Wilson, J.L, Sarg, J.F., and Read, J.F., (eds.), Controls on carbonate platform and basin development. Society of Economic Paleontologists and Mineralogists Special Publication 44, p.147-165.

Read, J.F., Grotzinger, J.P., Bova, J.A., and Koerschner, W.F., 1986. Models for generation of carbonate cycles. Geology, v.14, p.107-110.

Reed, J.K., 1985. Deepest distribution of Atlantic hermatypic corals discovered in the Bahamas. Proceedings 5th International Coral Reef Symposium, v.6, p.249-254.

Reijmer, J.J.G., Schlager, W., and Droxler, A.W., 1988. Site 632: Pliocene-Pleistocene sedimentation cycles in a Bahamian basin. *in* Austin, J. A., Schlager W., et al. (eds.), Proceedings of the Ocean Drilling Program, Scientific Results, Volume 101, Part B , p. 213-220.

Reiss, Z., and Hottinger, L., 1984. The Gulf of Aqaba. Springer-Verlag, Berlin, 354p.

Rinkevich, B., and Loya, Y., 1984. Does light enhance calcification in hermatypic corals? Marine Biology, v.80, p.1-6.

Ronov, A.B., Khain, V.E., Balukhovsky, A.N., and Seslavinsky, K.B., 1980. Quantitative analysis of Phanerozoic sedimentation. Sedimentary Geology, v.25, p.311-325.

Rose, P.R., 1976. Mississippian carbonate shelf margins, western United States. Journal of Research

U.S.Geological Survey, v.4, p.449-466.
Ross, C.A., 1986. Paleozoic evolution of southern margin of Permian Basin. Geological Society of America Bulletin, v.97, p.536-554.
Ross, R.J., James, N.P., Hintze, L.F., and Poole, F.G., 1989. Architecture and evolution of a Whiterockian (Early Middle Ordovician) carbonate platform, Basin Ranges of Western U.S.A.. *in* Crevello, P., Wilson, J.L, Sarg, J.F. and Read, J.F., (eds.), Controls on carbonate platform and basin development. Society of Economic Paleontologists and Mineralogists Special Publication 44, p.167-185.
Sadler, P.M., 1981. Sediment accumulation rates and the completeness of stratigraphic sections. Journal of Geology, v.89, p.569-584.
Saller, A.H., Barton, J.W., and Barton, R.E., 1989. Slope sedimentation associated with a vertically building shelf, Bone Spring formation, Mescalero Escarpe field, Southeastern New Mexico. *in* Crevello, P., Wilson, J.L, Sarg, J.F. and Read, J.F., (eds.), Controls on carbonate platform and basin development. Society of Economic Paleontologists and Mineralogists Special Publication 44, p.275-288.
Sarano, F, and Pichon, M., 1988, Morphology and ecology of the deep fore reef slope at Osprey Reef, (Coral Sea). Proceedings 6th International Coral Reef Symposium, v.2, p.607-611.
Sarg, J.F., 1988. Carbonate sequence stratigraphy. *in* Wilgus, C.K., Hastings, B.S., Kendall, C.G.St.C., Posamentier, H.W., Ross, C.A. and Van Wagoner, J.C., (eds.), Sea-level changes: an integrated approach. Society of Economic Paleontologists and Mineralogists Special Publication 42, p.155-181.
Scaturo, D.M., Strobel, J.S., Kendall, C.G.St.C., Wendte, J.C., Biswas, G., Bezdek, J., and Cannon, R., 1989, Judy Creek: A case study for a two-dimensional sediment deposition simulation. *in* Crevello, P., Wilson, J.L, Sarg, J.F. and Read, J.F., (eds.), Controls on carbonate platform and basin development. Society of Economic Paleontologists and Mineralogists Special Publication 44, p.63-76.
Schatzinger, R.A., Bebout, D.G., Loucks, R.G., and Reid, A.M., 1980. *in* Halley, R.B., and Loucks, R.G., (eds.), Society of Economic Paleontologists and Mineralogists Core Workshop 1, p.137-160.
Schlager, W., and Ginsburg, R.N., 1981. Bahama carbonate platforms - the deep and the past. Marine Geology, v.44, p. 1-24.
Schlager, W., 1963. Zur Geologie der ostlichen Lienzer Dolomiten. Mitteilungen der Gesellschaft der Geologie- und Bergbaustudenten in Österreich, v.13, p.41-120.
Schlager, W., 1981. The paradox of drowned reefs and carbonate platforms. Geological Society of America Bulletin, v.92 , p.197-211.
Schlager, W., 1989. Drowning unconformities on carbonate platforms. *in* Crevello, P., Wilson, J.L, Sarg, J.F. and Read, J.F., (eds.), Controls on carbonate platform and basin development. Society of Economic Paleontologists and Mineralogists Special Publication 44, p.15-25.
Schlager, W., 1991. Depositional bias and environmental change - important factors in sequence stratigraphy. Sedimentary Geology, v.70, p.109-130.
Schlager, W., 1992. Sedimentology and sequence stratigraphy of reefs and carbonate platforms. American Association of Petroleum Geologists, Continuing Education Course Note 34, 71p.
Schlager, W., Biddle, K.T., and Stafleu, J., 1991. Picco di Vallandro (Dürrenstein), a platform-basin transition in outcrop and seismic model. Dolomieu Conference on Carbonate Platforms and Dolomitization, Ortisei, Italy, Excursion Guidebook D, 22 p.
Schlager, W., Reijmer, J.J.G., Ten Kate, W.G.H.Z., and Sprenger, A., 1990. Exposure and flooding of carbonate platforms recorded in carbonate ooze and calciturbidites. American Association of Petroleum Geologists Bulletin, v.74, p.758 (abstract).
Schuhmacher, H., 1976. Korallenriffe. Bayerischen Landwirtschaftsverlag, München.
Schwab, F., 1976. Modern and ancient sedimentary basins: comparative accumulation rates. Geology, v.4, p.723-727.
Schwarzacher, W., and Haas, J., 1986. Comparative statistical analysis of some Hungarian and Austrian Upper Triassic peritidal carbonate sequences. Acta Geologica Hungarica, v.29, p.175-196.
Scoffin, T.P., Tudhope, A.W., Brown, B.E., Chansang, H., and Cheeney, R.F. , 1992. Patterns and possible environmental controls of skeletogenesis of *Porites lutea*, South Thailand. Coral Reefs, v.11, p.1-11
Shackleton, N.J., Backman, J., Zimmerman, H., Kent, D.V., Hall, M.A., Roberts, D.G., Schnitker, D., Baldauf, J.G., Desprairies, A., Homrighausen, R., Huddlestun, P., Keene, J.B., Kaltenback, A.J.,

Krumsiek, K.A.O., Morton, A.C., and Westberg-Smith, J., 1984. Oxygen isotope calibration of the onset of ice-rafting and the history of glaciation in the North Atlantic region. Nature, v.307, p.620-623.

Shinn, E.A., 1966. Coral growth-rate, an environmental indicator. Journal of Paleontology, v.40/2, p.233-241.

Shinn, E.A., 1980. Geologic history of Grecian Rocks, Key Largo Coral Reef Marine Sanctuary. Bulletin of Marine Science, v.30, p.646-656.

Shinn, E.A., Lidz, B.H., Halley, R.B., Hudson, J.H., and Kindinger, J.L. ,1989. Reefs of Florida and the Dry Tortugas. Field trip guidebook T176, 28th International Geological Congress, American Geophysical Union, Washington, 53 p.

Smith, S.V., 1978. Coral-reef area and the contributions of reefs to processes and resources of the world's oceans. Nature, v.273, p.225-226.

Smith, S.V., 1983. Coral reef calcification. *in* Barnes, D.J., (ed.), Perspectives on coral reefs. Australian Institute of Marine Science Contribution 200, p.240-247.

Sodero, D.E., and Hobson, J.P., 1979. Depositional facies of Lower Paleozoic Allen Bay carbonate rocks and contiguous shelf and basin strata, Cornwallis and Griffith Islands, Northwest Territories, Canada. American Association of Petroleum Geologists Bulletin, v.63, p.1059-1091.

Stanley, G.D., 1981. Early history of Scleractinian corals and its geological consequences. Geology, v.9, p.507-511.

Stanley, G.D., 1988. The history of early Mesozoic reef communities: a three-step process. Palaios, v.3, p.170-183.

Stanley, S.M., 1988. Climatic cooling and mass extinction of Paleozoic reef communities, Palaios, v.3, p.228-232.

Swart, P.K., 1983. Carbon and Oxygen isotope fractionation in scleractinean corals: A review. Earth Science Reviews, v.19, p.51-80.

Terry, C.E., and Williams, J.J., 1969. The Idris 'A' bioherm and oilfield, Sirte Basin, Libya -its commercial development, regional Paleocene geologic setting, and stratigraphy. *in* Hepple, P., (ed.), The exploration for petroleum in Europe and North Africa: London, Institute of Petroleum, p.31-48.

Tett, P., 1990. The photic zone. *in* Herring, P.J., Campbell, A.K., Whitfield, M., and Maddock, L., (eds.), Light and life in the sea. Cambridge University Press, Cambridge, 357p.

Tollmann, A., 1976. Analyse des klassischen nordalpinen Mesozoikums. Franz Deuticke, Wien, 580 p.

Tomascik, T., and Sander, F. ,1985. Effects of eutrophication on reef-building corals I: Growth rate of the reef-building coral *Montastrea annularis*. Marine Biology, v.87, p.143-155.

Toomey, D.F., and Winland, H.D., 1972. Rock and biotic facies associated with Middle Pennsylvanian (Desmoinesian) algal buildup, Nena Lucia Field, Nolan County, Texas. American Association of Petroleum Geologists, v.57, p.1053-1074.

Turcotte, D.L., 1992. Fractals and chaos in geology and geophysics. Cambridge University Press, Cambridge, 221p.

Turnsek, D., Buser, S., and Ogorelec, B., 1981. An Upper Jurassic reef complex from Slovenia, Yugoslavia. *in* Toomey, D.F., (ed.), European fossil reef models. Society of Economic Paleontologists and Mineralogists Special Publication 30, p.361-370.

Van den Hoek, C., Breeman, A.M., Bak, R.P.M., and Van Buurt, G., 1985. The distribution of algae, corals and gorgonians in relation to depth, light attenuation, water movement and grazing pressure in the fringing coral reef of Curaçao, Netherlands Antilles. Aquatic Botany, v.5, p.1-46.

Van Loon, H., (ed.), 1984. Climates of the oceans. World survey of climatology, Elsevier, Amsterdam, v.15.

Vaughan, T.W., 1919. Corals and the formation of coral reefs. Smithsonian Institution Annual Review, 1917, p.189-238.

Vincelette, R.R., and Soeparjadi, R.A., 1976. Oil-bearing reefs in Salwati basin of Irian Jaya, Indonesia. American Association of Petroleum Geologists Bulletin, v.60, p.1448-1462.

Walls, R.A., Mountjoy, E.W., and Fritz, P., 1979. Isotopic composition and diagenetic history of carbonate cements in Devonian Golden Spike reef, Alberta, Canada. Geological Society of America Bulletin, v.90, p.963-982.

Ward, R.F., Kendall, C.G.St.C., and Harris, P.M., 1986. Upper Permian (Guadalupian) facies and their association with hydrocarbons-Permian Basin, West Texas and New Mexico. American Association

of Petroleum Geologists Bulletin, v.70, p.239-262.

Watkins, D.K. and Verbeek, J.W., 1988. Calcareous nannofossil biostratigraphy from Leg 101, Northern Bahamas. *in* Austin, J. A., Schlager W., et al. (eds.), Proceedings of the Ocean Drilling Program, Scientific Results, Volume 101, Part B, p. 63-85.

Watts, A.B., 1982. Tectonic subsidence, flexure and global changes of sea level, Nature, v.29, p.469-474.

Weber, J.N., and Woodhead, P.M.J., 1970. Carbon and oxygen isotopic fractionation on the skeletal carbonate of reef-building corals. Chemical Geology, v.6, p.93-117.

Weber, J.N., and White, E.W., 1974. Activation energy for skeletal aragonite deposited by the hermatypic coral *Platygyra spp*. Marine Biology, v.26, p.353-359.

Weber, J.N., White, E.W., and Weber, P.H., 1975. Correlation of density banding in reef coral skeletons with environmental parameters: the basis for interpretation of chronological records preserved in the coralla of corals. Paleobiology, v.1, p.137-149.

Weber, J.N., Deines, P., Weber, P.H. and Baker, P.A., 1976. Depth related changes in the $^{13}C/^{12}C$ ratio of skeletal carbonate deposited by the Caribbean reef-frame building coral *Montastrea annularis*: further implications of a model for stable isotope fractionation by scleractinian corals. Geochimica et Cosmochimica Acta, v.40, p.31-39.

Weil, S.M., Buddemeier, R.W, Smith, S.V., and Kroopnick, P.M., 1981. The stable isotopic composition of coral skeletons: control by environmental variables. Geochimica et Cosmochimica Acta, v.45, p.1147-1153.

Weinberg, S., 1976. Submarine daylight and ecology. Marine Biology, v.37, p.291-304.

Wilkinson, B.H., and Walker, J.C.G., 1989. Phanerozoic cycling of sedimentary carbonate. American Journal of Science, v.289, p.525-548.

Williams, S.C, 1985. Stratigraphy, facies evolution, and diagenesis of late Cenozoic limestones and dolomites, Little Bahama Bank, Bahamas. Ph.D. Thesis, University of Miami, 217 p.

Wilson, J.L., 1975. Carbonate facies in geologic history. Springer-Verlag, New York, 471 p.

Winterer, E.L., and Bosellini, A., 1981. Subsidence and sedimentation on Jurassic passive continental margin, Southern Alps, Italy. American Association of Petroleum Geologists Bulletin, v.65, p.394-421.

Winterer, E.L., and Murphy, M.A., 1960. Silurian reef complexes and associated facies, central Nevada. Journal of Geology, v.68, p.117-139.

Woodroffe, C.D., 1992. Morphology and evolution of reef islands in the maldives. 7th International Coral Reef Symposium, p.109 (abstract).

Woodley, J.D., Chornesky, E.A., Clifford, P.A., Jackson, J.B.C., Kaufman, L.S., Knowlton, N., Lang, J.C., Pearson, M.P., Porter, J.W., Rooney, M.C., Rylaarsdam, K.W., Tunnicliffe, V.J., Wahle, C.M., Wulff, J.L., Curtis, A.S.G., Dallmeyer, M.D., Jupp, B.P., Koehl, M.A.R., Nigel, J., Sides, E.M.,1981. Hurricane Allen's impact on Jamaican coral reefs. Science, v.214, p.749-755..

Wyman, K.D., Dubinsky, Z., Porter, J.W., and Falkowski, P.G., 1987. Light absorption and utilization among hermatypic corals: a study in Jamaica, West Indies. Marine Biology, v.96, p.283-292.